Vanessa Gouveia Ramos

Bachelor of Science in Biomedical Engineering

Automatic classification of medical images based on functional connectivity measurements - methodological exploration

Dissertation submitted in partial fulfillment
of the requirements for the degree of

Master of Science in
Biomedical Engineering

Adviser: Alexandre Andrade, Assistant Professor,
Faculty of Sciences of the University of Lisbon

Examination Committee

Chairperson: Carla Maria Quintão Pereira
Raporteur: Ricardo Nuno Pereira Verga e Afonso Vigário
Member: Alexandre da Rocha Freire de Andrade

FACULDADE DE
CIÊNCIAS E TECNOLOGIA
UNIVERSIDADE NOVA DE LISBOA

March, 2019

Automatic classification of medical images based on functional connectivity measurements - methodological exploration

Copyright © Vanessa Gouveia Ramos, Faculdade de Ciências e Tecnologia, Universidade NOVA de Lisboa.
A Faculdade de Ciências e Tecnologia e a Universidade NOVA de Lisboa têm o direito, perpétuo e sem limites geográficos, de arquivar e publicar esta dissertação através de exemplares impressos reproduzidos em papel ou de forma digital, ou por qualquer outro meio conhecido ou que venha a ser inventado, e de a divulgar através de repositórios científicos e de admitir a sua cópia e distribuição com objetivos educacionais ou de investigação, não comerciais, desde que seja dado crédito ao autor e editor.

This document was created using the (pdf)LaTeX processor, based in the "novathesis" template[1], developed at the Dep. Informática of FCT-NOVA [2].
[1] https://github.com/joaomlourenco/novathesis [2] http://www.di.fct.unl.pt

Abstract

The study of patterns of neuronal activity constitutes a tool of extreme value in the attempt to unveil neural pathological mechanisms. Hence, functional connectivity studies using images from Resting State fMRI (rs-fMRI) are crucial, and there are several metrics which can be used to assess brain connections. Nonetheless, no clear evidence exists that some may be better than others.

In this study, in an attempt to discover if certain metrics better characterized certain connections, two different approaches were followed. Data from a public dataset was used - Addiction Connectome Preprocessed Initiative (ACPI) - as well as one toolbox for matrix construction - Multiple Connectivity Analysis (MULAN) - and another for statistical comparison - GraphVar. Both toolboxes run in MATLAB. Metrics under analysis were: correlation, coherence, mutual information, transfer entropy and non-linear correlation. To that end, 116 brain regions were considered.

First, considering only healthy subjects, it was done a pairwise comparison between results from different metrics. It was verified that each of them led to different results regarding the same connections. Then, connectivity results between a healthy and a pathological group of subjects with Attention-Deficit/Hyperactivity Disorder (ADHD) were compared. Concerning the differences, several similarities with the known affected areas described amongst the literature were found. However, discrepancies were observed which may be related to differences in sample size and/or the metric used in these studies.

In general, it was shown that there is indeed variability between functional metrics and regional specificity. Still, the anatomical and physiological reasons for these differences remain unknown. It was clear that using more than one metric may be important and that the use of more general metrics may have advantages in the study of the pathological brain as it may have more complex dynamics. Furthermore, ensemble tools that have into consideration more than one metric to characterize brain connections may represent invaluable tools for autonomic image classification.

Keywords: Functional connectivity, rs-fMRI, ADHD, functional connectivity metrics, regional specificity

Resumo

O estudo de padrões de atividade neuronal constitui uma ferramenta de extremo valor no deslindar de mecanismos patológicos. Neste sentido, estudar a conectividade funcional usando imagens de ressonância magnética funcional em repouso assume um papel chave. No entanto, várias são as métricas que podem ser usadas para aferir as conexões e não existem evidências claras que umas sejam mais vantajosas que outras.

Neste estudo, numa tentativa de perceber se certas métricas teriam uma melhor capacidade de caracterizar determinadas conexões, seguiram-se duas abordagens. Usaram-se dados provenientes de uma base de dados pública (ACPI), uma *toolbox* para construção de matrizes de conectividade (MULAN) e outra para comparação estatística (GraphVar). As métricas estudadas foram: correlação, coerência, informação mútua, transferência de entropia e correlação não linear. Foram consideradas 116 regiões do cérebro.

Primeiro, considerando sujeitos saudáveis, compararam-se dois a dois os resultados de diferentes métricas após devida normalização. Mostrou-se que cada métrica conduz a resultados diferentes para as mesmas conexões. Depois, compararam-se os resultados obtidos para as mesmas conexões entre um grupo saudável e outro patológico (ADHD) e confrontaram-se os resultados das comparações com dados referentes a diferenças que se sabem existir entre os grupos. Várias semelhanças com a literatura foram encontradas. No entanto, verificaram-se discrepâncias que se pensam dever a diferenças entre o tamanho das amostras e/ou métricas usadas nos diferentes estudos.

No geral, comprovou-se que existe de facto variabilidade entre as métricas e especificidade regional, permanecendo em aberto a que se devem tais diferenças. Sublinha-se a importância do uso de mais do que uma métrica. Para além do mais, sugere-se que o uso de métricas mais gerais pode trazer vantagens ao estudo do cérebro patológico dada a possibilidade de este envolver dinâmicas mais complexas. Tornou-se evidente que o uso de ferramentas que agregam informação de diferentes métricas poderá ser vantajoso no estudo de padrões de atividade neuronal e na classificação automática de imagens.

Palavras-chave: Conectividade funcional, rs-fMRI, ADHD, métricas de conectividade funcional, especificidade regional

Contents

List of Figures xi

List of Tables xiii

Acronyms xv

1 Introduction 1
- 1.1 Context and Motivation . . . 1
- 1.2 Goals . . . 2
- 1.3 Thesis Outline . . . 3

2 Theoretical Background 5
- 2.1 Magnetic Resonance Imaging . . . 5
  - 2.1.1 Blood Oxygen Level-Dependent Signal . . . 6
  - 2.1.2 Resting State Functional MRI . . . 7
- 2.2 Human Brain Connectivity . . . 8
  - 2.2.1 Functional Connectivity Metrics . . . 9
  - 2.2.2 Main Intrinsic Connectivity Networks . . . 14
- 2.3 Assessing Brain Connections with Neuroimage . . . 15
  - 2.3.1 Region Definition . . . 15
  - 2.3.2 Connectivity Measurement . . . 16

3 State-of-the-Art 17
- 3.1 Attention-Deficit/Hyperactivity Disorder . . . 17
  - 3.1.1 Altered ReHo and ALFF measurements on ADHD subjects . . . 18
  - 3.1.2 Altered connectivity measurements on ADHD subjects . . . 19
- 3.2 Comparison Between Different Measures of Connectivity . . . 21

4 Materials and Methods 23
- 4.1 Participants . . . 24
  - 4.1.1 ACPI Dataset . . . 24
- 4.2 Quantifying Functional Connectivity . . . 27
  - 4.2.1 Connectivity Matrices Computation . . . 28
  - 4.2.2 Connectivity Matrices Normalization . . . 29

4.3 Statistical Analysis 30
4.3.1 Group Comparisons 32

5 Results and Discussion **33**
5.1 Results Viewer Interface 33
5.2 Pairwise Functional Connectivity Metric Comparison 34
5.2.1 BCorrU-BMITU 35
5.2.2 BCorrD-BMITD1 35
5.2.3 BCohW-BCorrU 36
5.2.4 BCohF-BCorrU 38
5.2.5 BCohW-BMITU 41
5.2.6 BCohF-BMITU 43
5.3 Control versus Patient Comparison 48
5.3.1 Hsquare 49
5.3.2 Transfer Entropy 52
5.3.3 Mutual Information 56
5.3.4 Time Basic 60
5.3.5 Frequency Basic 63

6 Conclusion **79**

Bibliography **83**

List of Figures

2.1 Longitudinal and transverse relaxation. 6
2.2 Representation of some key determinants in Blood-Oxygen-Level-Dependent (BOLD) signal. 7
2.3 Flowchart with the fundamental steps involved in resting state connectivity analysis. 16

4.1 Scheme from the bootstrapping process followed to obtain the histogram used for matrix normalization. 30
4.2 Schematic workflow of GraphVar toolbox. 31

5.1 Example of a matrix displayed on the results display panel. 33
5.2 Results from pairwise functional connectivity metric comparison - matrices from BCorrU-BMITU and BCorrD-BMITD1. 34
5.3 Results from pairwise functional connectivity metric comparison - matrices from BCohW2-BCorrU and BCohW3-BCorrU. 36
5.4 Results from pairwise functional connectivity metric comparison - significant networks from BCohW2-BCorrU. 37
5.5 Results from pairwise functional connectivity metric comparison - significant network from BCohW3-BCorrU. 38
5.6 Results from pairwise functional connectivity metric comparison - matrices from BCohF2-BCorrU and BCohF3-BCorrU. 39
5.7 Results from pairwise functional connectivity metric comparison - significant networks from BCohF2-BCorrU. 39
5.8 Results from pairwise functional connectivity metric comparison - significant networks from BCohF3-BCorrU. 40
5.9 Results from pairwise functional connectivity metric comparison - matrices from BCohW2-BMITU and BCohW3-BMITU. 41
5.10 Results from pairwise functional connectivity metric comparison - significant networks from BCohW2-BMITU. 42
5.11 Results from pairwise functional connectivity metric comparison - significant networks from BCohW3-BMITU. 44
5.12 Results from pairwise functional connectivity metric comparison - matrices from BCohF-BMITU. 45

5.13 Results from control versus patient comparison using Hsquare family- matrices from BH2U, BH2D, PH2U, and PH2D. 49
5.14 Results from control versus patient comparison using Hsquare family- significant networks from BH2U. 50
5.15 Results from control versus patient comparison using Transfer Entropy family - significant network from BTEU (part I). 52
5.16 Results from control versus patient comparison using Transfer Entropy family - matrices from BTEU, BTED, PTEU, and PTED. 53
5.17 Results from control versus patient comparison using Transfer Entropy family - significant network from BTEU (part II). 54
5.18 Results from control versus patient comparison using Transfer Entropy family - significant networks from PTEU. 55
5.19 Results from control versus patient comparison using metrics from Mutual Information family - matrices from BMITU, BMITD1, PMITU, and PMITD1. 57
5.20 Results from control versus patient comparison using Mutual Information family - significant networks from PMITU (part I). 58
5.21 Results from control versus patient comparison using Mutual Information family - significant network from PMITU (part II). 59
5.22 Results from control versus patient comparison using metrics from Time Basic family - matrices from BCorrU, BCorrD, PCorrU, and PCorrD. 60
5.23 Results from control versus patient comparison using metrics from Time Basic family - significant networks from BCorrU and PCorrU. 61
5.24 Results from control versus patient comparison using metrics from Frequency Basic family - matrices from Fourier Based Coherence. 64
5.25 Results from control versus patient comparison using metrics from Frequency Basic family - significant networks from BCohF3 (part I). 65
5.26 Results from control versus patient comparison using metrics from Frequency Basic family - significant network from BCohF3 (part II). 66
5.27 Results from control versus patient comparison using metrics from Frequency Basic family - matrices from Wavelet Based Coherence. 67
5.28 Results from control versus patient comparison using metrics from Frequency Basic family - significant networks from BCohW1 and BCohW2. 68
5.29 Results from control versus patient comparison using metrics from Frequency Basic family - significant networks from BCohW1, BCohW2, and BCohW3. . 69
5.30 Results from control versus patient comparison using metrics from Frequency Basic family - significant networks from BCohW3. 70

List of Tables

3.1 Regions with altered ReHo measurements on ADHD subjects. 18
3.2 Regions with altered ALFF measurements on ADHD subjects. 19
3.3 Pairs of regions with altered connectivity measurements on ADHD subjects. . 22

4.1 List of the 116 brain regions that are comprised in the AAL atlas. 25
4.2 List of metrics used throughout the present study and respective notation. . . 28
4.3 Parameters used for matrices computation 29

Acronyms

AAL Automated Anatomical Labeling.

ACC Anterior Cingulate Cortex.

ACPI Addiction Connectome Preprocessed Initiative.

ADHD Attention-Deficit/Hyperactivity Disorder.

ALFF Amplitude of Low-Frequency Fluctuation.

ANCOVA Analysis of Covariance.

ANTs Advanced Normalization Tools.

BOLD Blood-Oxygen-Level-Dependent.

dACC Dorsal Anterior Cingulate Cortex.

dlPFC Dorsolateral Prefrontal Cortex.

DMN Default Mode Network.

dmPFC Dorsomedial Prefrontal Cortex.

dMRI Diffusion-Weighted MRI.

EEG Electroencephalography.

fMRI Functional Magnetic Resonance Imaging.

GLM General Linear Model.

MEG Magnetoencephalography.

MRI Magnetic Resonance Imaging.

MTA Multimodal Treatment of Attention Deficit Hyperactivity Disorder.

MULAN Multiple Connectivity Analysis.

OFC Orbitofrontal Cortex.

PCC Posterior Cingulate Cortex.

PET Positron Emission Tomography.

PFC Prefrontal Cortex.

ReHo Regional Homogeneity.

RF Radio Frequency.

ROI Region of Interest.

rs-fMRI Resting State fMRI.

SPECT Single-Photon Emission Computed Tomography.

vmPFC Ventromedial Prefrontal Cortex.

VS Ventral Striatum.

CHAPTER 1

Introduction

1.1 Context and Motivation

The human brain is a fascinating organ and because of its complexity it remains a mystery in many aspects. In an attempt to unveil its mechanisms and organization there are several levels of analysis that take part in neuroscience research, including: molecular, cellular, systems, behavioural, and cognitive neuroscience [7].

In this study the focus will be on systems neuroscience where two fundamental concepts are crucial to thoroughly understand brain functioning. These concepts are segregation and integration [36] and between them one finds connectivity as a major player.

Over the past, many functional impairments caused by regional brain lesions were observed and led to many pathological models emphasising a segregationist idea [33]. However, more recently, there has been a growing recognized understanding of the importance of brain connectivity in neuropathology. As a matter of fact, in recent years, functional connectivity patterns have been linked to different neurological and psychiatric disorders. The analysis of individual variations of these patterns may conduct to a better knowledge of these disorders and may even be used to differentiate healthy and diseased subjects.

In modern societies, disorders of the nervous system constitute a major issue afflicting millions of people worldwide. Unfortunately, some of these disorders lack of a reliable diagnostic test. Take for example Parkinson's disease, a disorder that at the time the symptoms arise at least half of the dopaminergic neurons have already been lost. Furthermore, there is no standard diagnostic test for this disease and the more objective existing diagnosis relies on the use of radioactive neuroimaging techniques [5].

The need for early stage biomarkers is noticeable and it's not exclusive of neurodegenerative disorders. Neuropsychiatric disorders also lack on objective reliable markers [50], for example, major depressive disorder, an important neuropsychiatric disorder, has its

diagnosis based on subjective evaluation of signs and symptoms [93]. It's not only this need for a better diagnostic but also for a better prognosis and treatment for neurological diseases that is one of the drivers of functional connectivity studies [33], with different techniques being used to measure functional connections.

Recent technological developments brought new methods to explore the brain and understand its mechanisms. For example, non-invasive neuroimaging techniques have allowed *in vivo* imaging and represent invaluable tools [8]. They enabled the study of previously unanswered questions about both healthy and unbalanced brain. Functional magnetic resonance, a relatively new imaging technique, was developed during the early 1990s [13] and has proved to be of extreme value as a brain research tool, as it was used in thousands of studies since its appearance.

Using data obtained from these new imaging techniques, different mathematical methods may be used to quantify the functional connectivity between brain regions, each of them accessing different characteristics of neural connections and leading to different results. Quantifying interactions constitutes a challenge and each metric has its pros and cons [6]. In fact, functional connectivity measurements will be the core of this study in an attempt to understand if there is any regional advantage when using a given metric.

Due to the problem's complexity, large datasets and data sharing are essential. However, at the same time, massive information being collected has led to the new problem of how to extract meaningful information from such huge amount of data [25]. This is where machine learning algorithms can play an essential role. Many different automatic classification techniques may be used to address the challenge and help find patterns among neuroimaging data.

1.2 Goals

With all this in mind, this study aims to give a solid contribution in the identification of computational analysis tools that may be useful in automatic neuroimage classification, more specifically functional magnetic resonance images of the human brain. To do so, we first compare the values of functional connectivity strength obtained when using different connectivity metrics for the same pairs of brain regions. Then we compare functional connectivity between brain regions from two sample groups: a pathological and a control group.

- **First Goal:** identification of functional connectivity metrics that allow to quantify the connectivity strength between different brain areas and comparison of these metrics in an attempt to infer if there is any significant pairwise differences.
- **Second Goal:** application of connectivity metrics to a specific case study for group comparison.

We expect to find regional differences when using different metrics and propose to study them, hoping to find metrics that better describe the connection between specific brain regions.

1.3 Thesis Outline

In the next chapter, Chapter 2, it will be presented the theoretical underpins that were considered crucial for a proper understanding of the following text, including notes regarding how is functional connectivity assessed using neuroimaging techniques and which are the mathematical metrics used to achieve this.

In Chapter 3, a brief review of previous work done in the field of this study will be done, that is, state-of-the-art on functional connectivity measurements comparison. In addition, it will be done a review on the work done on the pathology chosen for the specific case study, which is ADHD.

Next, materials and methods that were used will be described in detail in Chapter 4, with emphasis given on the methodology and several decisions that had to be done.

In Chapter 5, research results and the corresponding discussion having into account the current literature will be presented.

Finally, in Chapter 6, some conclusions and limitations of the present study will be exposed, as well as observations on future work.

CHAPTER 2

Theoretical Background

In this chapter, as it was said before, it is intended to introduce some key theoretical concepts essential for the understanding of the following chapters. For starters, basic concepts on Magnetic Resonance Imaging (MRI) will be provided. Then, the focus will be on human brain connectivity, how it may be quantified and some of the methods that can be followed to do so.

2.1 Magnetic Resonance Imaging

MRI is a non-invasive imaging technique that is based on the magnetic proprieties of atomic nuclei.

To produce magnetic resonance images several biologically relevant elements can be used. These must have a non zero-spin atom and include hydrogen, oxygen-16, fluorine-19, sodium-23, and phosphorus-31 [9]. Hydrogen is the most abundant of all within the human body, hence it is the most used in clinical MRI [18].

When in normal conditions, nuclear spins are randomly oriented and the total magnetization is zero. However, in the presence of a strong external magnetic field, $\vec{B_0}$, the spins align with this field and give rise to a measurable magnetic moment, $\vec{M_0}$, that has the direction of the given external field. As this happens, the nuclei precess around an axis with the direction of the field with a frequency called the Larmor frequency, given by $w_0 = B_0.\gamma$, where γ corresponds to the gyromagnetic constant which is characteristic of each nuclear specie.

The magnetization may be measured by disturbing the system through the application of a Radio Frequency (RF) pulse perpendicular to $\vec{B_0}$ with the Larmor frequency, $\vec{B_1}$. Hence it is applied, the nuclei resonate and absorb energy. The net magnetization vector is now precessing around the total magnetic field and can be described by its longitudinal

component along $\vec{B_0}$ and its transverse component perpendicular to $\vec{B_0}$. As the RF is turned off, the transverse magnetization progressively tends to zero and the system returns to a new equilibrium. This process is called relaxation and also occurs on the longitudinal magnetization which returns to its equilibrium, M_0. Transverse and longitudinal relaxation can, respectively, be described by the time constants T2 and T1 which are represented in figure 2.1.

These changes in energy generate an oscillating magnetic field which can be measured with a receive coil where a current proportional to the transverse relaxation is induced. The detected signal is called Free Induction Decay signal and, in practice, decays faster than expected for the T2 because of magnetic field inhomogeneities, this is described by another constant, T2* [13].

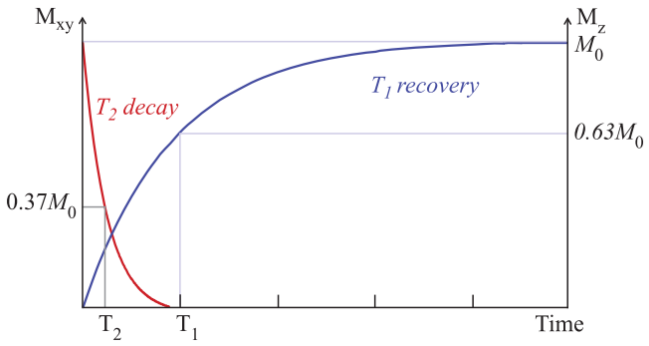

Figure 2.1: Longitudinal and transverse relaxation. T1 corresponds to the interval where 63% of longitudinal magnetization is recovered. T2 corresponds to the interval where 37% of transverse magnetization is present. From [57].

In order to obtain an image, it is necessary to spatially encode what is being imaged in such way that it is possible to know which point on space is responsible for the detected signal. This is done by using gradient coils.

2.1.1 Blood Oxygen Level-Dependent Signal

Functional Magnetic Resonance Imaging (fMRI) is a modality of MRI, thus being an entirely non-invasive technique. This technique allows the observation of the working brain [13], providing an indirect measure of neural activity. Comparing with Electroencephalography (EEG) it has a higher spatial resolution and a poorer temporal resolution [14].

BOLD is the most common contrast method used in fMRI and it is based on the magnetic proprieties of hemoglobin, the oxygen transporter in the blood vessels. Hemoglobin has two different forms: oxyhemoglobin and deoxyhemoglobin, the latter being a paramagnetic molecule and so influencing blood magnetization and MR signal [18].

In 1990, Ogawa et al. observed that variations on oxygen concentration in the blood altered MRI signal [62]. It was verified that brain activation upon stimulation led to MRI signal changes: initially one could observe a signal decrease and then a strong

increase. This was explained by means of changes on the ratio between oxyhemoglobin and deoxyhemoglobin in the blood surrounding the activated brain region.

Metabolically speaking, when an increase of neural activity occurs, there is an increase on adenosine triphosphate demand. Hence, oxygen consumption increases, leading towards an increase of deoxyhemoglobin concentration in the surrounding area [40]. This is followed by a blood flow increase and an oversupply of oxygenated blood, decreasing deoxyhemoglobin concentration in the surrounding area which translates to the verified increase in the MRI signal [32].

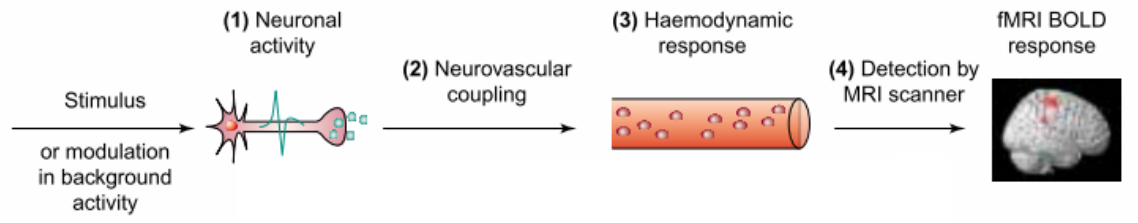

Figure 2.2: Representation of some key determinants in BOLD signal from neuronal activity to signal detection by MRI scanner. Adaptation from [4].

At the current spatial resolution, at the tinniest volume, BOLD signal reflects not only the activity of a population of neurons but also several other factors. It must be noted that there is a complex relationship between the neural activity and the correspondent hemodynamic response and, as seen with blood volume, not only neural activity leads towards changes in oxyhemoglobin concentration and many factors affect the detected signal, including the scanning parameters (figure 2.2). Hence, cerebral blood flow, cerebral metabolic rate of oxygen, vascular geometry, hematocrit, magnetic field strength, and echo time are just some of the key determinants of BOLD signal [4].

Very used in clinical research, BOLD fMRI has shown promising developments due to the growing use of a resting state approach.

2.1.2 Resting State Functional MRI

rs-fMRI contrasts with task-based fMRI and consists in signal acquisition with neither stimulus application or task performance.

While in resting condition, low frequency spontaneous fluctuations in the BOLD signal are registered in fMRI and there are several studies that support the neuronal basis of these fluctuations. In fact, patterns occur between regions that have common function and neuroanatomy. Furthermore, it was registered associations between these fluctuations and electrophysiological recordings [41].

The advantages of using rs-fMRI have been stated by several authors. For example, Fox et al. [34] highlights that there is a larger amount of energy consumption due to resting state neural activity opposed to the scarce variation of activity during task performance and a much better signal-to-noise ratio. In addition, it can be applied to a wider population

than task-based measurements because no motor requests are demanded, hence implying a negligible patient collaboration [28] and being suitable for patients with motor or cognitive impairments or that are for other reason incapable of collaboration during task-based measurements.

The use of resting state activity to identify functional connectivity patterns is promising and already widely used, not only for functional studies in healthy subjects but also, and perhaps most importantly, for studies of neurological pathologies. Therefore, functional connectivity rs-fMRI is suitable to study and compare healthy and pathological brains with several possible applications that range from pharmacology studies and disease monitoring to an evident diagnostic and prognostic potential.

2.2 Human Brain Connectivity

Neurons are the basic unit of the nervous system which comprises the spinal cord, the brain, and the peripheral nerves.

Millions of neurons are found in the human brain and interact with each other establishing complex dynamic neuronal networks. The information flow between neurons from different regions is dynamically coordinated through changes in neural oscillatory synchrony proprieties like strength, pattern, and frequency [6]. In fact, neural synchronous intrinsic fluctuations were shown to reflect the underlying connectivity of brain areas even at rest [19, 41] and are originated from spatially apart brain areas that are functionally linked [73].

Understanding the established interactions within the brain by looking at it as a system rather than just studying isolated regions may be crucial to have new insights into the underlying mechanisms of pathological brain functioning. Indeed, in recent years, there has been a shift from the study of local pathology to the study of interconnected systems disruption [33].

Since 2005, the term connectome has been applied when it comes to brain connectivity. It was used, independently, for the first time, by Sporns [74] and Hagmann [39] to describe the set of all structural neural connections. However, in recent literature, one can find it being used to refer to the ensemble of different brain regions and their structural and functional connections rather than just refer to structural connections itself [25].

Connectomes can be analysed at different spatial scales, from micro to macro-scale, each one closely linked to the others but providing different perspectives into brain's connections [24]. At the micro-scale we find single neurons and synaptic connections, at the meso-scale, connections within and between cell assemblies, like columns, and at the macro-scale, we have interregional pathways. At the current technological paradigm, macro-scale is the most feasible way to assess the human connectome [19].

Two main types of connectivity can be named, and they are: structural and functional connectivity. A brief description of each one is given bellow.

Structural (or anatomical) connectivity corresponds to actual physical connections, that is, connections established by fibre tracts wired to each other and linking spatially distant brain regions [74].

Functional connectivity refers to statistical dependences of activation patterns between different brain regions [36], representing undirected associations between them. Despite being somehow constraint by structural connectivity, it is not the same [44]. In fact, it was shown that if there is an anatomical connection, a functional connection exists, however, the opposite is not true, and there may exist a strong functional connection between two brain regions with no direct anatomical link [29]. Some authors also define another type of connectivity: effective connectivity, which corresponds to the effect that one neural population exerts over another, representing a direct influence [36].

2.2.1 Functional Connectivity Metrics

There are several ways to analyse functional connectivity. For example, one can do a seed wise analysis by choosing an hypothesis-driven seed (group of localized voxels) and studying its statistical dependencies with all the other voxels outside its boundaries, that is a seed to voxel analysis [41]. Another option is to either do a voxel or Region of Interest (ROI) wise analysis, where statistical dependencies between all the voxels or ROIs are studied, that is a voxel to voxel or seed to seed analysis.

Functional connectivity is typically evaluated through a pairwise analysis between all possible pairs of time-series [24]. In fact, there is no single method to analyse statistical dependencies between a pair of time-series. Different metrics may be used, and each one carries different information with respect to different signal proprieties, including spectral content, temporal evolution, and linear or non-linear characteristics [54]. This is important, as there is no unique way of interaction between different brain areas.

In terms of metrics' taxonomy, we have linear and non-linear metrics, as some can only detect linear dependencies, while others detect both linear and non-linear. Non-linear methods are based on non-linear functions between the signals. Metrics may be directed or undirected, whether they quantify or not the direction of the coupling between the regions whose time-series are being analysed. They may also be model-based or model-free and belong to time or frequency domain.

Bellow, there is a brief description of some of the metrics that were used to measure functional connectivity in this study. First of all, it is important to introduce some concepts that are essential for the understanding of the description of two of the metrics, which come from the field of information theory.

Information theory has its foundation on the paper "A Mathematical Theory of Communication"and provides tools to quantify information and communication [83]. Originally, the goal was to study information transmission through communication systems [47].

An important concept of information theory is entropy. Entropy measures the reduction of uncertainty of the values of a given discrete variable when it is actually measured [63, 83]. Given two discrete variables X and Y, the entropy of X and Y are given by:

$$H(X) = -\sum_{x \in X} p(x) \log p(x) \tag{2.1a}$$

$$H(Y) = -\sum_{y \in Y} p(y) \log p(y) \tag{2.1b}$$

where $p(x)$ and $p(y)$ are the probability distribution of X and Y, respectively. When the logarithm has base of 2, the result from equations 2.1 is given in bits [63]. Entropy equals to zero when one element of the sequence has unit probability, and has its highest value when all elements of the sequence are equally probable. This translates to: the higher the uncertainty, the greater the measure.

The joint entropy is given by:

$$H(X,Y) = -\sum_{x \in X} \sum_{y \in Y} p(x,y) \log p(x,y) \tag{2.2}$$

where, $p(x,y)$ is the joint probability distribution. The conditional entropy can, then, be computed by:

$$H(X|Y) = -\sum_{x \in X} \sum_{y \in Y} p(x,y) \log p(x|y) \tag{2.3}$$

If the knowledge of the past and present of one variable leads to a better prediction of the future of another variable comparing with the situation when only the present and past of the given variable is known, it is said that the first causes the latter.

Cross-correlation

Cross-correlation measures the linear association between two random variables x and y and is given by equation 2.4, where Cov_{xy} corresponds to the covariance between x and y, τ to the time lag between the signals and σ to the standard deviation [53, 69].

$$C_{xy}(\tau) = \frac{Cov_{xy}(\tau)}{\sigma_x \sigma_y} \tag{2.4}$$

When we have two samples, X_n and Y_n, with $n = 1, \ldots, N$, an estimator for the cross-correlation is:

$$\hat{C}_{xy}(\tau) = \frac{\sum_{n=1}^{N-\tau} (X_n - \overline{X})(Y_{n+\tau} - \overline{Y})}{\sqrt{\sum_{n=1}^{N-\tau} (X_n - \overline{X})^2 \sum_{n=1}^{N-\tau} (Y_{n+\tau} - \overline{Y})^2}} \tag{2.5}$$

If the variables are normalized, such that they have zero mean and unit variance, the cross-correlation ranges between -1 and 1, meaning liner inverse or direct correlation, respectively. The maximum value given by equation 2.5 yields an estimate for the linear association between the variables [55]. If $C_{x,y}$ equals to zero then the variables are not

linearly dependent, however, this does not exclude other types of dependency and the result is only unambiguous if there is a linear association between the variables.

If, besides considering normalized variables, τ equals to zero, then cross-correlation corresponds to the Pearson's product moment correlation coefficient [63], the most used method to evaluate functional connectivity.

Cross-correlation does not give any information about the direction of a given relationship between two time-series.

To remove indirect effects, that is, effects from other signals that are not being analysed, partial cross-correlation may be computed.

It must be noted that the neurophysiological meaning of anti-correlations remains unknown, nevertheless, anti-correlations were seen to occur between competing neural networks [19].

Cross-coherence

Cross-coherence is the analogous of the cross-correlation in the frequency domain and also quantifies linear associations [53, 63]. It corresponds to the normalized cross spectral density function [69] and expresses how each frequency component from one signal is related to the corresponding frequency component from the other signal [55].

Cross-coherence is given by equation 2.6 [6].

$$Coh_{x,y}(f) = \frac{|S_{xy}(f)|}{\sqrt{|S_{xx}(f)||S_{yy}(f)|}} \tag{2.6}$$

where S_{xy} is the cross spectrum, defined by equation 2.7a, and $S_{xx}(f)$ and $S_{yy}(f)$ the power spectrum of x and y, respectively, equations 2.7b and 2.7c.

$$S_{xy}(f) = \sum_u Cov_{xy}(u)e^{-jfu} \tag{2.7a}$$

$$S_{xx}(f) = \sum_u Cov_{xx}(u)e^{-jfu} \tag{2.7b}$$

$$S_{yy}(f) = \sum_u Cov_{xx}(u)e^{-jfu} \tag{2.7c}$$

In order to compute the coherence it is necessary to know the cross and power spectra, which are obtained from an infinite period. As real data has finite size, estimators of the true spectrum are usually used, including smoothing techniques [51].

An alternative to Fourier-based coherence is to do a time-frequency analysis, that is, to do a wavelet coherence analysis. This measure, in contrast to the former, allows the study of coherence on non-stationary signals.

Wavelets are functions that have zero mean and are localized in time and frequency [80]. There are several families of wavelet functions, each of them obtained through dilations and translations of a mother wavelet.

Similarly to Fourier-based coherence, wavelet based coherence is given by:

$$WCoh(t,f) = \frac{|SW_{xy}(t,f)|}{\sqrt{|SW_{xx}(t,f)SW_{yy}(t,f)|}} \tag{2.8}$$

where $SW_{xy}(t,f)$ is the wavelet cross-spectrum between X and Y around time t and frequency f which is given by equation 2.9.

$$SW_{xy}(t,f) = \int_{t-\frac{\delta}{2}}^{t+\frac{\delta}{2}} W_x(\tau,f)W_y^*(\tau,f)d\tau \tag{2.9}$$

where W_x and W_y are the wavelet transforms of the signals that is obtained through the convolution of the signal with the chosen wavelet function, * denotes the complex conjugate. δ is an important parameter and is adapted to the frequency of interest. This is an important feature of wavelet analysis, as it improves the temporal resolution of the calculations. For lower frequencies the time window is longer than for higher frequencies, that is, for low frequencies a bigger value of δ may be chosen.

Mutual information

Mutual information is one of the measures from information theory and can be used to assess both linear and non-linear dependencies between two time-series, as it detects second and higher order correlations. This metric quantifies how much can be known about a given variable by observing another [83]. In particular, it estimates how much information is shared between the two [32] by quantifying the reduction of uncertainty about one time-series when having into account what is known about the other at the same time.

Being X and Y two discrete variables, mutual information is given by:

$$MI(X,Y) = \sum_{x\in X}\sum_{y\in Y} p(x,y)\log\left(\frac{p(x,y)}{p(x)p(y)}\right) \tag{2.10}$$

which may be expressed, in terms of entropy, as:

$$MI(X,Y) = H(Y) - H(Y|X) = H(X) + H(Y) - H(X,Y) \tag{2.11}$$

If one variable does not depend on the other we have $H(Y|X) = H(Y)$ and mutual information has its minimum value. On the other hand, if the two variables are equal, mutual information has its maximum value. Hence, mutual information is always non negative.

As defined here, mutual information is symmetric and lacks on content about directionality. In addition, it must be noted that authors refer that its reliable estimation frequently requires large amount of data [63].

Transfer entropy

Transfer entropy is another measure that comes from information theory. It is a model free non-linear metric that quantifies the uncertainty on a given time-series when having

information about its past and the past of another one. Hence, in opposition to mutual information, it also reflects the dynamics of the processes [71].

Being X and Y two time-series, the transfer entropy is given by:

$$TE(X,Y) = \sum_{x_{t+1}\in X}\sum_{x\in X}\sum_{y\in Y} p(x_{t+1},x_t,y_t)\log\left(\frac{p(x,y)}{p(x_{t+1}|x_t,y_t)p(x_{t+1}|x_t)}\right) \tag{2.12}$$

As for mutual information, a reliable estimation of this metric relies upon a large sample size [63, 83].

h^2 - Non Linear Correlation Coefficient

h^2 is a non-linear correlation coefficient that describes the dependency between two signals whatever the type of relationship existent between them [55].

If we have two signals, x and y, and the value of y is considered as a function of the value of x, then, the value of the first given the second may be described according to a regression curve [55] given by equation 2.13. The correlation ratio, eta^2, expresses the reduction of the variance of y by using the given curve to predict its values. h^2 is an estimate of eta^2 [63].

$$\mu_{y|x}(x) = \int_{-\infty}^{\infty} yp(y|x)dy \tag{2.13}$$

In practice, it is done a scatter plot of y versus x. x is subdivided into bins and it is computed an approximation of the regression curve connecting certain points - a point per bin whose coordinates correspond to y's average and the bin's midpoint - using a certain algorithm. h^2 is given by equation 2.14, where $f(x_i)$ is the linear piecewise approximation of the non-linear regression curve [63].

$$h^2_{y|x} = \frac{\sum_{k=1}^{N} y^2(k) - \sum_{k=1}^{N}(y(k) - f(x_i))^2}{\sum_{k=1}^{N} y^2(k)} \tag{2.14}$$

In opposition to the correlation function, the correlation ratio, h^2, may be asymmetric which translates to different relationships between x, y and y, x. Its asymmetry gives insights on the of relationship between the signals. If the relationship is linear, then h^2 approximates the squared cross-correlation function [63].

The evaluation of effective connectivity is usually model based and requires *a priori* set of regions and hypothesized set of connections. The most used methods are: Structural Equation Models, Dynamic Causal Modelling, and Granger Causality. The last one is a model free metric as well as transfer entropy, which is also used to assess effective connectivity and measures information flow [71, 83].

Several studies have shown that brain activity is time-varying during the time it is acquired [45], hence, there is an urge to develop new statistical methods for a time-varying analysis. These methods include the use of a sliding window, Psychophysiological Interactions, Dynamic Connectivity Regression, Dynamic Bayesian Variable Partition Model, and others [32].

2.2.2 Main Intrinsic Connectivity Networks

There are methods that lead to the detection of large-scale neural networks. The most commonly used are seed based or data driven approaches [19]. This last approach includes several multivariate decomposition methods, like Independent Component Analysis, Principal Component Analysis, and Singular-Value Decomposition [32].

An intrinsic connectivity network corresponds to a large-scale network observed at rest [10]. With most interest being given to Default Mode Network (DMN) [34], there is, however, different intrinsic networks that have been identified using rs-fMRI. For example, Yeo et al. used data from 1000 subjects and found seven main networks [77]. A brief description of some of the main intrinsic networks found in the literature is given bellow.

Sensorimotor network: is comprised by the primary motor cortex, primary sensory cortex, secondary sensory cortex, supplementary motor area, ventral premotor cortex, putamen, thalamus, and cerebellum [19].

Dorsal attentional network: is comprised by the intraparietal sulci, parts of the superior parietal lobes and the frontal eye field, and the temporal lobe MT complex. It is especially involved in attention reorientation during visual attentional functioning [19, 35] and, together with the ventral attentional network, it is a key component of the attention regulation systems.

Ventral attentional network: is comprised by the temporal-parietal junction, the frontal operculum, and the supramarginal gyrus [35, 64]. This network is involved in environment monitoring for salient stimuli [19].

Frontoparietal control network or executive control network: is comprised by the lateral frontal pole, Anterior Cingulate Cortex (ACC), Dorsolateral Prefrontal Cortex (dlPFC), anterior Prefrontal Cortex (PFC), lateral cerebellum, anterior insula, caudate, and inferior parietal lobe [19].

This network is involved on the coordination of cognitive control, which is the process of voluntary goal-driven behaviour that requires accurate and rapid adaptation to different sets, including emotional and social cues. There is evidence of the integration of the frontoparietal control network with other networks to whom it provides support for a flexible modulation [56].

Default network: is comprised by the anterior medial PFC, Posterior Cingulate Cortex (PCC), precuneus, and angular gyrus, and by other two subsystems: the dorsomedial prefrontal cortex subsystem and the medial temporal lobe subsystem. The dorsomedial prefrontal cortex subsystem includes: temporal pole, lateral temporal cortex, temporoparietal junction, and Dorsomedial Prefrontal Cortex (dmPFC). The medial temporal lobe subsystem includes: hippocampal formation, parahippocampal cortex, retrosplenial cortex, posterior inferior parietal lobe, and Ventromedial Prefrontal Cortex (vmPFC) [19].

This network is also known as task-negative network, because during most tasks it is deactivated [66]. This is true for tasks that demand external focus of attention. When attentional focus is internal, like during daydreaming or memory retrieval, this network is also found to be activated [52]. This network is negatively correlated with the attentional network [76].

Salience network: is mainly comprised by the anterior insula and the ACC. This network identifies salient stimuli and coordinates cognitive resources [61].

2.3 Assessing Brain Connections with Neuroimage

Currently, several neuroimaging techniques can be used to study human brain connections, namely: MRI, Positron Emission Tomography (PET), Magnetoencephalography (MEG), and EEG [28]. MRI is the most commonly used due to its availability, non-invasiveness, and high spatial resolution [24]. Furthermore, it can provide both structural and functional characterization, as Diffusion-Weighted MRI (dMRI) and fMRI allow to study structural and functional connectivity, respectively [8].

As it is the scope of this study, it is important to mention that when studying functional connectivity there are confounds that may contribute to the appearance of patterns that are not related to neural activity [12]. These patterns need to be identified and removed from the data prior to any further analysis and may be related, for example, to physiological fluctuations due to respiration or heart beating [82]. In addition, other preprocessing steps are essential, such as motion correction.

From the literature, two main steps involved in imaging brain connections can be identified [24, 25, 33], they are: region definition and connectivity measurement.

2.3.1 Region Definition

The first step to analyse brain connectivity is region definition or brain parcellation. At the end of this phase, one gets the regions from which connectivity will be measured, as in the second image from the flowchart in figure 2.3. However there is no obvious best method for boundary definition and inter-subject variability does not make the problem easier. Despite the efforts being put in the search for the optimal clustering technique, this remains unsettled.

In fact, several heuristic methods have been used in the past to achieve brain parcellation, each having its advantages and disadvantages. Anatomical templates - brain atlases such as Harvard Oxford or Automated Anatomical Labeling (AAL) -, cytoarchitecture information, random parcellation, blinded source-separation techniques or data-driven parcellation are just some of the methods that have already been used [24, 33]. The favourite method tends to be the data-driven parcellation [25], through which clusters determined by unsupervised learning applied to functional data are obtained.

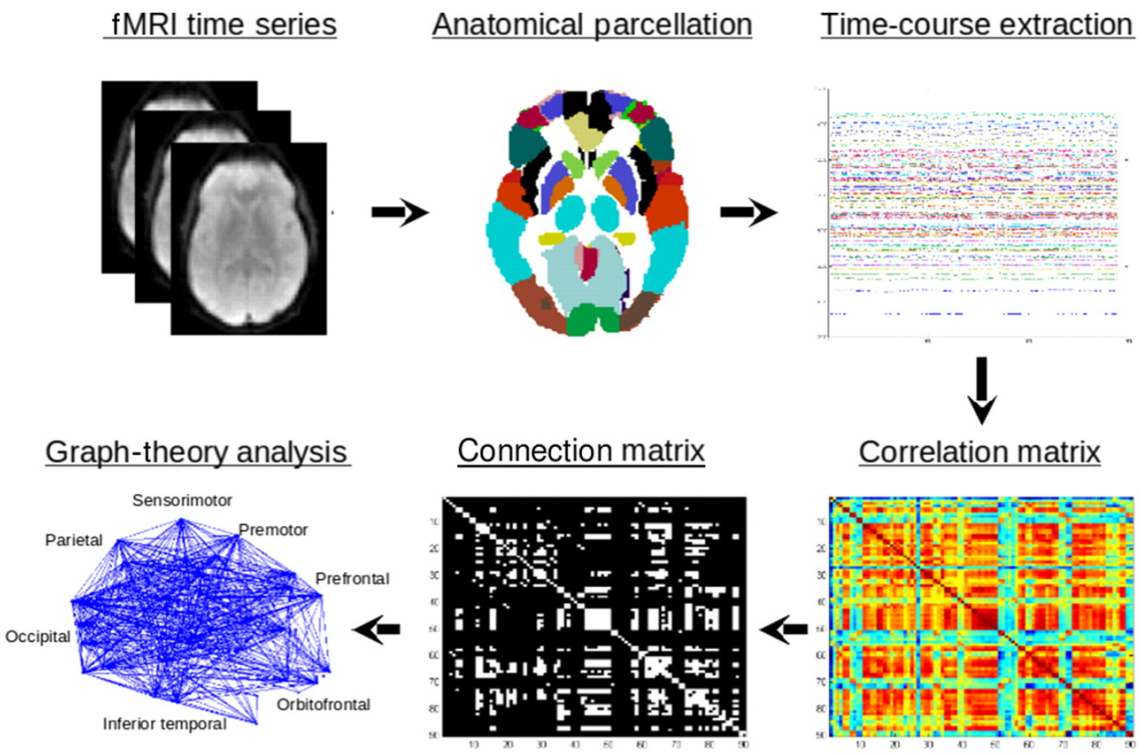

Figure 2.3: Flowchart with the fundamental steps involved in resting state connectivity analysis. From [37].

One must have in mind that this is a very important stage, as studies have shown that network analysis is influenced by parcellation [8, 10, 90].

As mentioned in the previous section, in subsection 2.2.1, individual voxels may be used as regions for connectivity analysis. This leads to a more complex statistical problem, hence, defining larger regions using one of the former techniques, significantly diminishes the computational costs, either related to running time or spatial constraints.

2.3.2 Connectivity Measurement

The second step corresponds to the assessment of connectivity between the regions previously defined. Here, the focus can be on each of the previously mentioned types of connectivity - structural or functional. At the end of this stage, each type of connectivity can be stored as a n x n connectivity matrix, n being the number of brain regions defined [8]. An example can be found on the forth image from the flowchart in figure 2.3. Connectivity studies may be done using these matrices or using graphs.

Graphs are representations of networks and are defined by a set of nodes with a set of ties between them, which are the edges. This corresponds to a set of brain regions with the corresponding connections. These graphs are defined using data from the matrices and may or not be weighted or directed as the matrices that were used to obtain them. Moreover, they can be represented by an adjacency matrix, as the one on the fifth image of figure 2.3, and analysed through graph theory methods.

CHAPTER 3

State-of-the-Art

In the present chapter, it will be done some notes regarding previous knowledge on the topics of this study. In particular, it will be mentioned some of the discovered neurological impairments occurring on subjects with ADHD, as this will be the disorder from the analysed case study. Moreover, results from studies regarding the effect of using different metrics on connectivity measures will be mentioned.

3.1 Attention-Deficit/Hyperactivity Disorder

ADHD is one of the most common neurodevelopmental disorders diagnosed during childhood and can persist through adulthood [19, 59]. Affecting around 5% of the children worldwide in 2007 [19], this disorder is diagnosed on the basis of subjective measures, that include clinical presentations and interviews [14, 27, 46].

It is characterized by age inappropriate behaviours of impulsivity, inattention and hyperactivity [16, 48, 91] and has effects either on social and academic realm. There are different ADHD subtypes, including hyperactivity-impulsivity (ADHD-H), persistent inattention (ADHD-I), and combined (ADHD-C) that is a combination of the former [23].

In the past years, many studies using different neuroimaging techniques as PET, Single-Photon Emission Computed Tomography (SPECT), and MRI were done hopping to contribute to a better understanding of the pathological mechanisms of ADHD and in the search for a better diagnosis and treatment. These studies have documented not only behaviour disturbances but also abnormalities on functional and structural connectivity and volumetric differences on several brain regions on subjects with ADHD [14, 15, 27].

At first, it was hypothesized that ADHD was caused by impairments in the prefrontal-striatal circuits and some authors even say that extreme focus on this model has held up the study of other regions that could also play important roles in ADHD [20]. However,

new discoveries, supported by new technological advances, have led to the emergence of other models, that have into account other regions of the brain like the occipital and temporal cortices [19]. Furthermore, there is a great number of studies that suggest that DMN impairment is a core player on ADHD pathophysiology.

Focusing on rs-fMRI studies, in the following paragraphs, a brief review on some of the findings from several studies on ADHD will be presented. In these studies, several different methods were used to assess population differences, including Regional Homogeneity (ReHo), Amplitude of Low-Frequency Fluctuation (ALFF), and pairwise functional connectivity measures. Most of these last studies used Pearson's correlation coefficient to characterize the connectivity strength between different brain areas.

3.1.1 Altered ReHo and ALFF measurements on ADHD subjects

ReHo measures how similar a time-series of a given voxel is from those of its closest neighbours and reflects the temporal synchrony of the BOLD signal.

Altered ReHo in ADHD subjects was registered in, at least, two rs-fMRI studies. Areas that showed decreased ReHo were: bilateral frontal pole, dlPFC [3], and fronto-striatal-cerebellar circuits [15]. Occipital, bilateral sensorimotor, and parieto-visual cortices, however, showed increased ReHo [3, 15].

Table 3.1: Regions with altered ReHo measurements on ADHD subjects.

	Brain Regions	**Study**
Decreased ReHo	- bilateral frontal pole	[3]
	- bilateral dlPFC	[3]
	- fronto-striatal-cerebellar circuits	[15]
Increased ReHo	- occipital cortex	[15]
	- bilateral sensorimotor cortex	[3]
	- bilateral parieto-visual cortex	[3]

When it comes to ALFF, in 2007, Zang et al. reported decreased ALFF in bilateral cerebellum and vermis, along with increased ALFF in the right ACC and bilateral brainstem [91]. Yang et al., however, found decreased ALFF in the in bilateral anterior and middle cingulate cortex [89].

Several differences in ALFF were reported on different regions comprising the frontal lobe. For example, decreased ALFF was reported in the inferior frontal cortex [86, 91] and in the right frontal gyrus [89].

Wang et al. also reported increased ALFF in several regions, including: bilateral middle frontal gyrus, left superior frontal gyrus, right rectus gyrus, left insula, and right inferior temporal gyrus [86]. Increased ALFF on the left superior frontal gyrus was also reported

by Yang et al. on another study [89]. Another region having reports of increased ALFF was the sensorimotor cortex [89, 91].

Table 3.2: Regions with altered ALFF measurements on ADHD subjects.

	Brain Regions	**Study**
Decreased ALFF	- bilateral cerebellum and vermis	[91]
	- bilateral anterior and middle cingulate cortex	[89]
	- inferior frontal cortex	[86, 91]
	- right frontal gyrus	[89]
Increased ALFF	- right ACC	[91]
	- bilateral brainstem	[91]
	- bilateral middle frontal gyrus	[91]
	- left superior frontal gyrus	[86, 89]
	- right rectus gyrus	[86]
	- left insula	[86]
	- right inferior temporal gyrus	[86]
	- sensorimotor cortex	[89, 91]

3.1.2 Altered connectivity measurements on ADHD subjects

Several studies have found abnormal connectivity patterns on subjects with ADHD when comparing to patterns from control subjects.

Increased connectivity was found between the Dorsal Anterior Cingulate Cortex (dACC) and several regions, including: bilateral thalamus, bilateral cerebellum, bilateral insula, and bilateral brainstem [78].

Sun et al. also found abnormal patterns involving the dACC, having reported a significant negative functional connectivity between the middle temporal gyrus and the dACC on subjects with ADHD while controls showed no significant functional connectivity between these areas. They also reported decreased inverse connectivity between the dACC and both the dmPFC and the PCC [76].

Within the basal ganglia it was also found impaired connectivity on ADHD subjects. Cao et al. studied the connections between brain areas using the putamen as a seed and found abnormal connectivity between this area and several others. More specifically, they reported increased connectivity between the left putamen and the right globus pallidus/thalamus. In addition, they found decreased negative connectivity between the left putamen and: the right declive and the right superior and middle temporal gyrus. They also reported decreased connectivity between the same region and: the right subcallosal gyrys/nucleus accumbens and right superior frontal gyrus. Decreased negative connectivity was also observed between the right putamen and both the right precuneus and left

decline [16]. Altered connectivity between the thalamus and basal ganglia was reported by Mills et al. [58].

Cocchi et al. reported other connections with increased connectivity, such as the connection between the left Orbitofrontal Cortex (OFC) and both the right lingual gyrus and the left superior frontal cortex and between the left amygdala and the right precentral gyrus. In the same study, they reported decreased connectivity between the OFC and the amygdala and temporal cortices [22].

There were other regions between which it was reported impaired functional connectivity, for example, Hoekzema et al. found increased connectivity between de left dlPFC and other regions, that included areas from sensorimotor network and DMN, including the precuneus and the PCC [43].

Posner et al. studied connectivity patterns involving dlPFC and Ventral Striatum (VS) and found altered connectivity. When it comes to the left dlPFC, they found decreased values with: left anterior operculum, left supplementary motor area, left dorsal caudate, left precentral gyrus, right dACC, and left supramarginal gyrus; and increased values with the middle occipital gyrus bilaterally and the left middle frontal gyrus. On the other hand, the right dlPFC showed decreased values with the left anterior operculum, left inferior frontal gyrus, and right dorsal caudate. Regarding the VS, decreased values for the left VS were reported with the left OFC and right hippocampus; and, for the the right VS, with the right anterior prefrontal cortex [64].

Tomasi et al., using short and long-range functional connectivity density, found impairments within reward-motivation regions and decreased functional connectivity between DMN regions and dorsal attentional networks. The superior parietal cortex, which is a region from the dorsal attentional network involved in attention processing, the precuneus, which is a region from the DMN, and the cerebellum had lower connectivity density; the VS, the OFC, and caudate, which are regions involved in reward and motivation, had higher connectivity density for ADHD. In particular, they reported: higher connectivity between the OFC and both the VS and ACC and lower connectivity between the OFC and the superior parietal cortex and between the VS and the precuneus, temporal pole, and parahippocampal gyrus [79].

Default Mode Network in ADHD

Dysfunctions involving the DMN are thought to be the cause of attentional problems in patients with ADHD [59, 81], in particular, due to its impaired suppression [79].

Concerning this network, Fair et al. found patterns suggestive of delayed neuromaturation [30] and in another study it was reported association between PCC and dACC connectivity and age for controls, which did not happened for ADHD subjects [76].

In addition, decreased functional connectivity was reported between vmPFC and PCC [20, 30], which are both components of the DMN.

Not only disturbances within the DMN were reported but also between this and other networks.

As mentioned above, Cao et al. observed decreased inverse functional connectivity between the right putamen and the right precuneus (component of DMN) [16], Sun et al. found decreased inverse functional connectivity between the DMN and the cognitive control network [76] and Tomasi et al. observed decreased functional connectivity between region from the DMN and dorsal attentional networks [79].

Castellanos et al. also reported abnormalities involving the DMN, in particular, they reported less negatively correlated activity between dACC and PCC/precuneus [20].

Sato et al. computed an abnormality index through unsupervised machine learning and, using this index, discovered an higher abnormality index for dACC and PCC connection in subjects with ADHD [70].

Furthermore, a less negative correlation for ADHD subjects between dlPFC and components from the DMN was also reported [43]. In the same study, it was found enhanced between network coherence and reduced within network coherence.

It must be noted that there are some inconsistencies across different studies, that some authors hypothesized as being caused by different methodological conditions, for example, different sample sizes, different disease subtypes sample representation, exclusion or not of subjects using or that used medication in the past, or even different age ranges [15, 26, 91].

3.2 Comparison Between Different Measures of Connectivity

Several studies have highlighted the importance of feature selection and dimensionality reduction in the classifier performance. However, data comparing the effect of different types of brain connectivity metrics in the classifier performance is scarce.

Smith et al. [72] simulated fMRI data to evaluate different functional connectivity metrics. The focus was rs-fMRI. Authors tested: correlation and partial correlation, regularized inverse covariance, mutual information, Granger causality and related lag-based measures, coherence, Bayes net methods, among others. They showed that inappropriate functional ROIs is bad for the estimation and noted that the sensitivity to detect a connection depends on the length of the fMRI session. In terms of detecting connection existence, the best ranked methods achieved at least 90% sensitivity (Partial correlation, Bayes net methods, and inverse covariance). On the other hand, detecting directionality, the best performance method (Patel's conditional dependence measure of connection directionality) had 70% of accuracy. Methods based on high-order statistics performed worse than the others.

Wang et al. [84] benchmarked 42 connectivity metrics using simulated datasets that where obtained using 5 different generative models. First, they performed an optimization of the parameters of each method and then applied those methods to different models.

Table 3.3: Pairs of regions with altered connectivity measurements on ADHD subjects.

	Pair of Brain Regions	**Study**
Decreased FC	- left putamen: right declive, right superior and middle temporal gyrus, right subcallosal gyrus/nucleus accumbens, and right superior frontal gyrus	[16]
	- right putamen: right precuneus, left declive	[16]
	- dACC: PCC and precuneus	[20]
	- dACC: dmPFC and PCC	[76]
	- vmPFC: PCC	[20, 30]
	- left dlPFC: left anterior operculum, left supplementary motor area, left dorsal caudate, left precentral gyrus, right dACC, and left supramarginal gyrus	[64]
	- right dlPFC: left anterior operculum, left inferior frontal gyrus, and right dorsal caudate	[64]
	- left VS: left OFC and right hippocampus	[64]
	- right VS: right anterior PFC	[64]
	- VS: precuneus, temporal pole, and parahippocampal gyrus	[79]
	- OFC: amygdala and temporal cortices	[22]
	- OFC: superior parietal cortex	[79]
	- left dlPFC: areas from DMN (precuneus, PCC)	[43]
Increased FC	- dACC: bilateral thalamus, bilateral cerebellum, bilateral insula, and bilateral brainstem	[78]
	- left putamen: right globus pallidus/thalamus	[16]
	- left dlPFC: middle occipital gyrus bilaterally, left middle frontal gyrus	[64]
	- left dlPFC: areas from sensorimotor network	[43]
	- left OFC cortex: right lingual gyrus and left superior frontal cortex	[22]
	- OFC: VS and ACC	[79]
	- left amygdala: right precentral gyrus	[22]

They studied, for example, which methods led to a correct connectivity inference and under which circumstances. Furthermore, they analysed performance with different signal-to-noise ratio and network configurations. They achieved better method performance than the previous study and proposed that this could be due to parameters optimization which was not done by in the former study. Authors stated that no single optimal method exists for all type of data.

A systematic analysis of functional connectivity metric reliability (capacity to obtain the same results for the same subject in different sessions) was carried by Fiecas et al. [31] in a study that comprised metrics such as cross-correlation, cross-coherence, and pairwise bivariate autoregressive model-based metrics. Stability was quantified using random-effects ANOVA model and cross-correlation was the best ranked metric.

CHAPTER 4

Materials and Methods

In this chapter, it will be presented a detailed description of the methodological framework used to obtain the results from this study, going from matrix construction, using different connectivity metrics, to statistical analysis.

We will start with a detailed description of the dataset that was used and then it will be given a brief outline of the used software and the methodology followed for data analysis. In particular, a general overview of the software, with special regard to the features used during this study, will be given along with a description of the followed steps.

Two different approaches were carried out. The first was to perform pairwise functional connectivity metric comparison. The second consisted on control versus patient functional connectivity comparison. These will from now on be referred as approach A and B:

- A. Pairwise Functional Connectivity Metric Comparison
- B. Control versus Patient Comparison

For both approaches, the first step was to construct several functional connectivity matrices using the time-series from each subject comprised on the dataset. For the same subject it was used several connectivity metrics. Following matrices construction, procedures were different for each approach and this will be explained later in detail. For approach B, matrices were directly used for statistical analysis, however, for approach A, normalization had to be done prior to statistical analysis.

Functional connectivity matrices were computed using MULAN toolbox and statistical analysis using GraphVar toolbox. Both toolboxes are freely available online.

4.1 Participants

4.1.1 ACPI Dataset

To perform the intended analysis, it was used rs-fMRI data from a dataset of 1000 Functional Connectomes Project, more specifically from the ACPI [2].

ACPI is an initiative which primary goal is to ease image processing and analysis of datasets generated by investigators from the National Institute on Drug Abuse. Both raw and preprocessed data are available to download at the homepage along with phenotypic information about data samples which were collected on 6 different sites, including university medical centres and hospitals. Preprocessing on the raw rs-fMRI data was done using Configurable Pipeline for the Analysis of Connectomes which is an open-source software pipeline that allows for automated preprocessing and analysis of rs-fMRI data.

There are 8 different preprocessing pipelines available to download. Each of these follow the same basic strategies: anatomical registration, tissue segmentation, functional registration, functional masking, nuisance correction, temporal filtering, motion correction, and spatial smoothing. The differences are related with specific preprocessing steps. For instance, regarding registration, there are two options: Advanced Normalization Tools (ANTs) or FMRIB's Non-linear Image Registration Tool. Other options are related with additional corrections, which are additional motion correction (scrubbing vs no scrubbing) and additional nuisance signal correction (global signal regression vs no global signal regression). Furthermore, the following parcellations are available among the preprocessed datasets: AAL, Craddock 200, Harvard-Oxford, and random parcels. A more detailed description of the preprocessing strategy is available at the previously mentioned homepage, as well as information about scan parameters [1].

Among ACPI there are different datasets with data coming from different investigations. For the present study it was used ACPI Multimodal Treatment of Attention Deficit Hyperactivity Disorder (MTA) dataset as it had more data samples available and allowed for control versus patient functional connectivity comparison opposed to the other available datasets which focused on drug addiction, having no specific disease under analysis. Furthermore, as it had been used on previous studies aiming classification it could allow for interesting confrontation with the outcomes from this study.

Data from MTA comes from a multisite study that intended to evaluate treatments for ADHD and includes samples from subjects with ADHD and control subjects, adding up to a total of 129 subjects, 104 males and 25 females with ages between 21 and 27 years. Moreover, this dataset comprises four different sample groups with 42 ADHD substance users, 46 ADHD non-substance users, 20 control substance users, and 21 control non-substance users.

More specifically, it was downloaded MTA 1 dataset with ANTs registered and chosen no scrubbing since it leads to less time points which is a critical quality for the intended analysis as it will be explained later. No global signal regression was also chosen as there is

controversial opinion upon its use [60]. All the samples were acquired at a 0.50 Hz sample frequency and have durations ranging from 4 to 6 minutes. Temporal filtering that had been applied consisted on a band pass filtering of 0.01 to 0.1 Hz.

In what concerns parcellation, it was chosen the AAL atlas following the standard procedure of the research institute where this study took place. A list with all the regions and the corresponding number in the atlas can be found in table 4.1. When two numbers are presented, the odd number corresponds to the left sided region and the even number to the right sided region.

Table 4.1: List of the 116 brain regions that are comprised in the AAL atlas.

Brain Area	**AAL Region Designation**	**AAL Region No.**
Frontal Lobe	Precentral gyrus	1, 2
	Superior frontal gyrus, dorsolateral	3, 4
	Superior frontal gyrus, orbital part	5, 6
	Middle frontal gyrus	7, 8
	Middle frontal gyrus, orbital part	9, 10
	Inferior frontal gyrus, opercular part	11, 12
	Inferior frontal gyrus, triangular part	13, 14
	Inferior frontal gyrus, orbital part	15, 16
	Rolandic operculum	17, 18
	Supplementary motor area	19, 20
	Olfactory cortex	21, 22
	Superior frontal gyrus, medial	23, 24
	Superior frontal gyrus, medial orbital	25, 26
	Gyrus rectus	27, 28
	Paracentral lobule	69, 70
Insula and Cingulate	Insula	29, 30
	Anterior cingulate and paracingulate gyri	31, 32
	Median cingulate and paracingulate gyri	33, 34
	Posterior cingulate gyrus	35, 36
Temporal Lobe	Hippocampus	37, 38
	Parahippocampal gyrus	39, 40
	Amygdala	41, 42
	Fusiform gyrus	55, 56
	Heschl gyrus	79, 80
	Superior temporal gyrus	81, 82
	Temporal pole: superior temporal gyrus	83, 84
	Middle temporal gyrus	85, 86

Continued on next page

Table 4.1: Continued from previous page

	Temporal pole: middle temporal gyrus	87, 88
	Inferior temporal gyrus	89, 90
Central Structures	Caudate nucleus	71, 72
	Lenticular nucleus, putamen	73, 74
	Lenticular nucleus, pallidum	75, 76
	Thalamus	77, 78
Occipital Lobe	Calcarine fissure and surrounding cortex	43, 44
	Cuneus	45, 46
	Lingual gyrus	47, 48
	Superior occipital gyrus	49, 50
	Middle occipital gyrus	51, 52
	Inferior occipital gyrus	53, 54
Parietal Lobe	Postcentral gyrus	57, 58
	Superior parietal gyrus	59, 60
	Inferior parietal, but supramarginal and angular gyri	61, 62
	Supramarginal gyrus	63, 64
	Angular gyrus	65, 66
	Precuneus	67, 68
Cerebellum and Vermis	Cerebelum Crus 1	91, 92
	Cerebelum Crus 2	93, 94
	Cerebelum 3	95, 96
	Cerebelum 4, 5	97, 98
	Cerebelum 6	99, 100
	Cerebelum 7b	101, 102
	Cerebelum 8	103, 104
	Cerebelum 9	105, 106
	Cerebelum 10	107, 108
	Vermis 1, 2	109
	Vermis 3	110
	Vermis 4, 5	111
	Vermis 6	112
	Vermis 7	113
	Vermis 8	114
	Vermis 9	115
	Vermis 10	116

4.2 Quantifying Functional Connectivity

MULAN is an open source toolbox that runs on MATLAB which was developed by Wang et al. and allows for functional connectivity matrices construction using different metrics [84].

Seven different families of metrics are available on MULAN toolbox, they are: correlation (time basic), coherence (frequency basic), Granger causality, transfer entropy, mutual information, h^2, and $\overline{\mathcal{A}}\mathcal{H}$. All these families comprise a total of 42 different metrics of functional connectivity. Detailed mathematical description of each metric can be found in the supplemental material from the study of Wang et al. [84].

To obtain connectivity matrices for every metric of a given family it has to be provided a .mat file and several parameters. The .mat file must have information regarding one single subject, which includes the time-series from each ROI and the sample frequency. Required parameters depend on the selected metric's family and include: size of the sliding window size, window overlap, minimal and maximal frequency for frequency domain metrics, maximum lags for model-free metrics, and model order for model-based metrics. The choice of these parameters is a critical step as it is known to conduct to different results.

After providing the required input (resting state data, metric's family and corresponding parameters) and pressing the Calculation button, for a given data sample and for each metric, each pairwise ROI time-series is analysed. This analysis is performed by window and the number of windows (N) depends upon the chosen size of the sliding window. At the end of the analysis, N connectivity matrices are obtained for each subject and for each metric.

To visualize the results regarding one single metric it must be pressed the button Demonstration that makes appear on the screen the matrix and corresponding network for the selected sliding window (obtained after selection of the intended threshold). Navigation between sliding windows is allowed and it is done by using control buttons from the Window Control panel. It is available the option to visualize the average of the N windows by pressing the Average button and also the option to see at the same time the connectivity strengths for each pair of time-series for the N windows and its average using the Analysis button.

Only five families were used in this study due to the computational cost that the other two implied. The families that were used are: frequency basic, h^2, mutual information, time basic, and transfer entropy. A list of the used metrics belonging to the mentioned families can be found in table 4.2. The chosen parameters for matrix construction were different for each approach and were chosen based on the optimization made by Wang et al. [84] with some adjustments that had to be done according to the features of the dataset.

Table 4.2: List of metrics used throughout the present study and respective notation. B- bivariate, P- partial; F- Fourier, W- wavelet; D- directed, U- undirected.

Family	**Metrics**
Frequency Basic	BCohF, BCohW
Hsquare	BH2D, BH2U, PH2D, PH2U
Mutual Information	BMITU, PMITU, BMITD1, PMITD1
Time Basic	BCorrU, BCorrD, PCorrU, PCorrD
Transfer Entropy	BTEU, BTED, PTEU, PTED

4.2.1 Connectivity Matrices Computation

A. Pairwise Functional Connectivity Metric Comparison

In this case, only control subjects were selected, maintaining a proportional ratio between the sample groups. Exams with less than 6 minutes were excluded, as it is recommended the use of longer time-series to obtain more reliable values of connectivity strengths when computing the matrices [84]. After selection, a total of 24 subjects remained left.

For this approach, a trade-off between window size and number of windows had to be done, as more than one window was necessary for the normalization process that was going to be done later. At first it was used 3 windows with the duration of 180 seconds each. However, it was decided to use 6 windows which had the duration of 100 seconds each, as the maximum number of windows would be the ideal situation and, at the same time, a certain minimum number of time points (which depends upon the metric) was an important requirement recommended by Wang et al. [84].

For the frequency band it was taken into account the filtering that was previously done and was selected the minimal and maximal frequency of 0.01 and 0.1 Hz. The maximum lag and window overlap was selected according to the optimization mentioned before.

A total of $17 \times 6 = 108$ matrices were obtained per subject (6 per metric). For each subject there were: 5 matrices from Frequency Basic (3 from BCohF and 2 from BCohW - corresponding to different frequencies), 4 matrices from Time Basic family, 4 matrices from Hsquare family, and 4 matrices from Mutual Information family. Matrices belonging to transfer entropy family are not considered here, as they had to be excluded, because their computation, in spite of the efforts, led to undefined strength weights indicated as NaN in MATLAB. The first frequency for BCohW was also not considered, because it also led to undefined weights, which could not be explained.

For each metric, the averaged connectivity matrix was computed as, according to the literature, the average corresponds to more stable value of connectivity strength. At the end, a total of 17 usable matrices per subject were obtained. Although, not all of them

were used for statistical analysis due to the great number of possible pairwise combinations ${}^{17}C_6 2 = 136$ which would imply an extensive analysis difficult to conduct during the available time. It was decided that only bivariate metrics would be considered for the next step and that metrics from the same family would not be compared with each other.

B. Control versus Patient Comparison

For this approach, a total of 80 subjects were selected, once again, maintaining a proportional ratio between sample groups: 40 control subjects (18 Grupo A e 22 do grupo B) and 40 ADHD patients (20 Grupo C e 20 Grupo D).

It was decided that only one sliding window would be used, having the size of the whole time-series, which varied between 4 and 6 minutes as no exclusion criteria was followed regarding the duration of the exams. This is not ideal, however, as mentioned on the previous section, it was important to have a minimum number of time points and, for some of the metrics, this corresponded to the use of the whole time-series. Furthermore, no normalization procedure would have to be done after matrix computation, which implies no need for more than one sliding window. In addition, using the whole time-series has the advantage of being less time consumption. Both the frequency band and the maximum lag selected was the same as in approach A for the same reasons.

It was obtained a total of 22 matrices per subject, that is, a total of 1760 matrices, each one having 116×116 weights. All these matrices were considered for statistical analysis.

Table 4.3: Parameters used for matrices computation for both approach A and B.

	Pairwise metric comparison	**Group Comparison**
Minimal frequency	0.010 Hz	
Maximal frequency	0.100 Hz	
Step frequency	0.033 Hz	
Model Order	5	
Max Delay	12	
Sample frequency	0.500 Hz	
Size of windows	100 seconds	Whole time-series
Number of windows	6 windows	1 window
Length of signals	6 minutes	4-6 minutes
Overlap	0.5	Not applicable

4.2.2 Connectivity Matrices Normalization

Aiming the comparison between different functional connectivity metrics, arises the problem that different metrics have different ranges of connectivity strengths. Therefore, to have comparable matrices, it was identified the need of some sort of normalization.

Different possibilities for normalization were studied, like using normalized versions of each metric, however, these were not found among the literature for all the metrics. The chosen procedure seemed to be the most appropriate and was based on one that was done by Wang et al. [85] which consists on a normalization based upon the probability distribution function of the connectivity strengths.

For each metric the non-normalized connectivity matrix corresponds to the average matrix of N sliding windows, which in this case corresponds to 6 windows. The procedure resides in obtaining a distribution function by bootstrapping on the total number of sliding windows (N) a certain number of times (Y). In each iteration, N sliding windows matrices are randomly selected with reposition from the initial N windows and the average matrix of the selected windows is then computed. At the end of the bootstrapping, we obtain Y averaged matrices that are used to build a histogram of all the connectivity strengths comprised on every matrix. Then, the cumulative distribution function is computed and used for normalization. In figure 4.1 a scheme of the process described here can be found. After this procedure, all the values of connectivity strengths range between 0 and 1.

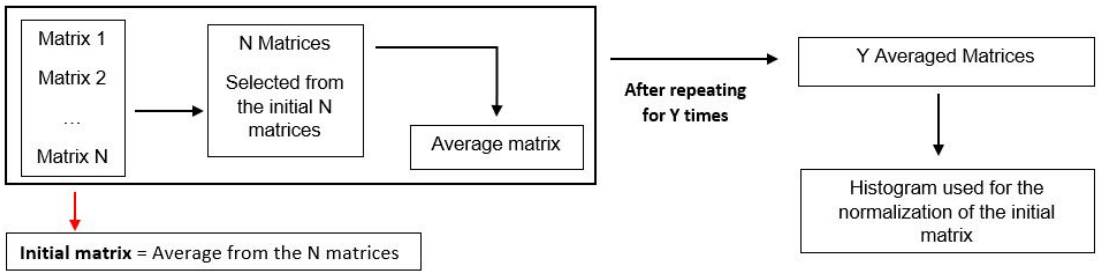

Figure 4.1: Scheme from the bootstrapping process followed to obtain the histogram used for matrix normalization.

For this study the probability distribution function was obtained by doing 500 times bootstrapping on 6 matrices. At the end, 17 normalized matrices per subject were obtained, that is 408 normalized matrices. Each matrix with 116×116 connectivity weights.

4.3 Statistical Analysis

To conduct statistical analysis, it was used the latest version of a toolbox named GraphVar (version 2.01b) which also runs on MATLAB [11, 49]. This toolbox provides a user-friendly GUI-based framework for brain connectivity analysis and results from the combination of several features from existent toolboxes, such as Brain Connectivity Toolbox, Graph Analysis Toolbox, and Network Based Toolbox.

GraphVar allows for brain network construction and characterization, statistical analysis, and interactive exploration of results. As input it takes a .mat file containing brain connectivity matrices or ROI time-series and a spreadsheet with the parcellation scheme. The schematic representation of GraphVar's workflow can be found in figure 4.2.

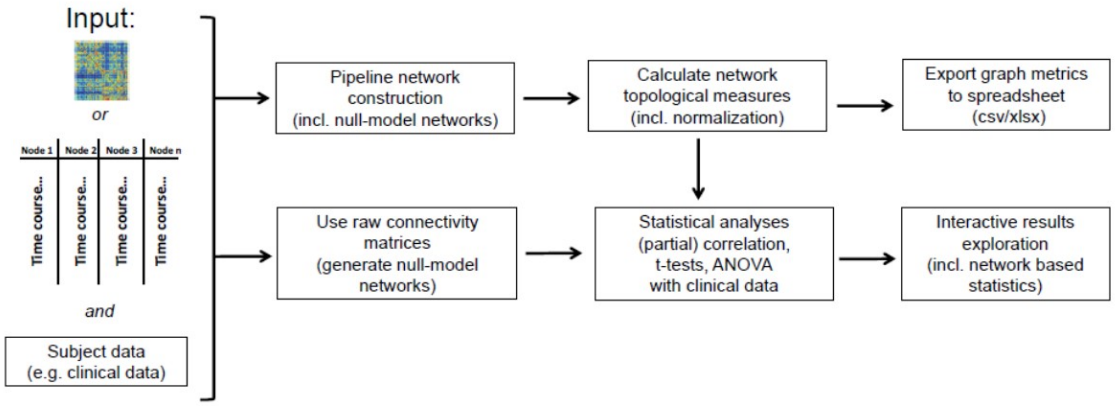

Figure 4.2: Schematic workflow of GraphVar toolbox. From [49].

If time-series are provided they will be used for the computation of connectivity matrices and the user can choose from the following available metrics: Pearson correlation, partial correlation, Spearman correlation, percentage bend correlation, and mutual information.

For graph network construction, different options are available concerning what kind of threshold is to be used or if any change in weights is supposed to be done. It is possible to choose to compute different graph topological measures from graph theory. As these features were not used, no further detail will be given.

An additional spreadsheet with information about any variable of interest, such as subject ID, clinical and demographic information must be provided when the purpose is to do statistical analysis. Statistical tests may be done on graph metrics or on the raw matrix data. Either way GraphVar runs a General Linear Model (GLM) and calculates F-tests which is equivalent to running t-tests, regressions, and Analysis of Covariance (ANCOVA). Parametric or non-parametric testing may be chosen. In parametric testing, data is assumed to be normally distributed. Non-parametric testing, on the other hand, allows for testing when nothing is known concerning data distribution.

As statistical tests may be done both on graph metrics or raw matrix data, the dependent variable may be a specific graph measure or the connectivity strength between pairwise regions and corresponds to the outcome whose variation is being studied. To perform the analysis, the user must select the variables of interest in terms of GLM. This includes: between covariates, between factors, within covariates, and nuisance covariates. A brief description of each of these terms, in accordance with GraphVar's user manual, is found below.

Between covariates are continuous variables that lead to the estimate of regression coefficients with regard to the dependent variables. They are regressed out prior to analysis to eliminate collinearity with the intercept term which is the predicted value of the dependent variable when all the independent variables are zero.

Between factors are categorical variables which should be selected when the goal is to

estimate the effects of categorical variables, individual group means, and pairwise differences between groups.

Within covariates are variables which should be selected when the estimation of regression coefficients is to be done having into consideration repeated measures with two time points. These variables, as between covariates, are regressed out prior to analysis to eliminate collinearity with the intercept term.

Nuisance covariates are variables that are to be regressed out from the dependent variables prior to analysis.

Within ID, is an option that is also available and allows to select repeated measures. It is also possible to choose interactions between categorical, continuous, and categorical-continuous variables.

Two types of non-parametric tests are available on GraphVar: testing against null model networks or non-parametric permutation testing. Either way data is permuted a certain number of times, specified by the user, to find the distribution of the test statistic. This is then used to assess significance: if the test statistic falls outside the distribution at a specified alpha level the result is assumed significant.

Detailed information about these and other features are available on GraphVar's user manual.

4.3.1 Group Comparisons

For approach A, non-parametric testing on raw matrix with no change in weights was performed. Thus, it was selected the option "raw Matrix"in the Raw Matrix panel with "no change"in weights. Furthermore, it was deselected all the options from Network Calculation panel. In the GLM panel, regarding the field of between factors, it was selected a given variable, depending on the approach. For both approaches permutation was chosen. In all cases, the statistical analysis was performed for all pairwise 116 AAL brain regions.

A. Pairwise Functional Connectivity Metric Comparison

After excluding several metrics for the reasons presented on the subsection 4.2.1, 24 different comparisons were done. To assess significance 2000 permutations were computed. The null hypothesis being tested is that the group mean for different metrics is equal.

B. Control versus Patient Comparison

For each metric it was done one single comparison, considering the group variable (ADHD vs Control) as a between factor. A total of 22 comparisons were done. To assess significance 1000 permutations were computed. The null hypothesis being tested is that the ADHD and control group means are equal.

CHAPTER 5

Results and Discussion

In the following chapter, results that were obtained from the statistical analysis performed using GraphVar toolbox will be presented and, in the meantime, a qualitative analysis and a brief discussion of these results at the light of the current literature and previous work will be done. A brief description about GraphVar's interactive results viewer will be first given.

5.1 Results Viewer Interface

GraphVar has an interactive user-friendly results viewer interface that is divided into three panels: results selection box panel, general functions panel, and the results display panel.

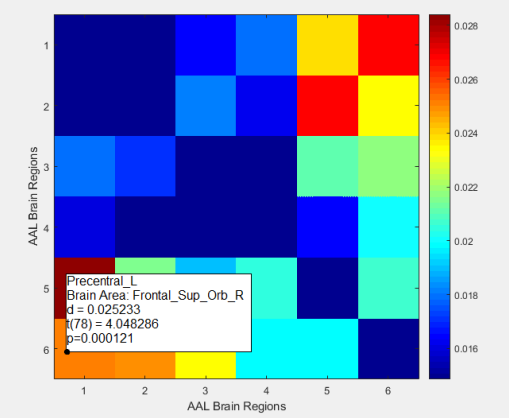

Figure 5.1: Example of a matrix displayed on the results display panel.

In the selection box, one may select the variables and the intended threshold according to which the results will be shown. Another selection that can be done in this panel regards the brain regions to be shown, as the user may select only a subsection of the previously selected brain regions that underwent statistical analysis.

The outcome from the statistical analysis is shown in the results display panel and its graphical representation depends upon the type of data being analysed. In the current case, as we performed a raw connectivity matrix analysis, what is obtained is a matrix whose rows and columns corresponds to the selected brain regions.

When passing over a certain matrix element, that corresponds to a certain pair of brain regions, a box with the statistical information is displayed, providing the mean group difference, the t-value, and the p-value. The mean group difference corresponds to the colour of the given matrix element which is in accordance with the colour scale provided on the right (figure 5.1).

In the general functions panel, the user may choose an alpha level and choose to hide non-significant mean group differences. Also within this panel, there is the option to apply either Bonferroni or False Discovery Rate correction. If any correction method is selected, a new alpha level is shown in accordance to this selection, corresponding to the corrected alpha level. There is also the option to show results according to p-values from the non-parametric testing by selecting the option Random Networks Groups.

Other settings are also available, including: the option to export or save the data, to show p-values instead of mean group differences in the colour scale, and to see significant subnetworks that can be found within the data.

In the following sections will be presented several matrices whose axis corresponds to AAL regions and the colour from each matrix element expresses the mean group difference. When existent, significant subnetworks obtained will also be presented. These networks were visualized using BrainNet Viewer [88] or GraphVar.

5.2 Pairwise Functional Connectivity Metric Comparison

To assess significance, 2000 permutations were computed and an alpha level of 0.01 was selected. It was selected Random Networks Groups so that non-parametric p-values would be considered. Only significant differences according to the applied significance level will be described.

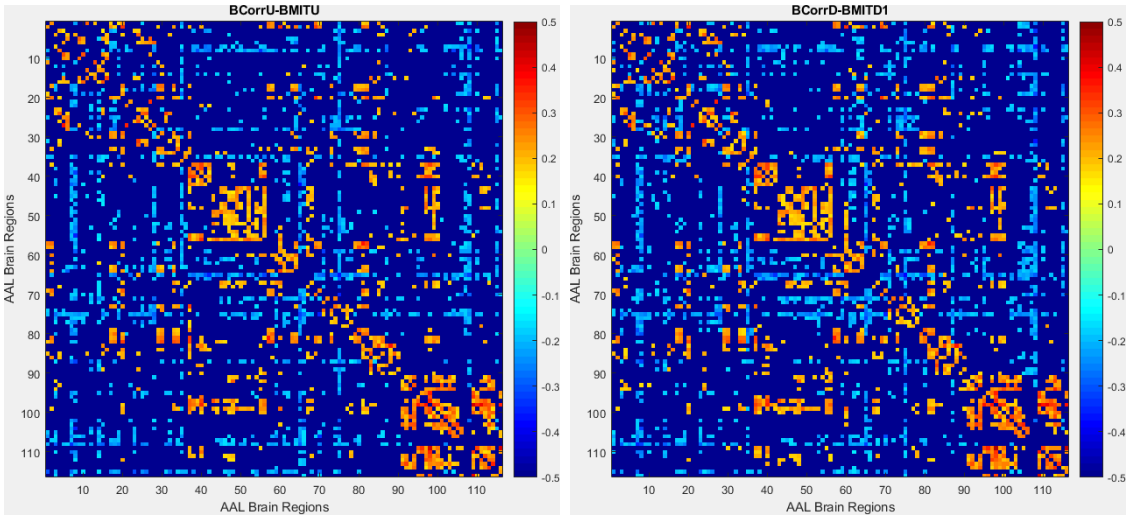

(a) BCorrU-BMITU (b) BCorrD-BMITD1

Figure 5.2: Results from pairwise functional connectivity metric comparison - matrices from BCorrU-BMITU and BCorrD-BMITD1.

Some comparisons will not be presented here and were excluded from further analysis. In particular, comparisons involving Hsquare family because normalized matrices from this family were almost homogeneous with values close to 1. Hence, its comparisons were difficult to interpret as Hsquare matrices had consistently bigger values. In addition, it was chose not to present comparisons between directed and undirected metrics. Therefore, a total of 11 comparisons were studied and will be next described.

5.2.1 BCorrU-BMITU

Figure 5.2a shows the results from metric comparison between BCorrU and BMITU.

It is noticeable that there are several pairs of brain regions showing significant positive mean group differences. These pairs correspond to connections where connectivity is bigger for the BCorrU metric. In particular, regions adjacent to the diagonal were registered to have mostly positive mean group differences. Connections between areas from both the cerebellum and vermis (except for cerebellum 10 and 9, and vermis 9) and areas from the temporal and occipital lobes also had mainly positive mean group differences.

When it comes to stronger connectivity for measurements from BMITU, almost every connection with the following regions may be mentioned: vermis 9, left posterior cingulate gyrus, left angular gyrus, right gyrus rectus, cerebellum 8, 9 and 10, bilateral middle frontal gyrus, and left pallidum. Furthermore, connections between the frontal and occipital lobes and between the frontal lobe and cerebellum and vermis were also mostly negative.

One significant network with more than 100 nodes was obtained for this comparison. It is not depicted here due to the large number of nodes which makes it illegible.

5.2.2 BCorrD-BMITD1

The comparison between the directed versions from the previously analysed metrics led to a similar matrix, that was almost symmetric and can be found in figure 5.2b.

Regions adjacent to the diagonal were, once again, registered to have mostly positive mean group differences. Other regions that had many connections with significant positive mean group differences, included: bilateral cerebellum 4, 5 and 6, bilateral median cingulate and paracingulate gyri, and right supplementary motor area.

On the other side, bigger values for BMITD1 were found for almost every connection with: cerebellum 9 and 10, and vermis 9. In particular, connections between the cerebellum and: frontal lobe, insula, and cingulate and paracingulate gyri mostly corresponded to negative mean group differences. Connections between the frontal and occipital lobes also had significant negative mean group differences.

The following regions may be highlighted for having lots of significant negative mean group differences: left angular gyrus, bilateral middle temporal gyrus (temporal pole), left pallidum, bilateral posterior cingulate gyrus, and bilateral middle frontal gyrus.

As in the last comparison, one significant network with more than 100 nodes was obtained and is, for the same reason, not shown here.

5.2.3 BCohW-BCorrU

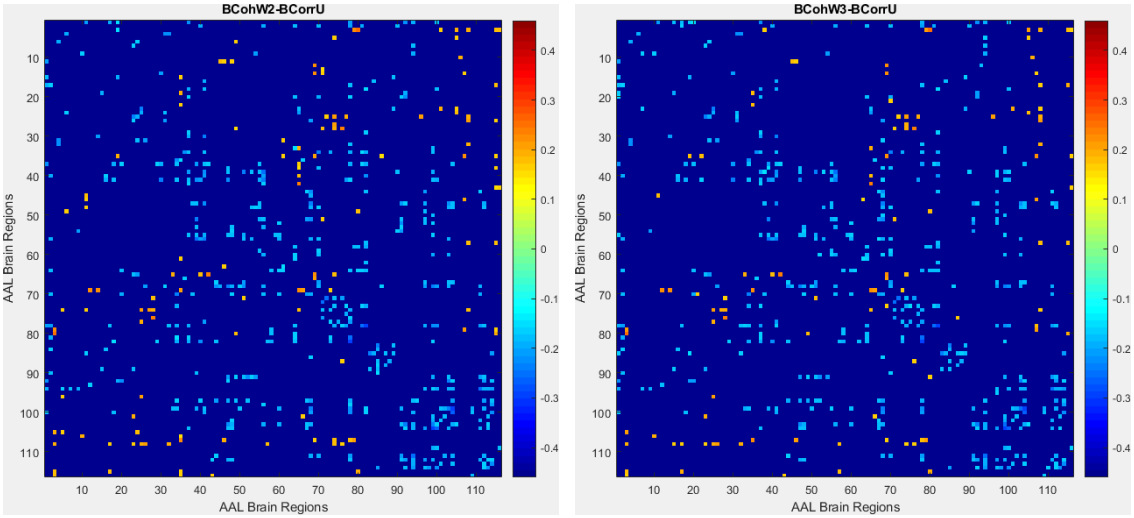

(a) BCohW2-BCorrU (b) BCohW3-BCorrU

Figure 5.3: Results from pairwise functional connectivity metric comparison - matrices from BCohW2-BCorrU and BCohW3-BCorrU.

BCohW2-BCorrU

Results from the comparison BCohW2-BCorrU can be found in figures 5.3a and 5.4. For this comparison, significant mean group differences were mostly negative.

Significant positive mean group differences were registered, for example, for connections between: the left angular gyrus and hippocampus, parahippocampal gyrus, and amygdala; left superior frontal gyrus and heschl gyrus, cerebellum and vermis; left posterior cingulate gyrus and the orbital part of the inferior frontal gyrus, the left supplementary motor area, and the right olfactory cortex. The left angular gyrus was, in fact, found on one of the significant subnetworks obtained for this comparison. This subnetwork is depicted in figure 5.4b and is comprised exclusively by connections with positive mean group differences.

Other regions that had several significant connections with positive mean group differences across all the brain were: vermis 9, 10 and cerebellum 9, 10. The biggest positive mean group difference was registered for: right heschl gyrus - left dorsolateral superior frontal gyrus.

Significant negative mean group differences were found within cerebellar and vermis areas, and along the diagonal, in particular, within the central structures, parahippocampal gyrus, and the amygdala. These last regions belong to a subnetwork from which the left middle occipital gyrus also belongs and that only has connections with negative mean group differences (figure 5.4a).

Both the right precuneus and the right dorsolateral superior frontal gyrus had several significant connections with negative mean group differences. The biggest negative mean

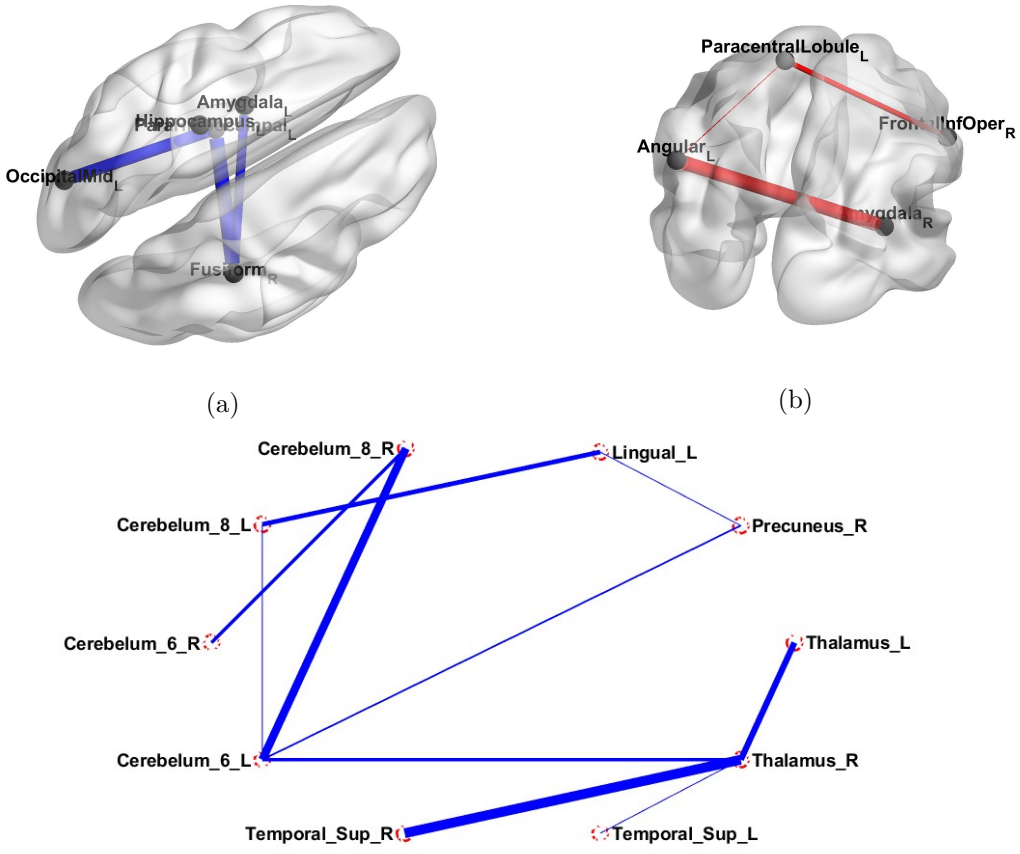

Figure 5.4: Results from pairwise functional connectivity metric comparison - significant networks from BCohW2-BCorrU. Blue line - negative mean group difference. Red line - positive mean group difference. Line thickness - strength of the measure.

group difference was found for: right superior temporal gyrus - right thalamus. In fact, these regions belong to another subnetwork obtained for the present comparison that, besides regions from the temporal lobe and the central structures, also comprises regions from the parietal lobe and the cerebellum (figure 5.4c).

BCohW3-BCorrU

In figure 5.3b, can be found the results from the comparison between BCohW3 and BCorrU. It can be seen that significant mean group differences were, again, mostly negative.

Significant positive mean group differences were specially found for connections between the frontal lobe and cerebellum and vermis, and for connections with: the left angular gyrus (right putamen, left paracentral lobule, right amygdala, right parahippocampal gyrus, median cingulate and paracingulate gyri) and the left posterior cingulate gyrus (left paracentral lobule, left cerebellum 10, vermis 10, left olfactory cortex, and left supplementary motor area).

Significant negative mean group differences were mostly found for regions adjacent to

the diagonal, connections between the cerebellum and vermis and for connections within the frontal lobe. A subnetwork only composed by connections with negative mean group differences can be seen in figure 5.5. In this subnetwork, the strongest connection for BCorrU is represented and happens between the right superior temporal gyrus and the right thalamus.

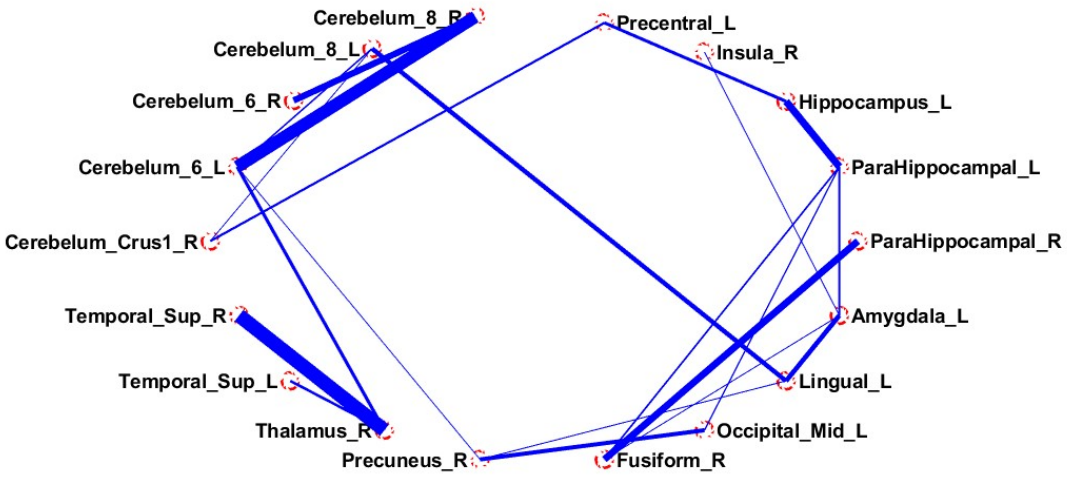

Figure 5.5: Results from pairwise functional connectivity metric comparison - significant network from BCohW3-BCorrU. Blue line - negative mean group difference. Red line - positive mean group difference. Line thickness - strength of the measure.

5.2.4 BCohF-BCorrU

The comparison BCohF1-BCorrU had no significant differences at the selected significance level.

BCohF2-BCorrU

This comparison had mostly positive mean group differences. These were, with special regard, registered for several connections involving the following brain regions: vermis 9 and 10 (except for connections with the central structures and cerebellum and vermis), left gyrus rectus (specially with central structures and supramarginal gyrus), vermis 1, 2 and cerebellum 10 (except for connections with cerebellum and vermis itself). Maximum value was found for: left cerebellum 7 b - right olfactory cortex. Several of the previously mentioned regions belong to two of the significant subnetworks obtained for this comparison. These networks can be found in figures 5.7b and 5.7c.

The following regions had several significant negative mean group differences: right rolandic operculum (lingual gyrus, cerebellum 6 and vermis 6), cerebellum 8 (right hippocampus, lingual gyrus, right fusiform, left cerebellum 4,5), and paracentral lobule. The

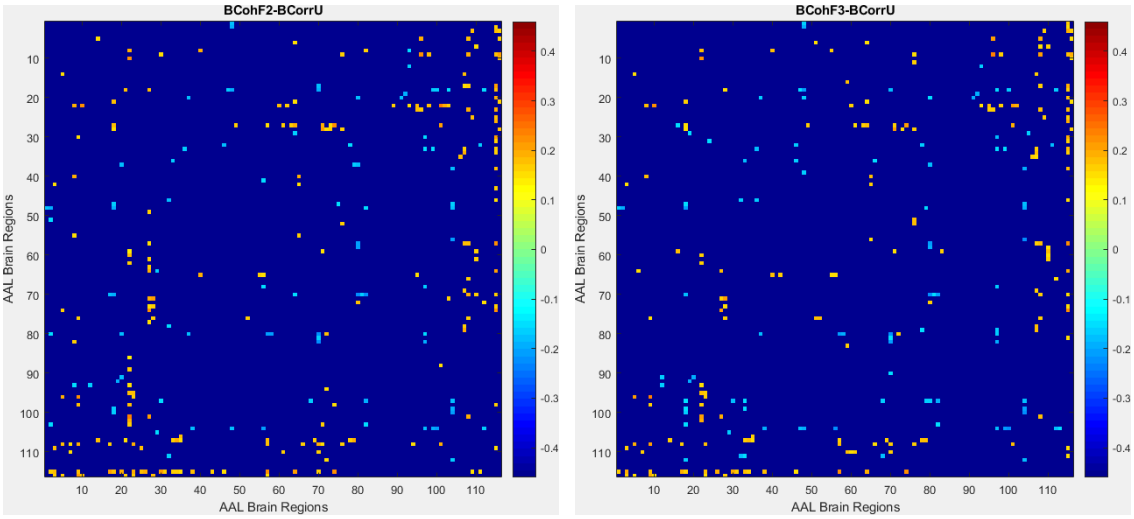

(a) BCohF2-BCorrU (b) BCohF3-BCorrU

Figure 5.6: Results from pairwise functional connectivity metric comparison - matrices from BCohF2-BCorrU and BCohF3-BCorrU.

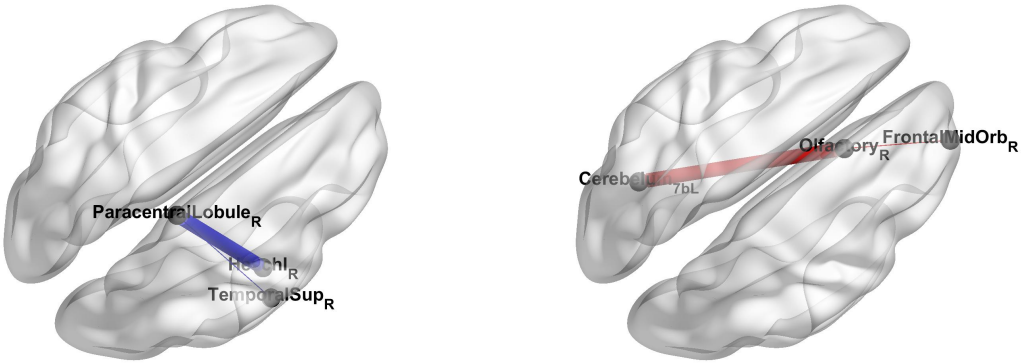

(a) (b)

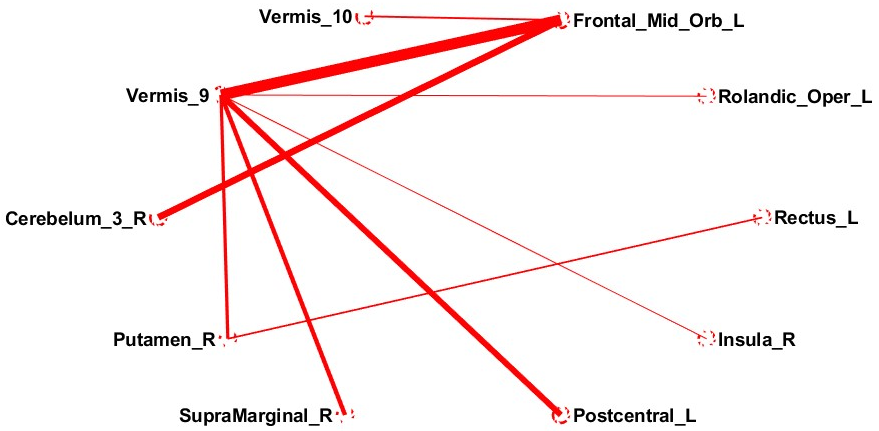

(c)

Figure 5.7: Results from pairwise functional connectivity metric comparison - significant networks from BCohF2-BCorrU. Blue line - negative mean group difference. Red line - positive mean group difference. Line thickness - strength of the measure.

biggest negative mean group difference was registered for: right heschl gyrus - right paracentral lobule and is one of the connections found on a subnetwork with only negative mean group differences (figure 5.7a).

BCohF3-BCorrU

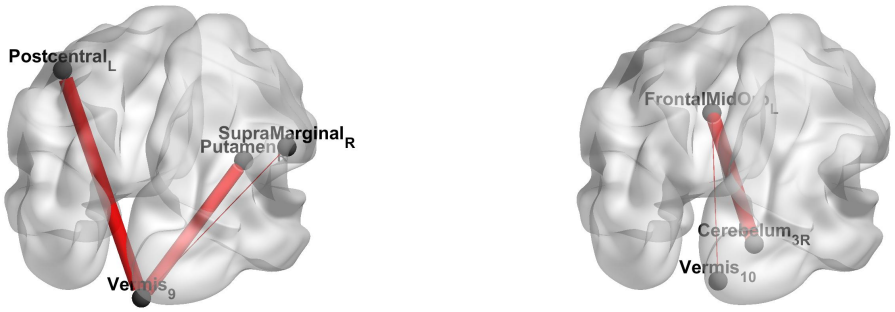

(a) (b)

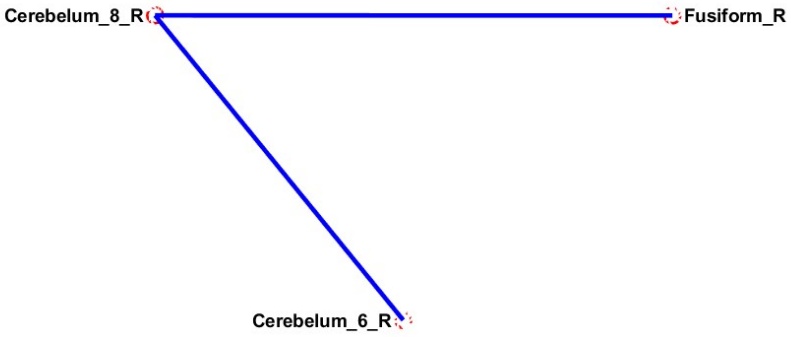

(c)

Figure 5.8: Results from pairwise functional connectivity metric comparison - significant networks from BCohF3-BCorrU. Blue line - negative mean group difference. Red line - positive mean group difference. Line thickness - strength of the measure.

This comparison led to the matrix found in figure 5.6b, that mostly has significant positive mean group differences. These positive differences were registered, for example, for the following connections: vermis 9 and 10 - several regions (except from the occipital lobe, cerebellum and vermis); gyrus rectus - central structures and supramarginal gyrus; and also for connections between cerebellum 10, vermis 1 and 2 - some regions from the frontal and parietal lobes. The biggest difference was found for the connection: right cerebellum 3 - left orbital part of the middle frontal gyrus that, together with vermis 10, belong to the subnetwork found in figure 5.8b. Other significant subnetwork was found that has vermis 9 as one of its nodes and can be seen in figure 5.8a.

Negative mean group differences were specially found for connections with the left rolandic operculum. The biggest negative difference was registered for: right cerebellum 8 - right cerebellum 6 and, together with the right fusiform, these regions form one of the significant networks that were obtained (figure 5.8c).

5.2.5 BCohW-BMITU

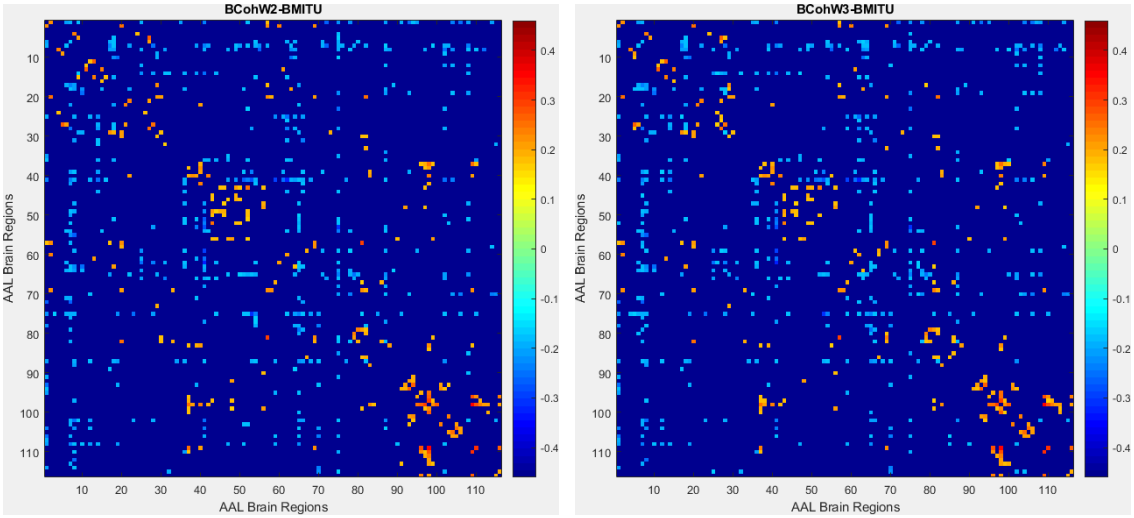

(a) BCohW2-BMITU (b) BCohW3-BMITU

Figure 5.9: Results from pairwise functional connectivity metric comparison - matrices from BCohW2-BMITU and BCohW3-BMITU.

BCohW2-BMITU

Figure 5.9a depicts the results from the comparison between BCohW2 and BMITU. Significant negative mean group differences were in majority.

Significant positive mean group differences were specially registered for connections within the frontal lobe, for connections between the left hippocampus and the cerebellum 3, 4, 5, and 6, and between the left calcarine fissure and surrounding cortex and regions from the occipital lobe. The cerebellum 4 and 5 had several significant connections, mainly with areas from the vermis and the cerebellum itself. In fact, this region comprises, with vermis 1 and 2, the pair with the biggest positive difference. Furthermore, two significant subnetworks only with positive mean group differences were obtained (figures 5.10a and 5.10c). Figure 5.10c comprises the connection with the biggest difference and includes specially areas from the cerebellum and vermis, while figure 5.10a includes areas from the frontal, parietal, and temporal lobes.

When it comes to significant negative mean group differences, the following brain regions had several significant connections: left pallidum, bilateral middle frontal gyrus, and left amygdala.

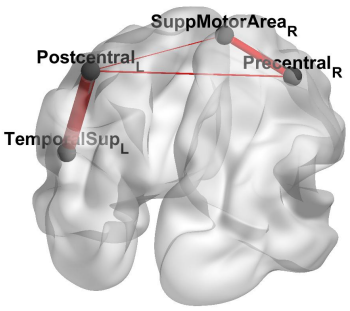

(a)

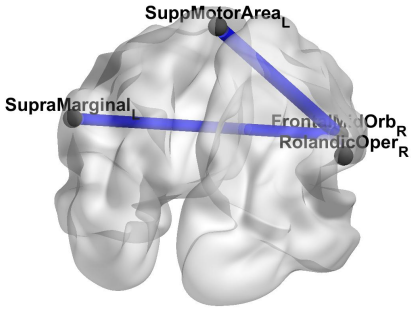

(b)

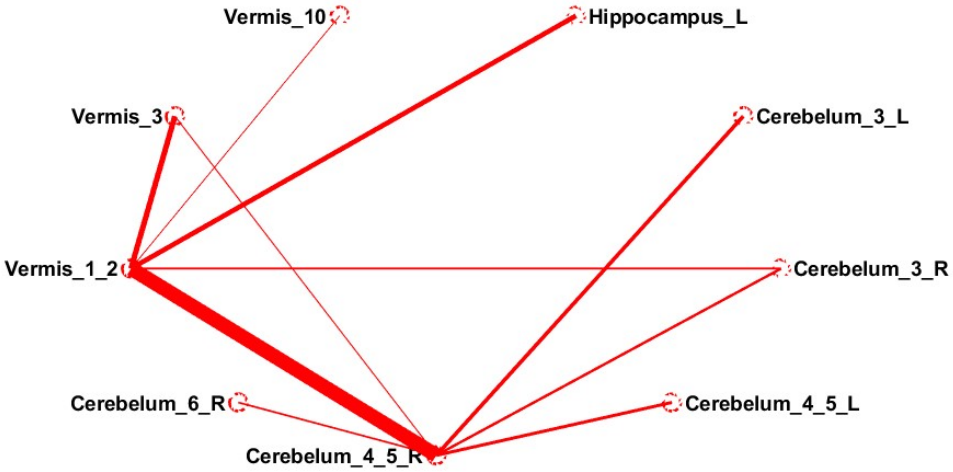

(c)

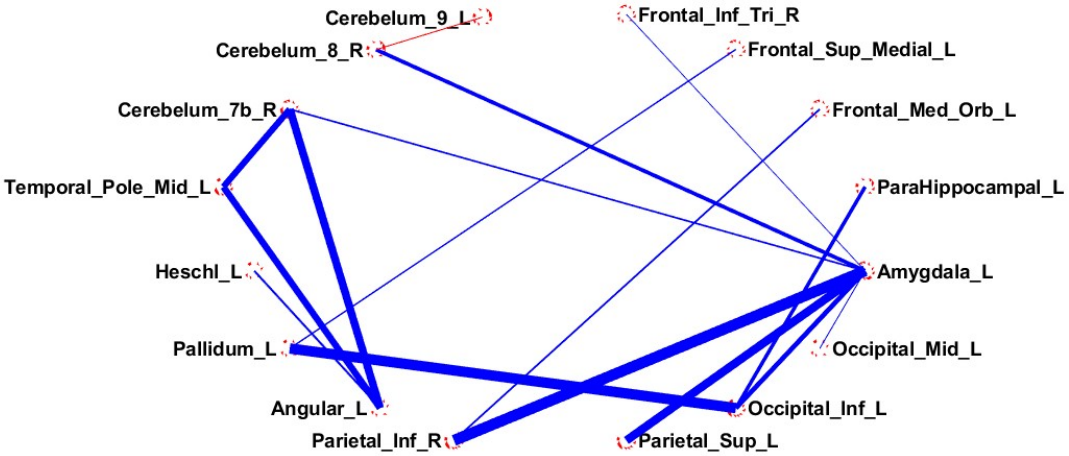

(d)

Figure 5.10: Results from pairwise functional connectivity metric comparison - significant networks from BCohW2-BMITU. Blue line - negative mean group difference. Red line - positive mean group difference. Line thickness - strength of the measure.

The triangular part of the inferior frontal gyrus also had several significant connections, in particular with: orbital part of the middle frontal gyrus, anterior cingulate and paracingulate gyri, right posterior cingulate gyrus, left amygdala, and right calcarine fissure and surrounding cortex.

The biggest negative mean group difference was registered for the pair: right inferior parietal gyrus - left amygdala. This connection is represented in figure 5.10d which depicts a significant subnetwork obtained for the comparison BCohW2-BMITU that almost has only negative mean group differences. Another significant subnetwork that was obtained can be found in figure 5.10b and has nodes from the frontal and parietal lobes.

BCohW3-BMITU

The matrix resultant from this comparison is very similar to the previously analysed matrix and can be found in figure 5.9b. Once again, significant mean group differences are mostly negative.

Significant positive mean group differences were found for pairs of regions adjacent to the diagonal with some exceptions (central structures and regions from the parietal lobe). Differences for connections within cerebellum and vermis were mostly positive. In fact, these connections constitute a significant subnetwork obtained for this comparison, that can be found in figure 5.11a. This subnetwork is very similar to one of those obtained for the comparison BCohW2-BMITU seen in figure 5.10c. There were other brain regions with mostly significant positive mean group differences, which were: bilateral cerebellum 4 and 5, vermis 1 and 2, right supplementary motor area, and right fusiform gyrus. The first two also appearing on the subnetwork mentioned above.

The biggest negative mean group differences were found for connections with the following regions: left pallidum, bilateral middle frontal gyrus, left amygdala, and bilateral angular gyrus.

In figure 5.11b a bigger subnetwork that was also obtained for the present comparison is shown. This network is comprised by several of the regions mentioned here.

5.2.6 BCohF-BMITU

For all these comparisons the fraction of positive and negative mean group differences was approximately the same (figure 5.12). Furthermore, concerning significant networks, one big network with more than 100 nodes was found for each comparison. It is not shown here as it is illegible due to its large amount of nodes.

BCohF1-BMITU

Positive mean group differences were registered for connections within areas from the cerebellum and vermis and within regions from the frontal lobe (olfactory, medial superior frontal gyrus, orbital part of the middle frontal gyrus, and gyrus rectus). The cerebellum

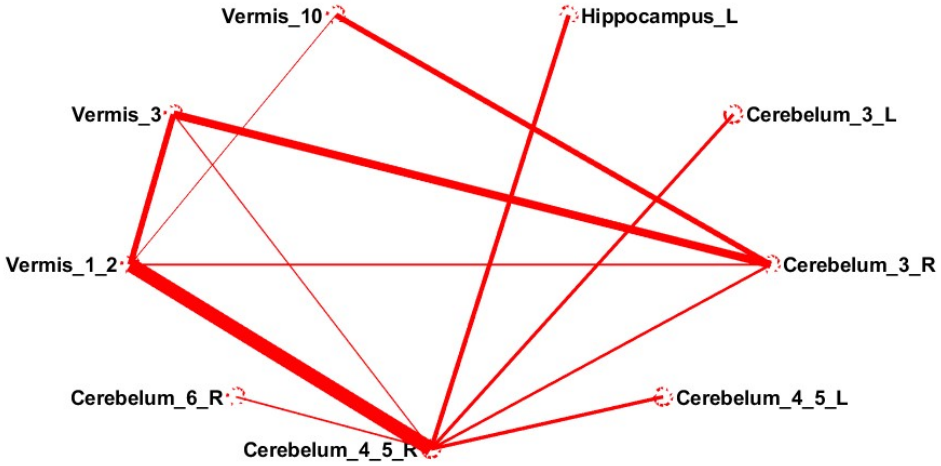

(a)

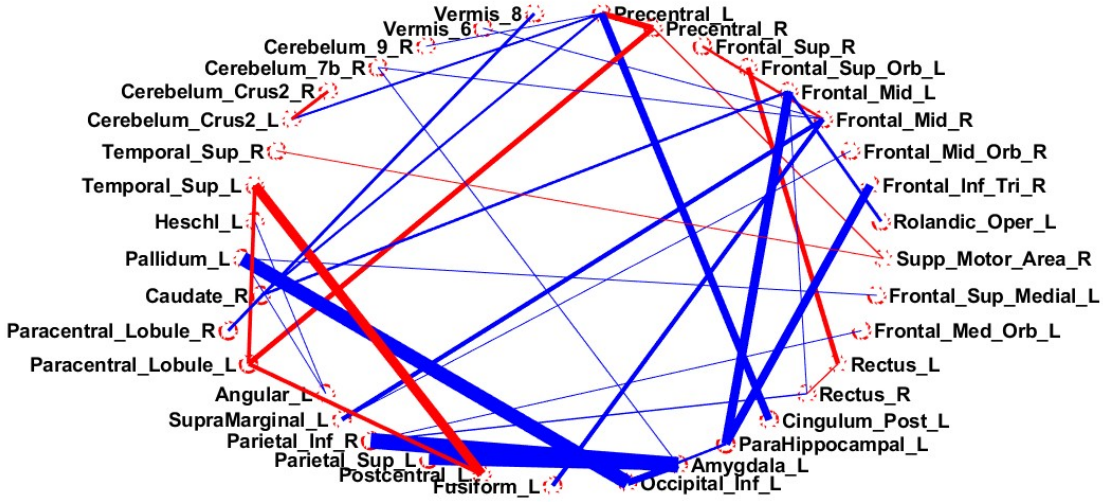

(b)

Figure 5.11: Results from pairwise functional connectivity metric comparison - significant networks from BCohW3-BMITU. Blue line - negative mean group difference. Red line - positive mean group difference. Line thickness - strength of the measure.

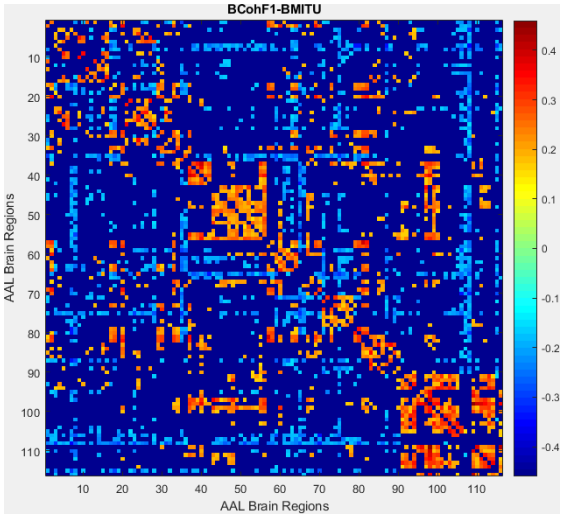

(a) BCohF1-BMITU

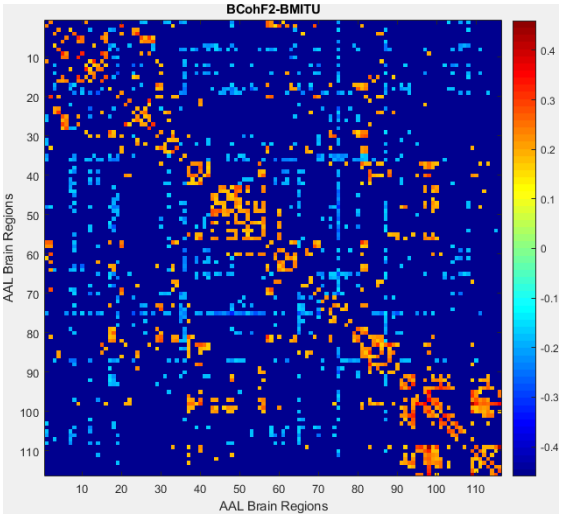

(b) BCohF2-BMITU

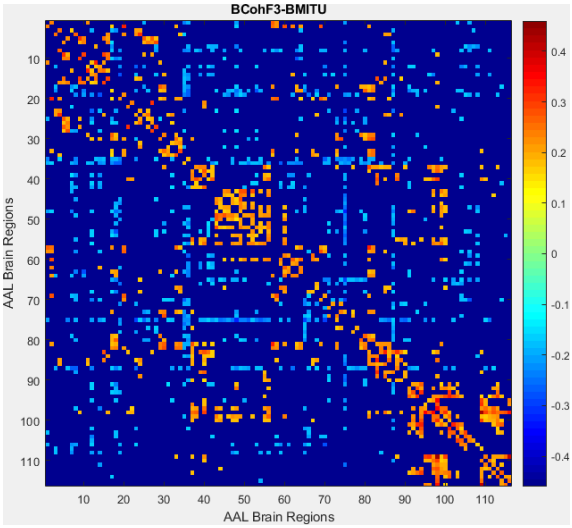

(c) BCohF3-BMITU

Figure 5.12: Results from pairwise functional connectivity metric comparison - matrices from BCohF-BMITU.

4, 5, and 6 had several significant connections, including with: median cingulate and paracingulate gyri, hippocampus, parahippocampal gyrus, amygdala, calcarine fissure and surrounding cortex, cuneus, and lingual gyrus. A cluster with positive differences was found that includes: amygdala, parahippocampal gyrus, and hippocampus. Connections with the right supplementary motor area and the right posterior cingulate gyrus and connections between regions from the occipital lobe and fusiform gyrus also had positive mean group differences. The biggest positive mean group difference was found for: vermis 1, 2 - right cerebellum 4, 5.

Significant negative mean group differences were specially registered for connections with the following areas: middle frontal gyrus, posterior cingulate gyrus, and left angular gyrus. The cerebellum 9, 10 had several significant connections with almost every brain

region, except the hippocampus, parahippocampal gyrus, amygdala, and the cerebellum itself. The biggest negative mean group difference was found for the connection: right cerebellum 10 - left middle frontal gyrus.

BCohF2-BMITU

Results were similar to those from the previously analysed comparison. Same type of difference was registered for connections within the cerebellum, vermis and within regions from the frontal lobe. Once again, a cluster with positive mean group differences was found, involving: amygdala, parahippocampal gyrus, and hippocampus. The cerebellum 4, 5, and 6 had significant connections, involving calcarine fissure and surrounding cortex, cuneus, and lingual gyrus. The biggest positive mean group difference was registered for the same pair as in BCohF1-BMITU.

The posterior cingulate gyrus had several significant connections across the whole brain with negative mean group differences, except with cerebellum and vermis, olfactory cortex, medial superior frontal gyrus, orbital part of the middle frontal gyrus, gyrus rectus, and insula. The left pallidum, the orbital part of the middle frontal gyrus, and the left middle temporal pole had several significant connections with negative mean group differences. The biggest negative mean group difference was found for: left pallidum - right lingual gyrus.

BCohF3-BMITU

Positive mean group differences were registered for cerebellum 4, 5, and 6 for connections with: hippocampus, parahippocampal gyrus, calcarine fissure and surrounding cortex, and lingual and fusiform gyri. The left hippocampus had several significant connections with positive mean group differences as well as regions along the diagonal (for example, cerebellum and vermis, frontal lobe, occipital and fusiform). The biggest positive mean group difference was found for the same pair as in BCohF1-BMITU.

With bigger values for BMITU, an highlight for the following regions can be made: left pallidum, posterior cingulate gyrus, and left middle temporal gyrus, which all had several significant connections. The pair with the biggest negative mean group difference was the same as for the last comparison.

Overall Discussion of Results from Approach A

Unfortunately, only metrics from Mutual Information, Time Basic, and Frequency Basic were compared, as metrics from other families had to be excluded on account of processing issues.

Overall, regarding the networks that were obtained, almost no similarities between different comparisons were found. Nevertheless, in the following paragraphs, the few that were seen will be pointed out.

When it comes to comparisons involving correlation it was seen that pairs along the diagonal always had stronger values for this metric. These pairs, in general, correspond to regions closer to each other, which are expected to have higher correlation. However, this overestimation may lead to false positive results and our findings are suggestive that a multi-metric approach may help to mitigate and control this problem. When the comparison was between frequency domain metrics and mutual information, pairs closer to the diagonal had stronger values for frequency domain metrics. This is also expectable, as coherence is the analogous metric of correlation in the frequency domain.

It was seen that matrices obtained for some comparisons were similar, even when different families where being compared. This happened, for example, for the comparisons: BCohF-BMITU, BCohW-BMITU, and BCorrU-BMITU (for the first two, similarities were found for all the frequencies). Regarding these comparisons, BCohW-BMITU was the one that led to fewer significant differences.

Other comparisons had similar results, such as BCorrU-BMITU and BCorrD-BMITD1 which both led to one significant network with more than 100 nodes, emphasizing the differences between these two metrics. In what concerns these two families, mutual information is a non-linear metric and, in past studies, was seen to outperform other metrics in time-series characterization [92], having good generality and equitability[1] [68]. On the other hand, correlation is a linear, static, and global metric [21] which assumes Gaussianity [42].

Several efforts have been made in order to discover if linear association is enough to describe neuronal dynamics and gaussianity assumption is important here. In fact, authors stated that deviation from gaussianity has different effects in functional networks depending on the spatial scale, being relatively minor within networks and significant between networks [21].

BCorrU-BMITU and BCorrD-BMITD1 had similar results with BCohW-BCorrU, however, with opposite polarities, as positive differences in one correspond to negative differences in the other. Regarding pairs along the diagonal this is expectable, as correlation tends to have higher values for this regions.

In what concerns comparisons between metrics from the frequency domain and mutual information, BCohW-BMITU had less significant differences than BCohF-BMITU. For comparisons with Wavelet based coherence, six significant networks were found. Amongst these networks and across different frequencies it was found connections that appeared in more than one network. In particular, networks depicted in figures 5.10a, 5.10b, and 5.10d had several connections that appeared in another network depicted in figure 5.11b. In addition, the network depicted in figure 5.10c is very similar to the one in figure 5.11a. For comparisons with Fourier based coherence, similarly to comparisons between metrics from Time Basic and Mutual Information, for each frequency one significant network with more than 100 nodes was found.

[1] One metric has good generality if it is capable of detecting a wide range of associations with sufficient sample size and good equitability if it gives similar values to equally noisy associations of different types.

Regarding comparisons between metrics from frequency domain and correlation, all the matrices obtained had a similar outline. From all the comparisons done in the present work, comparisons between Fourier based coherence and correlation were the ones with less significant differences and BCohF1-BCorrU had no significant differences at all. This is expected as these are the most similar metrics being compared, both detecting linear associations and being analogous metrics in different domains. However, some conceptual differences between these two metrics may be pointed out. For instance, coherence is sensitive to both phase and amplitude of the signal [63] and is not sensitive to the regional hemodynamic response function, whereas correlation is [75]. This is important, as recent study found that regional hemodynamic response function variability may lead to the identification of false functional connections when ignored [67].

Six significant networks were obtained for comparisons between Fourier based coherence and correlation. These networks only had one common connection with another network and no similarities between themselves at all. This common connection happened between right cerebellum 6 and right cerebellum 8 (see figures 5.4c, 5.5, and 5.8c).

On its turn, comparisons between Wavelet based coherence and correlation led to four significant networks which had similarities between themselves as connections from two of them appeared in other network from a different frequency, in particular, connections from 5.4c and 5.4a appeared in 5.5.

5.3 Control versus Patient Comparison

For all the control versus patient comparisons it was selected an alpha level of 0.05 prior to analysis and selected Random Networks Groups so that non-parametric p-values would be considered. Only significant differences according to the applied significance level will be described.

As aforementioned, mean group differences are shown according to a colour scale. For all the metrics, the considered difference was: $d = Control - ADHD$. Thus, when the mean group value of connectivity is higher for controls we have a positive difference which corresponds to the warm colours in the colour scale, otherwise, there is a negative difference, meaning that the connectivity is stronger for ADHD subjects over controls for the given pair of brain regions.

It was verified, as expected, that while some pairs of regions had a stronger connection for the control group, others were stronger for the ADHD group.

For each family of metrics, results from bivariate methods will be firstly presented, starting with undirected metrics and then the corresponding directed metric. The same procedure will be then followed for partial metrics. For directed metrics it will done special notes regarding the direction of the connections under analysis.

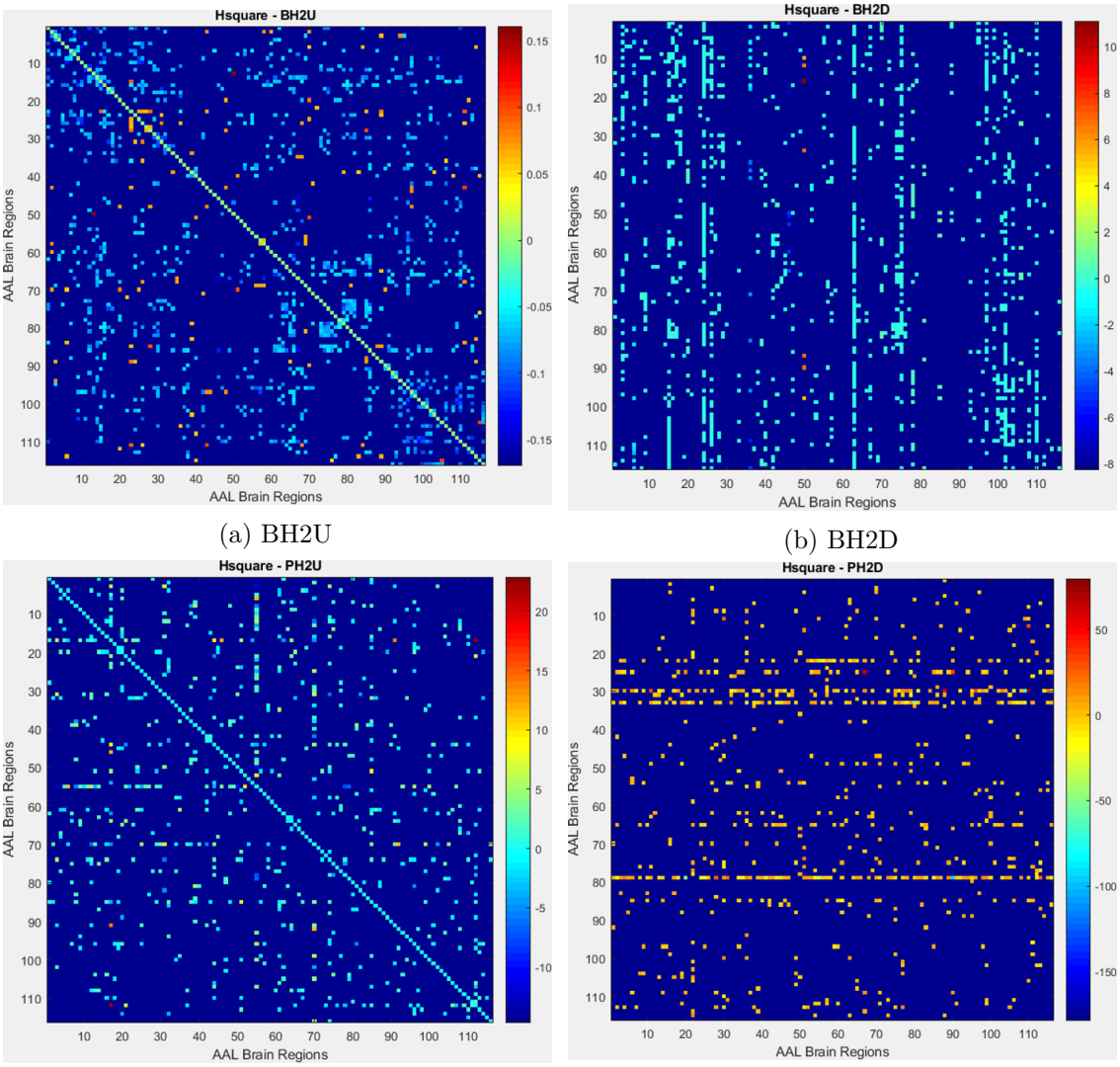

(a) BH2U

(b) BH2D

(c) PH2U

(d) PH2D

Figure 5.13: Results from control versus patient comparison using Hsquare family- matrices from BH2U, BH2D, PH2U, and PH2D.

5.3.1 Hsquare

Figures 5.13 and 5.14 show the results obtained for the group comparison using matrices computed through the application of metrics from Hsquare family.

BH2U

Significant mean group differences were mostly negative, revealing a greater number of stronger connections for the ADHD group in comparison with controls (figure 5.13a).

In particular, some negative clusters were registered for connections happening between both the parietal and temporal lobes and the central structures. The parietal lobe had several significant negative mean group differences happening with other regions besides the central structures, such as the temporal lobe and the cerebellum. It was seen that

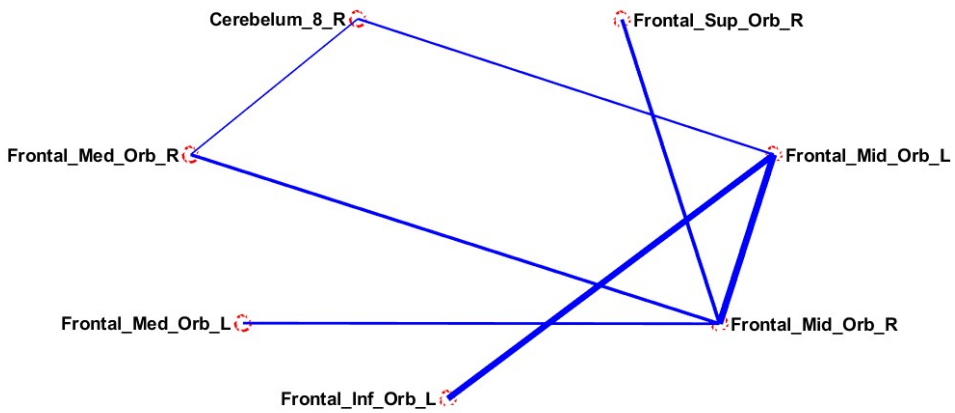

(a)

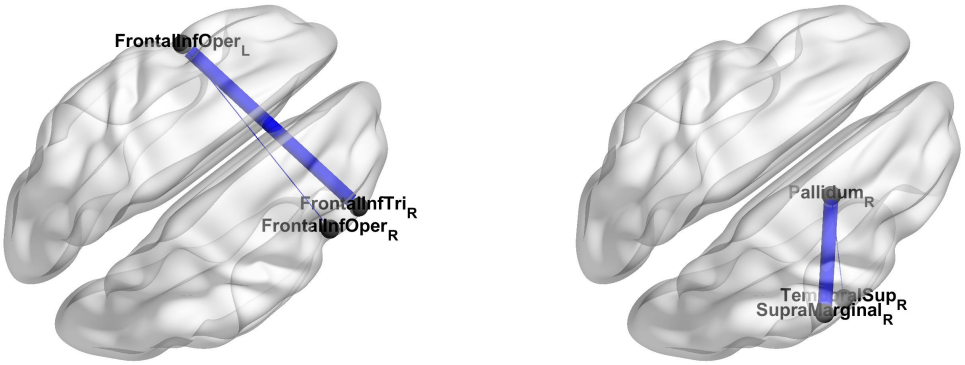

(b) (c)

Figure 5.14: Results from control versus patient comparison using Hsquare family- significant networks from BH2U. All of these networks show connections that were stronger for the ADHD group.

connections between areas from the vermis and the cerebellum were also stronger for the ADHD group as well as connections within the frontal lobe.

Furthermore, some regions had consistently stronger connections across all the brain for the ADHD group, these were: rolandic operculum, inferior frontal gyrus (triangular, opercular, and orbital part), and middle frontal gyrus.

Stronger connections for the ADHD group were also seen amongst the significant subnetworks obtained from the matrix (figures 5.14a, 5.14b, and 5.14c). These networks, in particular, pointed out the differences between the two groups regarding connections within the frontal lobe (figures 5.14a and 5.14b).

Positive mean group differences were sparse and registered, for example, for connections with the following brain regions: medial superior frontal gyrus, orbital part of the middle frontal gyrus, parahippocampal gyrus, paracentral lobule, posterior cingulate gyrus, vermis 8, and vermis 4, 5. The pair of regions which had the strongest connection for the control group was: right superior occipital gyrus - left triangular part of the inferior frontal gyrus.

BH2D

Once again mean group differences were mostly negative with even fewer positive mean group differences (figure 5.13b). These positive differences were, in particular, registered for connections with the right superior occipital gyrus with the direction: other regions → right superior occipital gyrus.

Some of the strongest connections for the ADHD group were observed (with this direction) between several brain regions and the left dorsolateral superior frontal gyrus, the orbital part of the left inferior frontal gyrus, the right medial superior frontal gyrus, the left supramarginal gyrus, the right putamen, the left pallidum, the right cerebellum 7b, and vermis 3.

The connection between the right cuneus and the left supplementary motor area was particularly higher for the ADHD group.

PH2U

The outcome from the comparison of the two groups when using PH2U can be seen in figure 5.13c.

On one hand, it was found that the biggest negative mean group differences, that is, the strongest connections for the ADHD group, were registered between: the left fusiform gyrus and the left superior frontal gyrus, the left fusiform gyrus and the right superior occipital gyrus, and the right calcarine fissure and surrounding cortex and vermis 6.

On the other hand, the biggest positive mean group differences were found to happen between vermis 6 and the left rolandic operculum and between the left fusiform and the right orbital part of the superior frontal gyrus.

Several regions had a particularly high number of connections showing significant between group differences, they were: the left rolandic operculum, the left fusiform gyrus (specially for connections with regions from the frontal and occipital lobes), and the right paracentral lobule.

PH2D

The matrix resultant from the comparison of the two groups when using PH2D can be seen in figure 5.13d.

Significant mean group differences were observed for the following regions with several others: right olfactory cortex, orbital part of the left middle frontal gyrus, right insula, left median cingulate and paracingulate gyri, left heschl gyrus, and left angular gyrus.

As in BH2D, left pallidum and right putamen were also involved in connections with both positive (right putamen → left middle occipital gyrus, left pallidum → left inferior parietal gyrus) and negative (left pallidum → right insula, left pallidum → vermis 7) significant mean group differences.

The biggest negative difference on mean group connectivity strength was registered for the following pairs of brain regions: left heschl gyrus → right inferior temporal gyrus; right insula → vermis 1, 2; left heschl gyrus → left precuneus; left heschl gyrus→ right supplementary motor area.

On the other extremity, the biggest positive difference was registered for the pair: right insula → vermis 3.

General considerations on the results from Hsquare

Using metrics from Hsquare family, several differences between the control and the ADHD group were found across the whole brain. In particular, connections within the frontal lobe and within the cerebellum were stronger for the ADHD group. This was specially seen when using bivariate metrics which may indicate that these connectivity differences are related to the interaction with a third region.

Connections with insula, cingulate, and the temporal lobe also registered connectivity differences between the groups. For example, the left fusiform had both stronger and weaker connections for the ADHD group, when using PH2U, regarding the frontal and occipital lobes. The posterior cingulate gyrus and the right insula also had connectivity differences between the groups. The right superior occipital gyrus had decreased functional connectivity with several brain regions for the ADHD group when using bivariate metrics and an increased functional connectivity for the same group regarding the connection with the left fusiform when using PH2U.

Central structures also were registered to have connectivity differences between the control and the ADHD groups.

5.3.2 Transfer Entropy

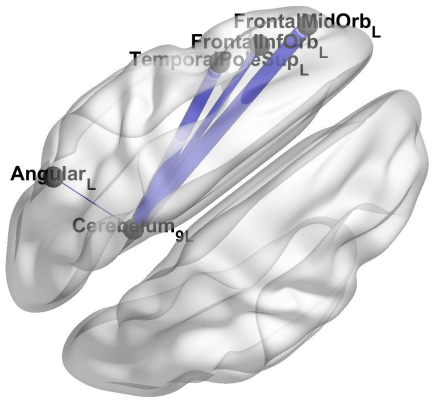

Figure 5.15: Results from control versus patient comparison using Transfer Entropy family - significant network from BTEU (part I). Blue line - negative mean group difference. Red line - positive mean group difference. Line thickness - strength of the measure.

Figures 5.15, 5.16, 5.17, and 5.18 show the results obtained for the group comparison using matrices computed through the application of metrics from Transfer Entropy family.

BTEU

Results from the comparison between ADHD and control groups using BTEU are depicted in figure 5.16a.

Mean group differences were mostly negative, with positive mean group differences specially registered for connections between regions from the frontal

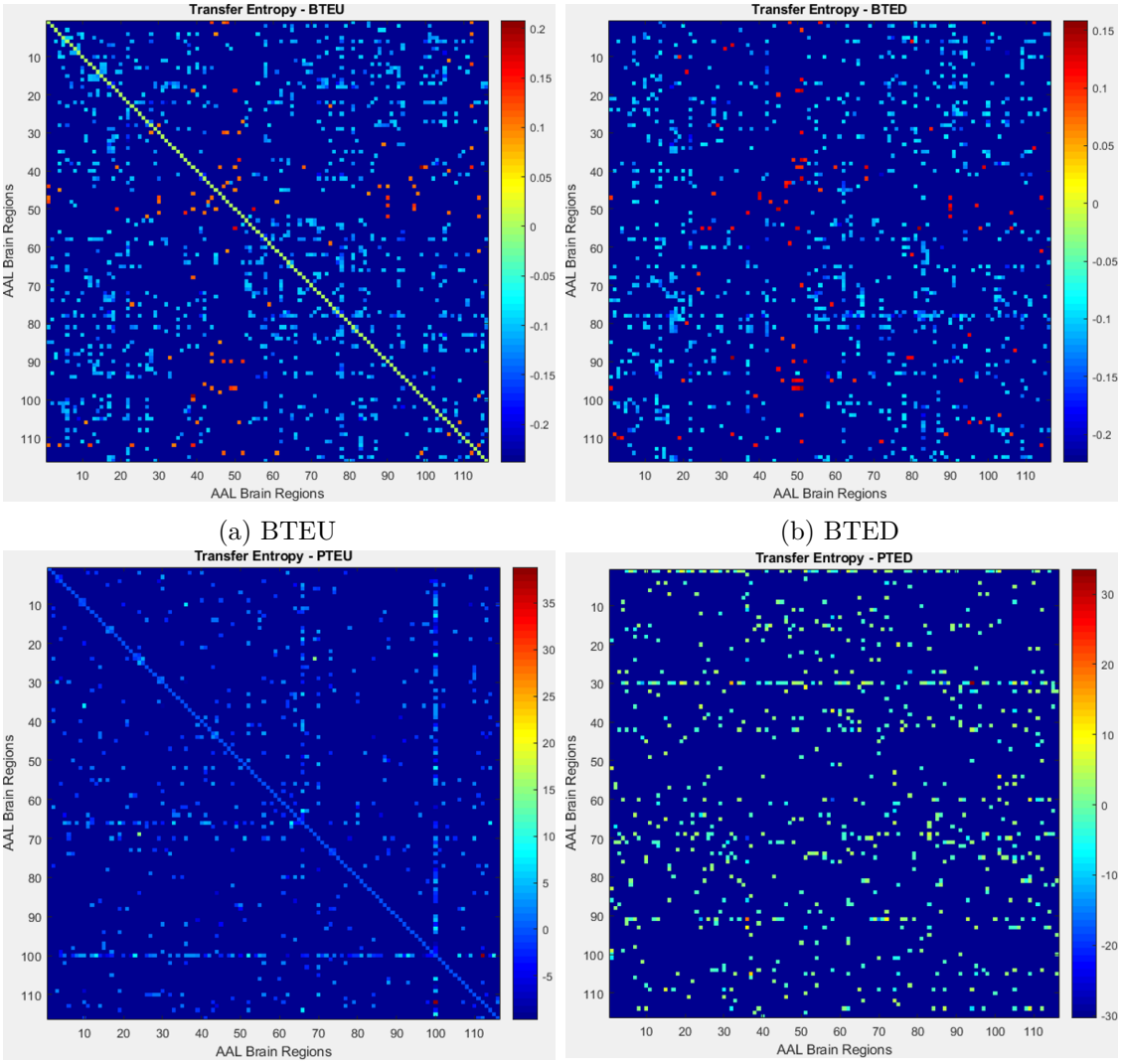

(a) BTEU

(b) BTED

(c) PTEU

(d) PTED

Figure 5.16: Results from control versus patient comparison using Transfer Entropy family - matrices from BTEU, BTED, PTEU, and PTED.

lobe and vermis 6 as well as between occipital and temporal lobe regions.

Significant positive mean group differences happened, for example, between the left supplementary motor area and the right superior occipital gyrus and between vermis 6 and both the right opercular part of the inferior frontal gyrus and the left parahippocampal gyrus. The biggest positive mean group difference was registered for the connection between the left cerebellum 6 and the left parahippocampal gyrus.

Connections were stronger for the ADHD group between regions from the temporal lobe and both the frontal and the parietal lobes.

Two significant subnetworks can be found in figures 5.15 and 5.17, both showing only connections with negative mean group differences. In particular, figure 5.15 shows connectivity differences occurring only on the left side with cerebellum 9 occupying a central position, and figure 5.17 shows differences in connections from the whole brain.

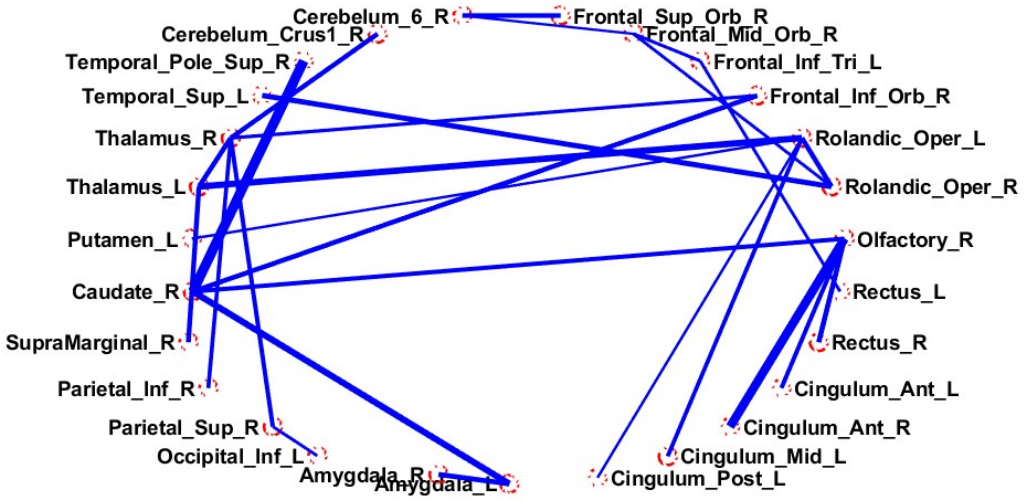

Figure 5.17: Results from control versus patient comparison using Transfer Entropy family - significant network from BTEU (part II). Blue line - negative mean group difference. Red line - positive mean group difference. Line thickness - strength of the measure.

The biggest negative mean group difference was registered for the connection between the right caudate gyrus and the right superior temporal gyrus (temporal pole).

BTED

Once again, mean group differences were mostly negative and the obtained results were very similar to those obtained for the previously described metric. Results can be seen in figure 5.16b.

Significant positive mean group differences were observed between several areas, including between: both the right inferior temporal gyrus and right parahippocampal gyrus and regions from the occipital lobe (like cuneus and lingual gyrus) and between the superior and middle occipital gyri and the left cerebellum 3, 4 and 5 (in this direction). Significant positive mean group differences that were mentioned in the previous metric, and were, once again, significant in the current comparison, happened with the following directions: left supplementary motor area → right superior occipital gyrus; vermis 6 → left parahippocampal gyrus; left parahippocampal gyrus → left cerebellum 6. The biggest positive mean group difference was registered for the connection: left cerebellum 4 and 5 → left middle occipital gyrus.

On the other hand, significant negative connections were registered, for example, between bilateral thalamus and other regions (left heschl gyrus, right and left supramarginal gyrus, right superior temporal gyrus, and vermis 1 and 2) and for connections between regions from the cerebellum and vermis and the left superior temporal gyrus (temporal pole). Some other significant connections with negative mean group difference were: orbital

part of the left middle frontal gyrus → right amygdala; bilateral triangular part of the inferior frontal gyrus → right amygdala.

PTEU

For this comparison, positive and negative mean group differences registered were almost in equal number, as depicted in figure 5.16c.

Significant mean group differences were particularly registered for connections with: the right angular gyrus (left orbital part of the superior frontal gyrus, left rolandic operculum, left supplementary motor area, right postcentral gyrus, and left supramarginal gyrus) and the right cerebellum 6 (right middle occipital gyrus and left cerebellum crus 2).

A small subnetwork involving some of the previously mentioned regions (the right angular gyrus, the right postcentral gyrus, and the left supplementary motor area) with all the connections showing higher values for the control group was found (figure 5.18a). Another significant subnetwork that was obtained can be seen in figure 5.18b and involves: the right triangular part of the inferior frontal gyrus, the left anterior cingulate and paracingulate gyri, and the left fusiform.

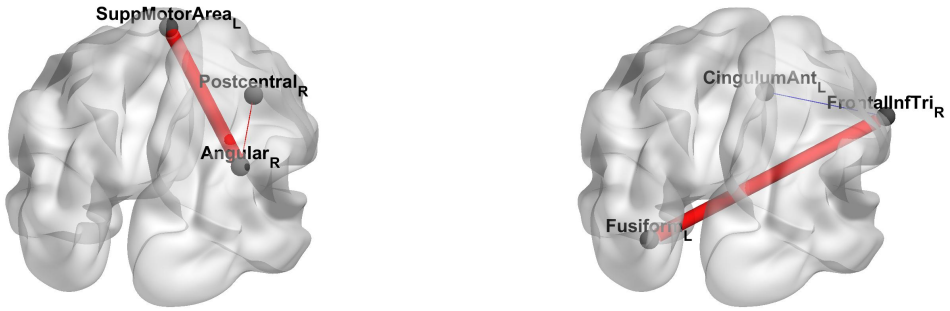

(a) (b)

Figure 5.18: Results from control versus patient comparison using Transfer Entropy family - significant networks from PTEU. Blue line - negative mean group difference. Red line - positive mean group difference. Line thickness - strength of the measure.

An extremely positive mean group difference was registered for the connection between vermis 6 and the right cerebellum 6. The most negative connections were registered for: right posterior cingulate gyrus and right insula; right cerebellum 6 and orbital part of the left inferior frontal gyrus.

PTED

Results obtained through the application of this metric can be seen in figure 5.16d.

Significant mean group differences were registered for connections between the left precentral lobule, right insula, left cerebellum crus 1, bilateral paracentral lobule and several brain regions.

The most positive mean group difference was registered for: right insula → right cerebellum crus 2. On the other hand, the most negative connections were registered for: left precentral lobule → left superior temporal gyrus (temporal pole) and right insula → vermis 1, 2.

General considerations on the results from Transfer Entropy

Results from bivariate metrics showed connectivity differences between the control and the ADHD groups specially on the temporal and occipital lobes, not only for connections within these lobes but with other regions.

Stronger connections for controls were mostly registered for connections with the occipital lobe, including the right superior occipital gyrus, cuneus, and lingual gyrus. These stronger connections specially occurred with regions from the frontal and temporal lobes, for example, the left supplementary motor area and the parahippocampal gyrus.

Using partial metricss group differences mostly regarded insula and cingulate and occipital regions. For example, the right insula, was one important region with significant positive and negative differences across all the brain when using PTED.

From the frontal lobe, the left supplementary motor area had significant group differences registered across different metrics regarding connections with several brain regions.

Group differences involving the cerebellum were seen when using all the metrics and regarded connections with regions from all brain lobes, including insula and cingulate and cerebellar regions itself.

5.3.3 Mutual Information

Results from group comparison obtained by using matrices computed with metrics from the Mutual Information family can be found in figures 5.19, 5.20, and 5.21.

BMITU

Results from the comparison between ADHD and control groups using BMITU are depicted in figure 5.19a.

Mean group differences were mostly positive, suggesting the existence of many stronger connections for controls in comparison with ADHD subjects. Differences between almost all the connections were considered significant, however, one must note that this difference had a very small range.

Within these stronger connections for the control group, there were several brain areas for which the biggest differences were registered, for example: right orbital part of the

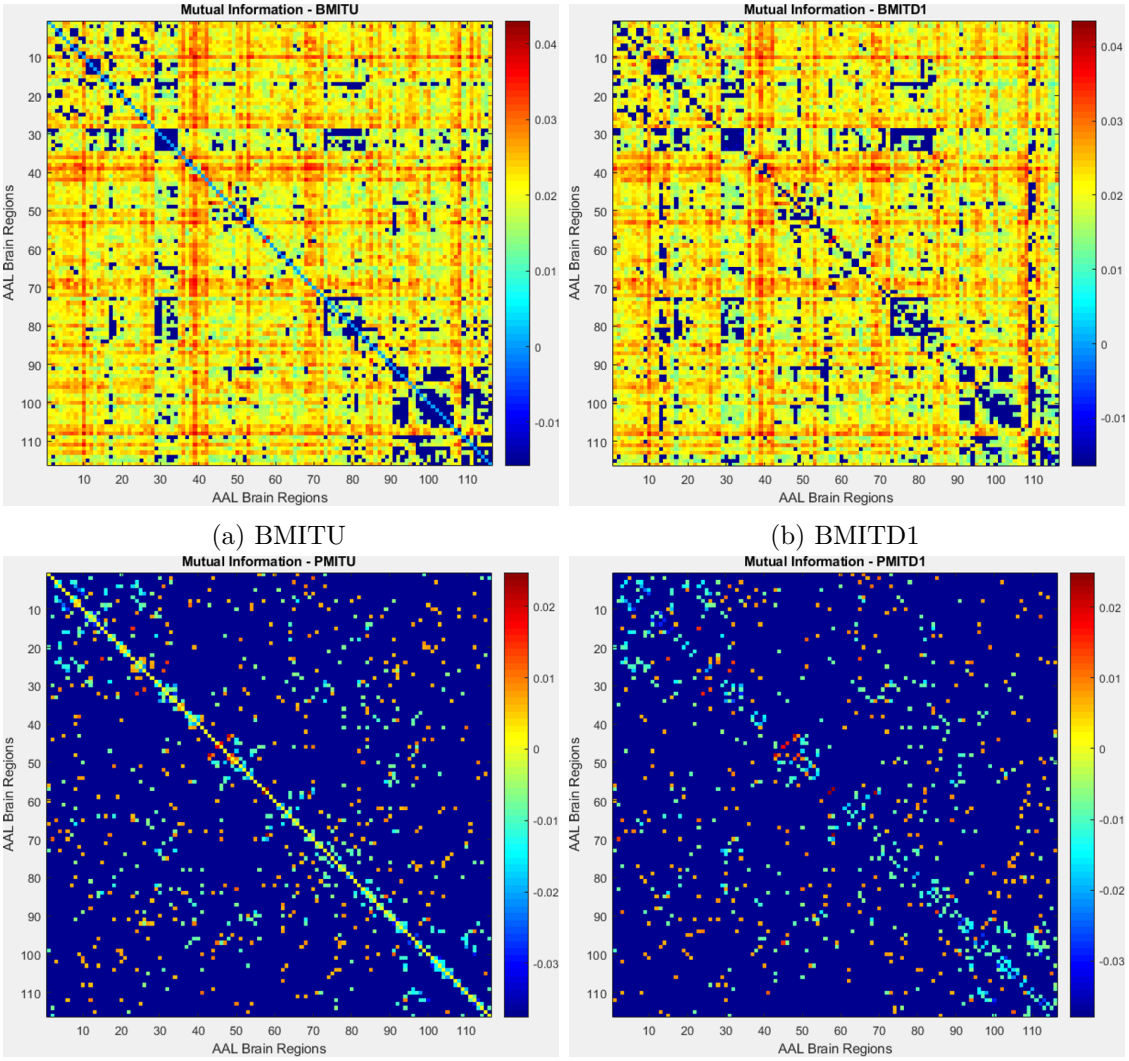

(a) BMITU (b) BMITD1

(c) PMITU (d) PMITD1

Figure 5.19: Results from control versus patient comparison using metrics from Mutual Information family - matrices from BMITU, BMITD1, PMITU, and PMITD1.

middle frontal gyrus, posterior cingulate gyrus, hippocampus, parahippocampal gyrus, amygdala, precuneus, paracentral lobule, caudate nucleus, and left inferior occipital gyrus.

BMITD1

Once again, mean group differences were mostly positive and almost identical results were obtained, which can be seen in figure 5.19b.

The biggest positive mean group differences were registered for the same regions mentioned above and were significant in both directions, leading to an almost symmetrical matrix.

Significant negative mean group differences were registered for the following group of connections: right insula - right median cingulate and paracingulate gyri, left cerebellum

7b - left cerebellum 8. Applying a more conservative significance level almost no negative differences arise.

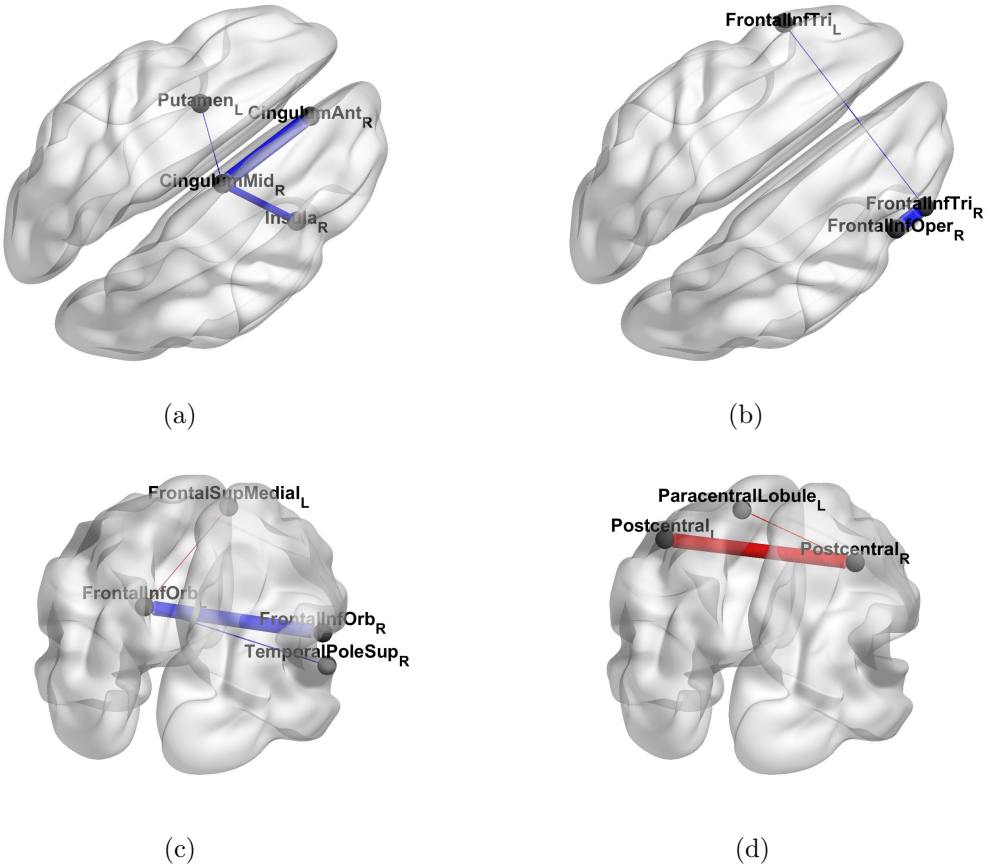

(a) (b)

(c) (d)

Figure 5.20: Results from control versus patient comparison using Mutual Information family - significant networks from PMITU (part I). Blue line - negative mean group difference. Red line - positive mean group difference. Line thickness - strength of the measure.

PMITU

Results from the group comparison done using matrices obtained through the application of PMITU can be found in figure 5.19c.

Significant positive mean group differences were registered for several connections across the whole brain. The biggest differences were registered for the following connections: left postcentral gyrus and right postcentral gyrus; right postcentral gyrus and left paracentral lobule; left calcarine fissure and surrounding cortex and right lingual gyrus. The first two pairs comprise one of the significant subnetworks that were found (figure 5.20d).

Significant mean group differences for connections within the frontal lobe were mostly negative and registered, for example, for the following connections: right superior frontal gyrus and right middle frontal gyrus; orbital part of the left superior frontal gyrus and orbital part of the left middle frontal gyrus; orbital part of the right superior frontal gyrus

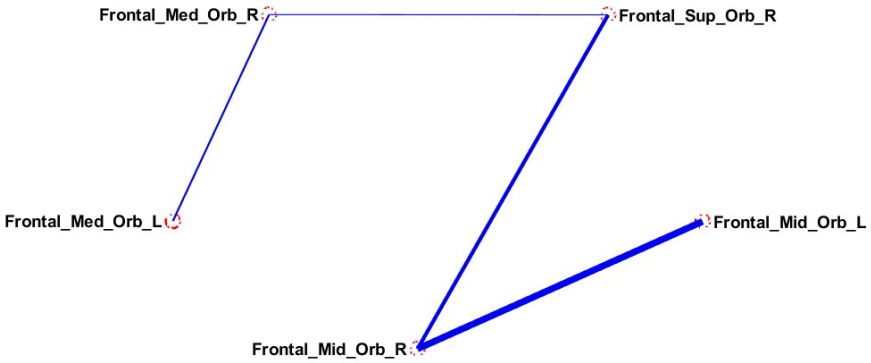

(a)

Figure 5.21: Results from control versus patient comparison using Mutual Information family - significant network from PMITU (part II). Blue line - negative mean group difference. Red line - positive mean group difference. Line thickness - strength of the measure.

and bilateral orbital part of the middle frontal gyrus; left middle frontal gyrus and right middle frontal gyrus. Furthermore, several networks involving regions from the frontal lobe were obtained. These can be seen in figures 5.20b, 5.20c and 5.21.

PMITD1

Once more, it was obtained an almost symmetrical matrix (figure 5.19d) where significant mean group differences were mostly negative and registered, in particular, for connections within the frontal lobe and within the cerebellum and vermis.

Significant positive mean group differences were registered for connections with cerebellum and vermis except connections within these areas themselves, which, as mentioned above, had negative mean group differences.

Biggest positive differences registered were the same as for the previous metric, happening for: left postcentral gyrus and right postcentral gyrus; right postcentral gyrus and left paracentral lobule; left calcarine fissure and surrounding cortex and right lingual gyrus.

General considerations on the results from Mutual Information

Mean group differences using metrics from Mutual Information family were small and significant differences from partial metrics seemed to appear for connections that had no significant difference when using bivariate metrics.

When using bivariate metrics, insula and cingulate regions had some of the biggest negative mean group differences that were registered for connections within these regions. This was also seen for partial metrics, in particular, among significant networks that were obtained.

Areas with connectivity differences between the two groups when using partial

metrics included, mostly, parietal, frontal, and cerebellar regions. Connections within the frontal lobe were generally stronger for the ADHD group as well as connections within the cerebellar region.

The right postcentral gyrus took part on several of the stronger connections for controls, which included the connection with the left postcentral gyrus and the left paracentral lobule.

5.3.4 Time Basic

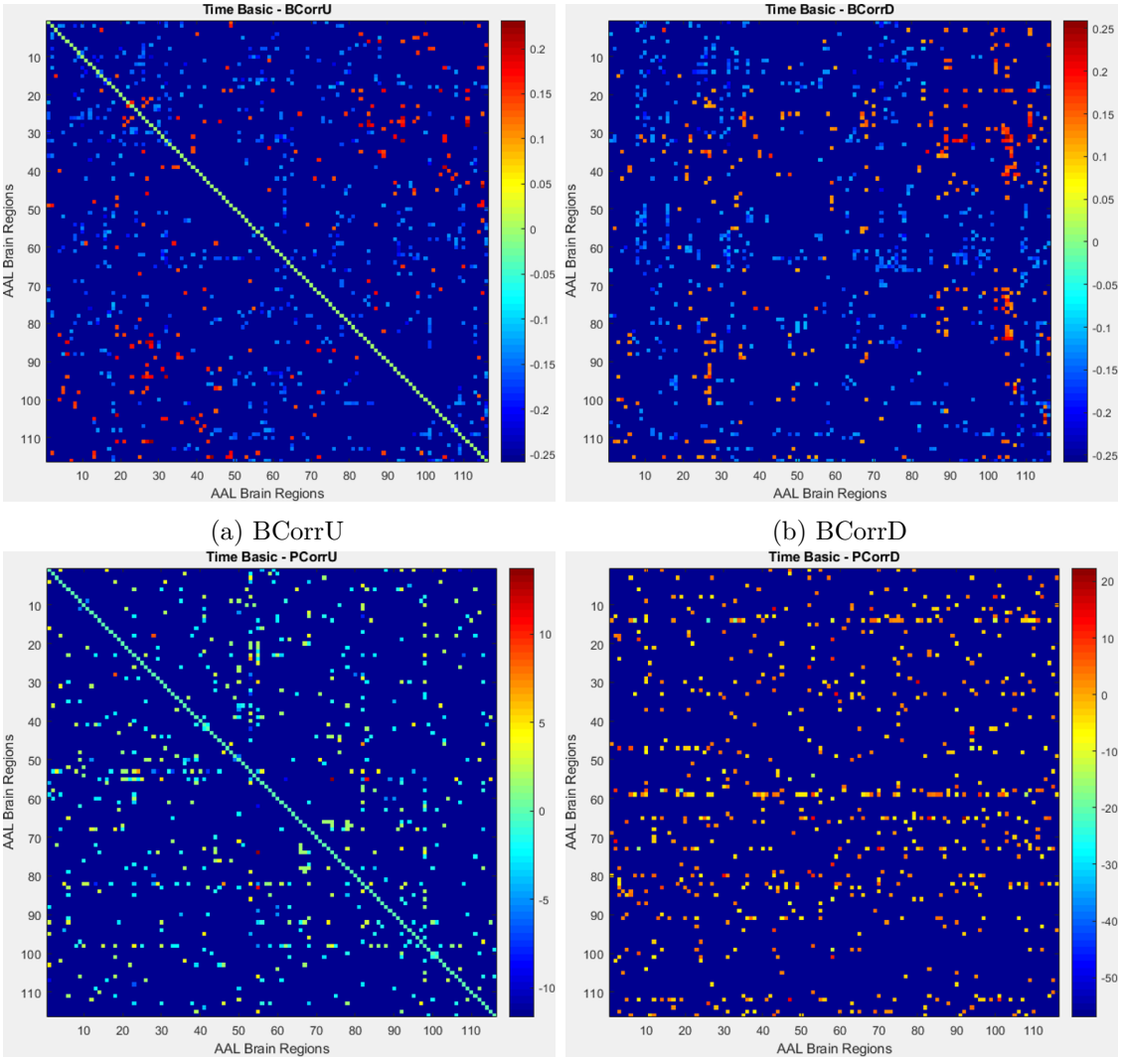

(a) BCorrU (b) BCorrD

(c) PCorrU (d) PCorrD

Figure 5.22: Results from control versus patient comparison using metrics from Time Basic family - matrices from BCorrU, BCorrD, PCorrU, and PCorrD.

Figures 5.22 and 5.23 show the results obtained for the group comparison using matrices computed by the application of metrics from Time Basic family.

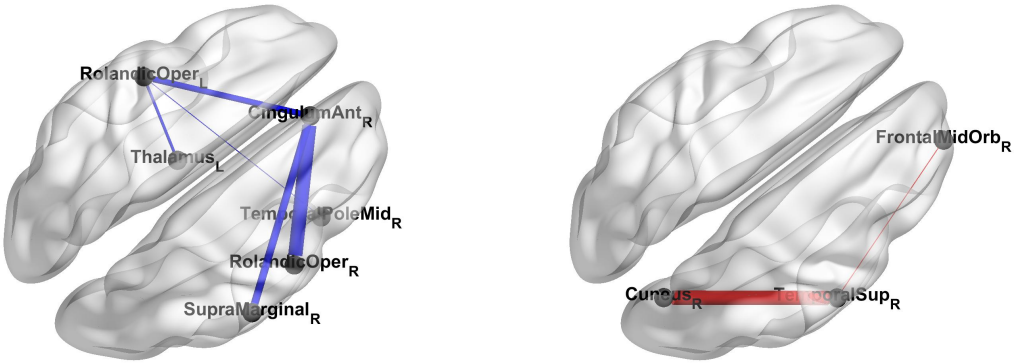

(a) BCorrU (b) PCorrU

Figure 5.23: Results from control versus patient comparison using metrics from Time Basic family - significant networks from BCorrU and PCorrU. Blue line - negative mean group difference. Red line - positive mean group difference. Line thickness - strength of the measure.

BCorrU

Significant negative mean group differences, that is, stronger connections for the ADHD group were in majority and were registered, for example, for almost every significant connection with: the left supramarginal and angular gyri, left putamen, and vermis 7. Connections within the frontal lobe mostly had significant negative mean group differences.

Biggest negative differences were registered for the following connections: left putamen and right medial superior frontal gyrus; right hippocampus and vermis 7; right rolandic operculum and right anterior cingulate and paracingulate gyri. This last pair is one of the constituents of a significant network that was obtained and involves other regions (figure 5.23a). In this subnetwork all the connections correspond to negative mean group differences.

Significant positive mean group differences were registered for several areas from the temporal lobe and for connections between the cerebellum and the frontal lobe, and also for connections with the left supplementary motor area (including with: left superior occipital gyrus, right superior parietal gyrus, left superior temporal gyrus, and left inferior temporal gyrus).

Significant connections with vermis 8 and 9 mostly had positive mean group differences. In addition, significant positive mean group differences were also registered for connections between cerebellum 8 and 9 and both amygdala and parahippocampal gyrus.

BCorrD

In this comparison, significant mean group differences were similar, as expected, with the previous metric.

Once again, significant mean group differences for connections with the left supramarginal gyrus were mostly negative as well as connections within the frontal lobe. Significant negative mean group differences were also registered for connections with the right anterior cingulate and paracingulate gyri and the right caudate.

Biggest negative differences were registered for the following connections: left putamen→ right medial superior frontal gyrus; left middle cingulate and paracingulate gyri→right anterior cingulate and paracingulate gyri; right insula → right medial superior frontal gyrus; right anterior cingulate and paracingulate gyri → right rolandic operculum.

Significant positive mean group differences were registered for the same areas as mentioned above (areas from the temporal lobe and connections between the cerebellum and the frontal lobe). However, some clusters were registered this time, for example, for connections between the central structures and the following cerebellar regions: right cerebellum 7b, right cerebellum 8, and left cerebellum 9. Another cluster appeared for connections happening between all the following areas and the previously mentioned cerebellar regions: bilateral insula, bilateral anterior cingulate and paracingulate gyri, right middle cingulate and paracingulate gyri, and parahippocampal gyrus.

PCorrU

The biggest positive mean group differences were registered for the connections: right putamen and left fusiform; left superior temporal gyrus (temporal pole) and left fusiform; right rolandic operculum and right gyrus rectus.

On the other hand, the biggest negative mean group differences, were registered for: left middle frontal gyrus and left inferior occipital gyrus; left fusiform and right inferior parietal gyrus.

The following regions had more connections with significant mean group differences: left inferior occipital gyrus, right superior temporal gyrus, and right cerebellum 4 and 5. In fact, the right superior temporal gyrus comprises a significant network obtained for this metric that only has connections with positive mean group differences and includes two other regions, the right cuneus and the right orbital part of the middle frontal gyrus (figure 5.23b).

PCorrD

For this comparison, the biggest positive mean group differences were registered for: left angular gyrus → right cerebellum crus 1; left angular gyrus → left superior temporal gyrus (temporal pole); opercular part of the left inferior frontal gyrus → left calcarine fissure and surrounding cortex; right insula → right heschl gyrus.

Biggest negative mean group differences were registered for: right cerebellum crus 2 → left lingual gyrus; triangular part of the right inferior frontal gyrus → orbital part of the right middle frontal gyrus; right postcentral gyrus → left supplementary motor area.

The following regions had several connections with significant mean group differences: triangular part of the right inferior frontal gyrus, left superior parietal gyrus, left angular gyrus, left putamen, right superior temporal gyrus, and vermis 6.

General considerations on the results from Time Basic

When using bivariate metrics it was evident that connections within the frontal lobe were stronger for the ADHD group as well as connections with the central structures, insula, and cingulate, including the left putamen.

Connectivity differences between the groups for connections with insula and cingulate were registered with all the metrics, specially for the right insula and right anterior cingulate and paracingulate gyri.

With bivariate metrics it was also evident that connections between frontal and cerebellar regions were stronger for controls.

The left supplementary motor area had connectivity differences with regions from the parietal lobe that were registered with several metrics, having both stronger connections for controls and ADHD subjects.

Areas from the temporal lobe were registered to have connectivity differences using all the metrics. For example, the left superior temporal gyrus had stronger connections for controls regarding connections with frontal, parietal, and temporal regions itself.

5.3.5 Frequency Basic

BCohF

For all of the considered frequencies, the connectivity strength was, for the most part, registered to be stronger for the ADHD group, as the significant mean group differences were mostly negative (figure 5.24). Positive mean group differences were registered for few pairs of brain regions.

BCohF1: Negative mean group differences were registered across almost every brain region, in particular, for connections with the parietal, temporal, and occipital lobes, and with regions from the cerebellum and vermis. The biggest negative difference was seen for the pair left cerebellum 7b - left cerebellum 6.

Positive mean group differences were registered for the connections: left anterior cingulate and paracingulate gyri - left orbital part of the inferior frontal gyrus (biggest difference); left medial superior frontal gyrus - left orbital part of the inferior frontal gyrus; right olfactory cortex - right orbital part of the middle frontal gyrus and left gyrus rectus; left medial superior frontal gyrus - gyrus rectus; left anterior cingulate and paracingulate gyri - left orbital part of the middle frontal gyrus; left angular gyrus - left posterior cingulate gyrus; vermis 9 - left cerebellum 9.

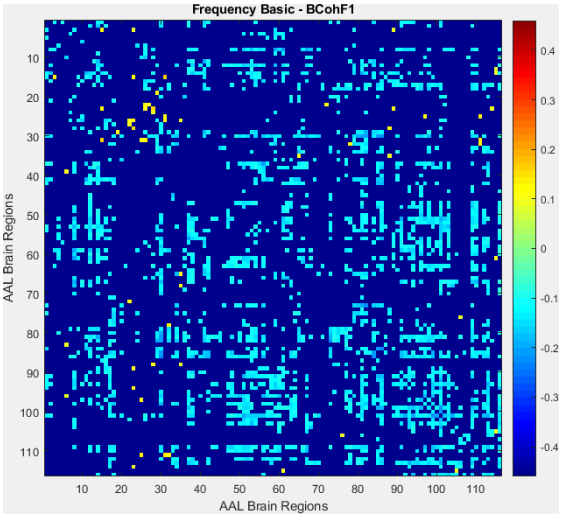

(a) BCohF1

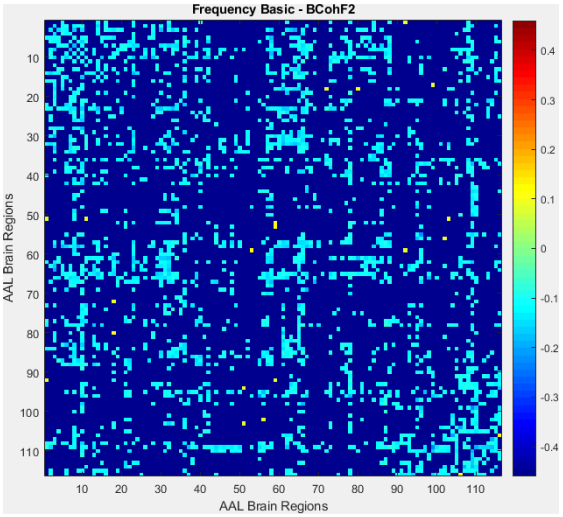

(b) BCohF2

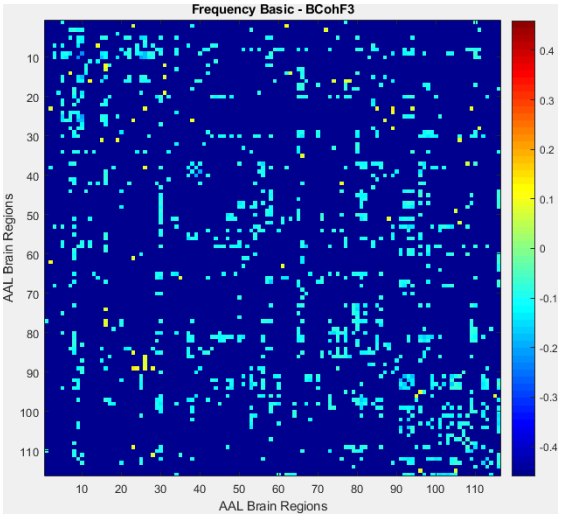

(c) BCohF3

Figure 5.24: Results from control versus patient comparison using metrics from Frequency Basic family - matrices from Fourier Based Coherence.

BCohF2: Positive mean group differences were registered for the pairs: left superior parietal gyrus - left inferior occipital gyrus (biggest difference); right caudate nucleus - right rolandic operculum; right heschl gyrus - right rolandic operculum; left cerebellum 6 - left rolandic operculum.

Negative mean group differences were registered across almost every brain region, including frontal and parietal lobes, insula and cingulate regions, and within regions from the cerebellum and vermis. In addition, there were several significant negative mean group differences for cerebellum 10, vermis 1, 2 and 3. The biggest mean group difference was registered for the pair: vermis 1 and 2 - left cerebellum 6.

BCohF3: Positive mean group differences were found for connections happening with several areas from the frontal lobe, including the connections: right triangular part of the

inferior frontal gyrus - left middle frontal gyrus; right orbital part of the inferior frontal gyrus - right opercular part of the inferior frontal gyrus, right putamen and thalamus; left medial superior frontal gyrus - left inferior temporal gyrus and left middle temporal gyrus. The pair right pallidum - right amygdala also had a connection with a positive mean group difference. The biggest positive mean group difference was observed for: left inferior temporal gyrus - left medial superior frontal gyrus.

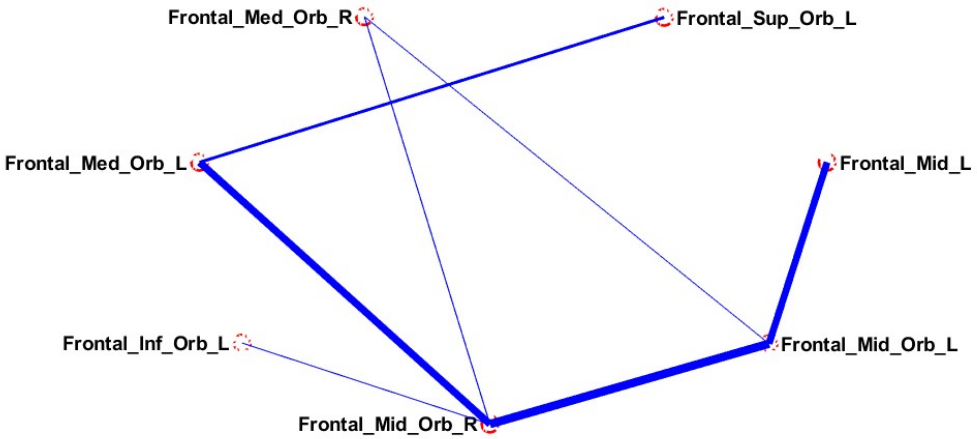

(a)

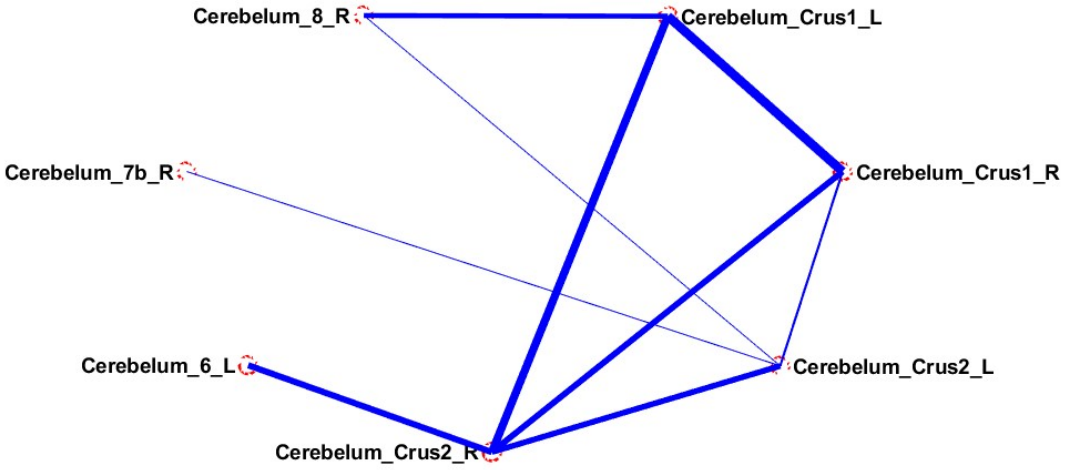

(b)

Figure 5.25: Results from control versus patient comparison using metrics from Frequency Basic family - significant networks from BCohF3. Blue line - negative mean group difference. Red line - positive mean group difference. Line thickness - strength of the measure.

Several significant negative mean group differences were registered for connections with: middle frontal gyrus, insula, and heschl gyrus. On the left hemisphere, the superior temporal gyrus had several connections with significant negative mean group differences. The biggest negative difference was registered for: right orbital part of the middle frontal

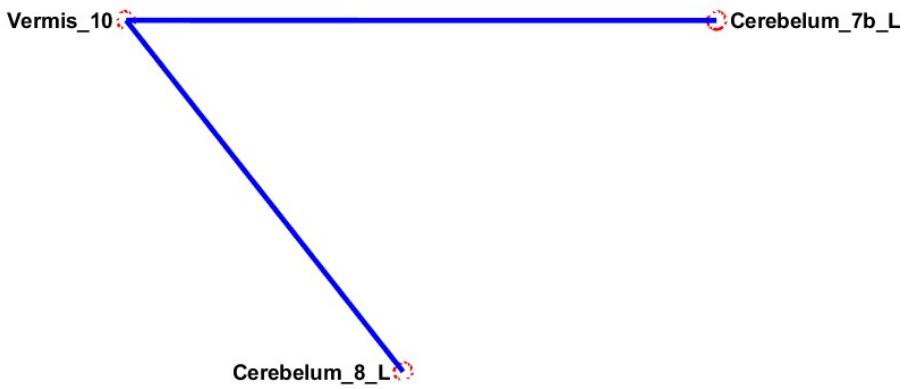

(a)

Figure 5.26: Results from control versus patient comparison using metrics from Frequency Basic family - significant network from BCohF3. Blue line - negative mean group difference. Red line - positive mean group difference. Line thickness - strength of the measure.

gyrus - left orbital part of the middle frontal gyrus. These two regions belong to a subnetwork that was obtained and only comprises connections that are stronger for the ADHD group, involving several regions from the frontal lobe (figure 5.25a).

Other two significant subnetworks were obtained for this metric, both of them only composed by regions from the cerebellum (figure 5.25b and 5.26) and with connections that only showed negative mean group differences, that is, higher value of connectivity strength for the ADHD group.

BCohW

For all of the considered frequencies, the number of significant positive and negative mean group differences was approximately the same. Furthermore, the three matrices obtained had several significant connections in common (see figure 5.27).

Significant positive mean group differences were registered between the left angular gyrus and regions from the frontal lobe, the medial superior frontal gyrus and several brain regions, the left cerebellum 9 and regions from the occipital lobe and the central structures, and between the right posterior cingulate gyrus and regions from the frontal lobe. These last connections could be seen on one subnetwork, that only had connections with positive mean group differences and was obtained for BCohW1 (figure 5.28b).

The left angular gyrus was found to be comprised in another subnetwork obtained for the same metric, making up, with the orbital part of the left inferior frontal gyrus, the only pair with a connection having a positive mean group difference in the given subnetwork (figure 5.28a). This same connection also appeared on another subnetwork obtained for BCohW3 (figure 5.30a).

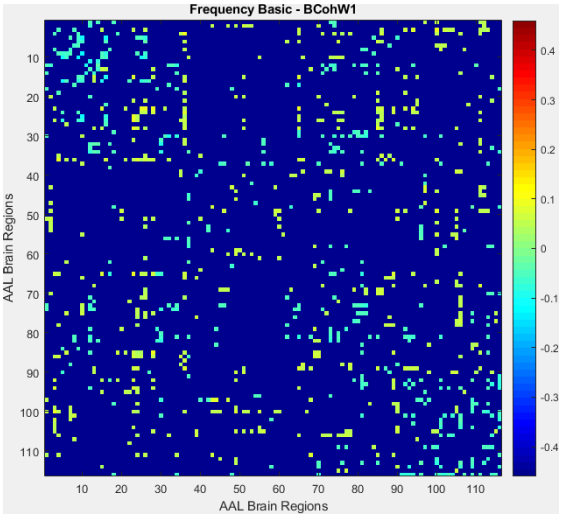

(a) BCohW1

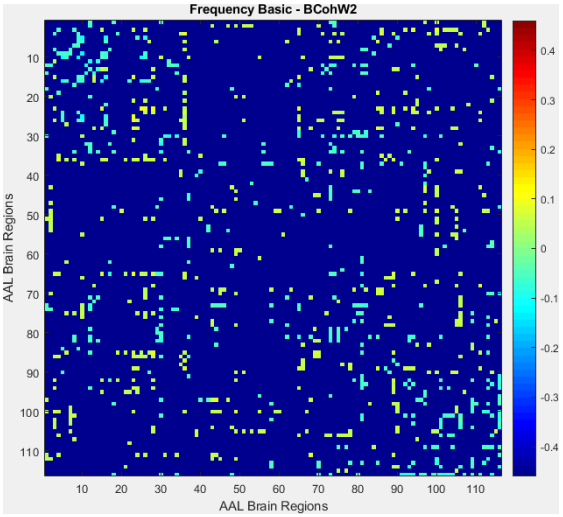

(b) BCohW2

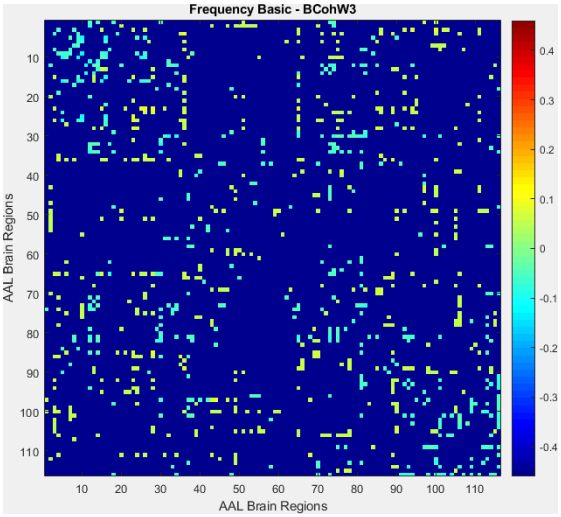

(c) BCohW3

Figure 5.27: Results from control versus patient comparison using metrics from Frequency Basic family - matrices from Wavelet Based Coherence.

One of the biggest positive mean group differences that was significant for all the frequencies happened for the connection right gyrus rectus - left medial superior frontal gyrus and can be found in the subnetworks depicted in figures 5.28d and 5.30a.

Significant negative mean group differences were found within the frontal lobe, and within cerebellum and vermis. In addition, they were found for connections happening between the insula and the central structures and between some regions from the temporal lobe and both the left putamen and pallidum.

The previously mentioned brain regions were seen in several significant subnetworks. For example, a subnetwork obtained for BCohW3 with several regions from the frontal lobe, the cerebellum, and the central structures that only had significant negative mean group differences (figure 5.30b). Other networks that showed the negative differences within connections from the frontal lobe can be seen in figures 5.28a and 5.28c obtained for

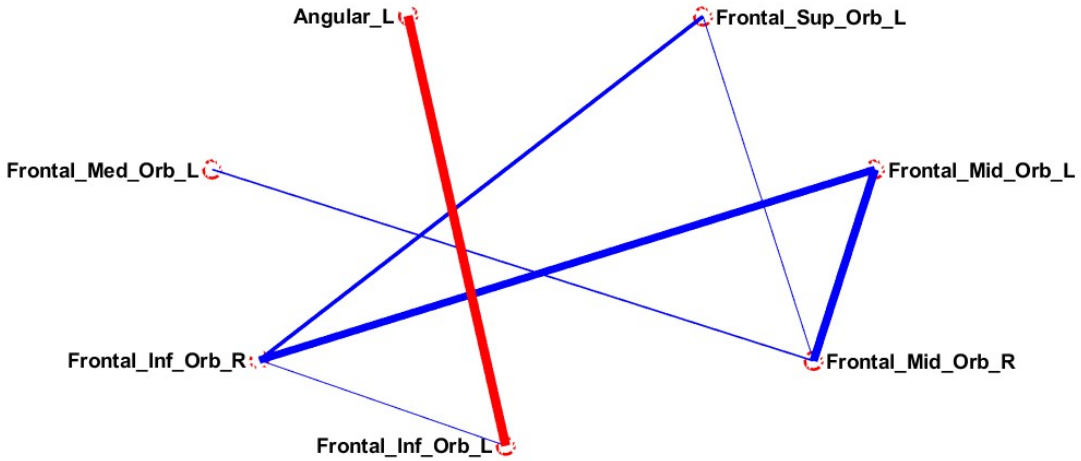

(a) BCohW1

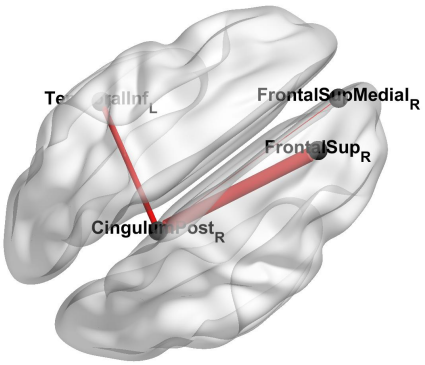

(b) BCohW1

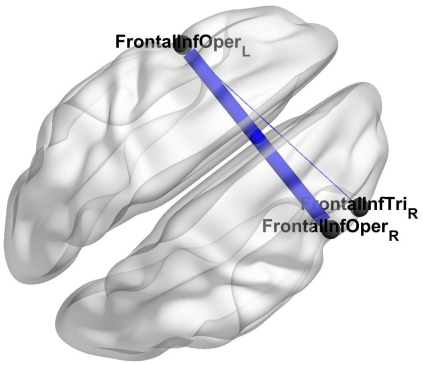

(c) BCohW1

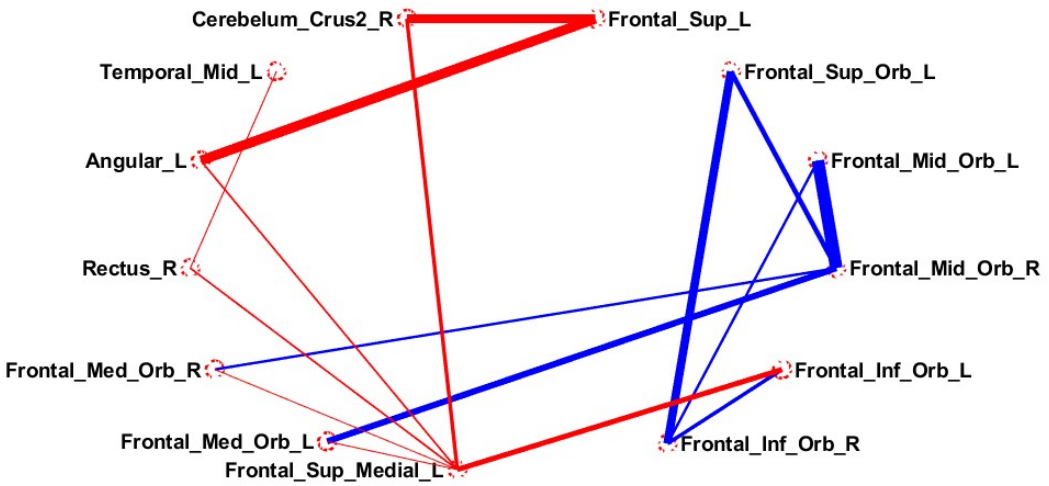

(d) BCohW2

Figure 5.28: Results from control versus patient comparison using metrics from Frequency Basic family - significant networks from BCohW1 and BCohW2. Blue line - negative mean group difference. Red line - positive mean group difference. Line thickness - strength of the measure.

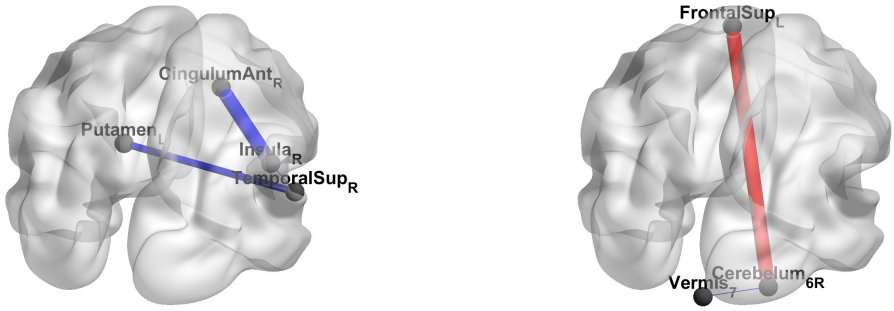

(a) BCohW1 and BCohW2 (b) BCohW3

Figure 5.29: Results from control versus patient comparison using metrics from Frequency Basic family - significant networks from BCohW1, BCohW2, and BCohW3. Blue line - negative mean group difference. Red line - positive mean group difference. Line thickness - strength of the measure.

BCohW1, and in figure 5.28d, obtained for BCohW2. This last network is almost identical to the one depicted in figure 5.30a that was obtained for BCohW3.

As for positive mean group differences, the biggest significant negative mean group difference was the same for all the frequencies and happened between the right and left orbital part of the middle frontal gyrus.

General considerations on the results from Frequency Basic

Using Fourier based coherence, several connectivity differences between the control and the ADHD groups were found. In particular, it was evident that connections within regions from the cerebellum and vermis were stronger for the ADHD group.

Regarding connections within the frontal lobe, the last two frequencies showed several significant connections with negative mean group differences. On the other side, positive differences, that is, stronger connections for the control group, were found for connections happening with the frontal lobe.

Central structures and regions from the insula and cingulate also showed both positive and negative connectivity differences between the groups.

Using wavelet based coherence, stronger connections for the ADHD group were, once again, found within the frontal lobe and within the cerebellum and vermis.

The central structures, as before, had both connections with positive and negative mean group differences.

Stronger connections for the control group, as in Fourier based coherence, were observed for connections with regions from the frontal lobe, in particular, with cingulate and angular gyri. The left angular gyrus had several connections with significant positive mean group differences.

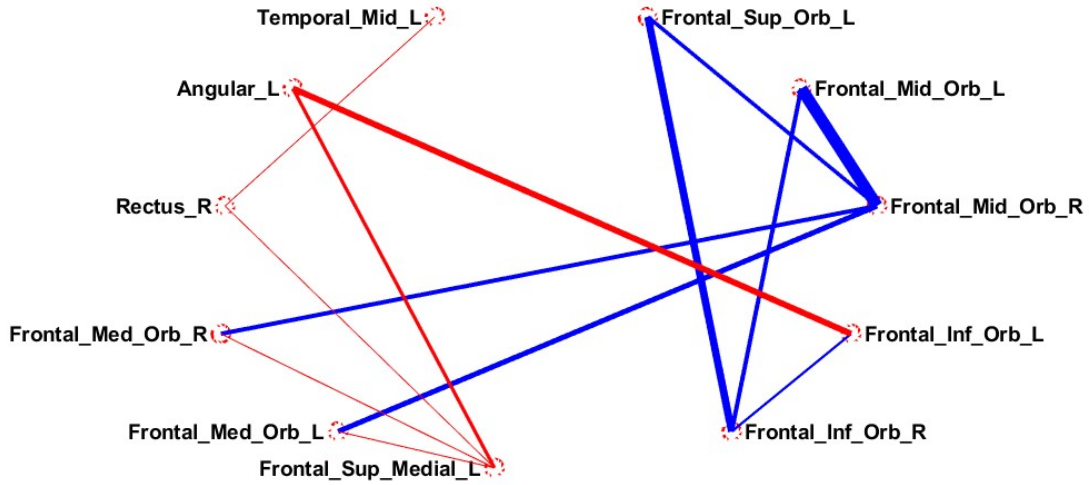

(a)

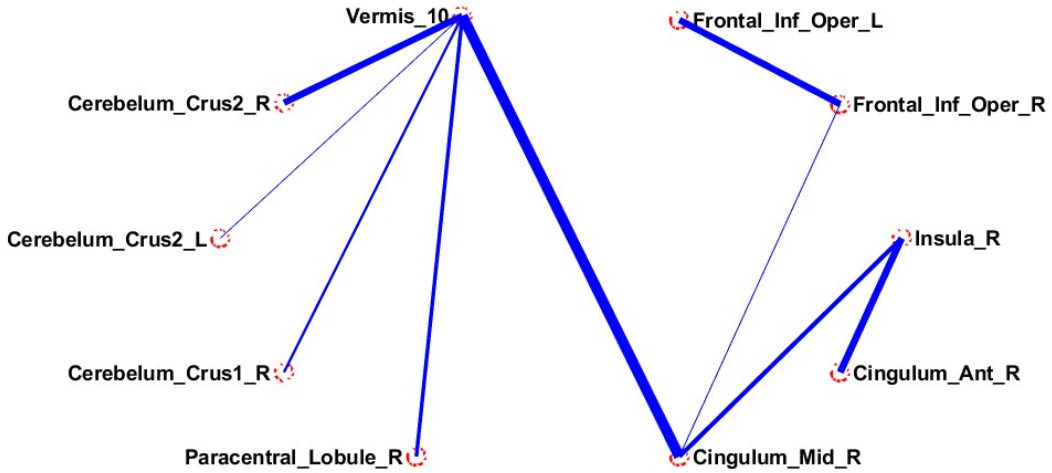

(b)

Figure 5.30: Results from control versus patient comparison using metrics from Frequency Basic family - significant networks from BCohW3. Blue line - negative mean group difference. Red line - positive mean group difference. Line thickness - strength of the measure.

Overall Discussion of Results from Approach B

When comparing the pathological and the healthy subjects, some regions had connectivity differences which were consistent even across different metrics. In the following paragraphs some of these differences will be pointed out. A brief description of some of the functions of each region will be provided as well as notes concerning previous studies.

Frontal lobe:

Regarding the frontal lobe, the rolandic operculum, the supplementary motor area, and the paracentral lobule had several connections with significant mean group differences. The frontal gyrus (inferior, middle, and superior) was also seen to have connectivity differences between the two groups when using different metrics. In fact, several networks that were obtained showed stronger connections for the ADHD group within the frontal lobe. Take, for example, the ones depicted in figures 5.14b, 5.20b, and 5.28c.

The rolandic operculum had several significant connectivity differences that were seen with: PTEU, PH2U, BH2U, BCorrU, BCorrD, PCorrU, and BCohF2. These significant connections comprised both positive and negative mean group differences and happened with areas from the whole brain. In particular, stronger connections for the ADHD group involving the right rolandic operculum were found when using bivariate Time Basic metrics. In this case, the connection with the right anterior cingulate and paracingulate gyrus was one of the strongest. When using BH2U, the right rolandic operculum also had several significant connections that were stronger for the ADHD group.

The supplementary motor area had stronger connections for controls happening with the occipital and frontal regions that were found with BTEU, BTED, and BCorrU. On the other hand, this region had stronger connections for the ADHD group when using PCorrD, BH2D, and PH2D, which happened, respectively, with the postcentral gyrus, cuneus, and heschl gyrus.

Studies regarding ADHD mention one area several times, stating that it is involved in the pathological mechanisms of this disease: the PFC. The PFC is the cerebral cortex located in the frontal part of the frontal lobe. This region can be functionally subdivided into smaller regions which do not have clear boundaries defined on the literature and are: dorsolateral, dorsomedial, ventromedial, ventrolateral, and orbitofrontal cortex. In addition, some also consider the ACC as belonging to the PFC [17].

Regarding its function, the PFC is related with cognitive control, including planning, attention, decision making, and working memory. In particular, the dlPFC is an important component of the executive control network that plays an important role in the signalling of several cognitive processes, such as attention and working memory. In fact, as component of the executive control network, it receives information from the ventral and dorsal attentional networks and integrates attentional cues to control behavioural responses in the context of the frontostriatal system [64]. The frontostriatal system is comprised by the dlPFC, the dorsal caudate, the putamen, and the thalamus.

For the sake of simplicity, as the boundaries of the given structure are not clear, it will be considered that the dlPFC is comprised by part of the middle frontal gyrus (including the orbital part). Hence, focusing on the middle frontal gyrus, several connectivity differences between the two groups were found. For example, there were several stronger connections for the ADHD group, when using BH2U and BCohF3, and several stronger connections for the control group, when using BH2U and BMITU. However, none of the connections that were pointed out has the same direction of abnormality as found in the literature. For example, in the study from Posner et al. they reported decreased connectivity for ADHD subjects between the left dlPFC and the right dACC, both components of the executive control network [64], whereas in the present study it was found increased functional connectivity between the left anterior cingulate and paracingulate gyri and the left orbital part of the middle frontal gyrus, using BCohF1. Nevertheless, this is in accordance with findings from another study in which subjects with ADHD were found to have enhanced coherence between different networks and reduced coherence within the same network [43].

The OFC was also reported to have several connectivity differences for subjects with ADHD among the literature. This area is a core component of the emotional regulation system, which is one of the systems involved in the dual pathway model of ADHD [64]. In the present study, considering orbital parts of the of the superior, middle and inferior frontal gyri, several connectivity abnormalities were found. In particular, stronger connections for the ADHD group were registered between the orbital part of the left middle frontal gyrus and amygdala, using BTEU. Furthermore, with BCohW, bivariate metrics from Hsquare and Time Basic families, and metrics from Mutual Information, several stronger connections for the ADHD group were registered within the frontal region. Using BTEU, stronger connections for the ADHD group between regions from the frontal and temporal lobes were found.

On the other hand, decreased connectivity for the ADHD group was found: with Hsquare metrics and BMITU, between several regions and the orbital middle frontal gyrus; with BCohF1, between the orbital part of the inferior and middle frontal gyrus and other frontal areas and the ACC; with BCohF3, between the orbital part of the right inferior frontal gyrus and the putamen, thalamus, and the opercular part of the inferior frontal gyrus; with Time Basic metrics, between cerebellar and frontal regions. Furthermore, several significant networks with connectivity differences involving regions from the OFC were found, such as the ones depicted in: 5.14a, 5.21a, 5.25a, 5.28a, 5.28d, and 5.30b.

Regarding some of the previously mentioned connections, it is important to say that both the putamen and the thalamus are components of the frontostriatal system whose main function is to respond to environmental demands by inhibiting or facilitating the needed responses [64]. Our findings are in accordance with group differences reported on the cortico-striato-thalamo loops [65], in particular, decreased connections between regions from the striatum and thalamus and cortical areas found by Cao et al. [15]. Nonetheless, opposite findings where reported in another study [78], which have been suggested to be

related to the size of the used sample, as it was much smaller in this last study.

Insula:

The right insula had stronger connections for controls happening with several brain regions. Using BCorrD, this area had bigger connectivity strength for controls for connections with several cerebellar regions, that included: right cerebellum 7b and 8 and left cerebellum 9. Using PCorrD, the right insula had stronger connectivity with the right heschl gyrus. In addition, this region comprised, along right cerebellum, the connection showing the biggest positive mean group difference when using PTED, and, along vermis 3, the connection with the biggest positive mean group difference when using PH2D.

Connections involving the right insula not only had stronger values for the control group but also for the ADHD group. Using BMITD1 and BCorrD, the connections with the right median cingulate and paracingulate gyri and with the right medial superior frontal gyrus, respectively, were stronger for the patient group. Using PTEU, the connection with the right posterior cingulate gyrus, and, using PH2D, the connections with the left pallidum, and vermis 1 and 2, were also stronger for the patient group. Using PTED, the connection with vermis 1 and 2 was also significant and had a negative mean group difference. In addition, when it comes to metrics from the frequency domain, the insula had several connections which were stronger for the ADHD group. Regarding, significant subnetworks involving the right insula, two were found for PMITU and BCohW1/2 depicted, respectively, in figures 5.20a and 5.29a.

The insular cortex can be macroscopically divided into anterior and posterior insula, each of these having different structural connections [38, 61]. This area is involved in complex functions and represents an important integration hub that takes part on sensory processing, feeling representation, motor control, decision making, and empathy. Together with the dACC, the insular cortex plays an important role in the coordination of functional networks in accordance with demands [38].

In particular, the anterior insula is involved in integration of information coming from autonomic and visceral systems into several functions, such as: emotional, cognitive, and motivational functions. In fact, studies have suggested that the dlPFC gets salient information from the anterior insula that is needed to cognitive processes (e.g. attention and working memory), and that the vmPFC gets information from the same region related with past behavioural outcomes, and uses it to make future decisions [61]. The posterior insula, in its turn, is also involved with integration and has an important role in somatosensory, vestibular, and motor functions.

Hence, the insular cortex connects different systems related with different processes (sensory, emotional and cognitive) and, by monitoring the environment and taking into consideration past experience, it is able to predict actions, contributing to the decision making process [38].

In the present study, stronger connectivity between the insula and the anterior cingulate and paracingulate gyri was found for the ADHD group, which was also found by Tian et

al. in a study which focused on the dACC. In Tian's study, authors proposed that this connectivity difference could indicate abnormalities of autonomic control functions, which had support on findings from previous studies regarding ADHD [78].

Cingulate and paracingulate:

Regarding the posterior cingulate gyrus and the median and anterior cingulate and paracingulate gyri several connections with significant group differences were found.

The anterior cingulate and paracingulate gyri had several stronger connections for the ADHD group, that happened, for example, with: the right rolandic operculum and the left median cingulate and paracingulate gyrus, when using BCorrU and BCorrD. This same region also had stronger connections for controls with several cerebellar regions, when using BCorrD. In addition, other stronger connections for controls were also seen when using BCohF1 for connections with the orbital part of the left middle and inferior frontal gyrus. Three significant networks were found involving the anterior cingulate and paracingulate gyri that can be found in figures: 5.18b, 5.23a, and 5.29a.

The median cingulate and paracingulate gyrus had several significant differences detected when using PH2D. For BCorrU, this region had a connection, that was already mentioned, happening with the right anterior cingulate and paracingulate gyri, which was one of the strongest for the ADHD group. With the same metric, this region was seen to have significant connections that were stronger for the control group and happened with several regions from the cerebellum. For BMITD1, the connection between the median cingulate and paracingulate gyrus and the insula was also stronger for the ADHD group.

The posterior cingulate gyrus, on its turn, had connectivity differences registered with BH2U, BMITU, PTEU, BH2U, and metrics from the frequency domain. Except for PTEU, the most significant connections involving the posterior cingulate gyrus, were stronger for the control group. With PTEU, this region was seen to be involved in one of the strongest connections for the ADHD group, registered with the right insula. One significant network involving the right posterior cingulate gyrus was found using BCohW1 (figure 5.28b).

The ACC is an important component from the executive control network and constitutes the focus of several studies regarding ADHD, in which it was reported decreased connectivity between this region and components from the DMN. These were postulated to offer a neurocognitive model of impaired attentional functioning as this decreased connectivity was found associated with attentional lapses [65].

Mostert et al. [59] found increased connectivity within executive control network. Tian et al. [78] found increased connectivity between the dACC and the thalamus, cerebellum, insula, and brainstem.

The PCC is a highly structurally connected region and one of the regions with the higher metabolic rate across all the brain. In fact, it is an important hub for information processing [52] and was seen to have complex patterns of functional connectivity, taking part in different intrinsic networks, including the DMN.

Authors have shown that the changes in activity magnitude from the PCC are related with cognitive load and that its improper deactivation is linked with inefficient cognitive function. Leech et al. [52] showed that different parts of PCC functionally interact with distinct intrinsic networks suggesting that it plays a role in coordinating these networks.

Alterations regarding PCC were seen to be associated with clinical impairments in several conditions, including ADHD. In particular, Castellanos et al. [20] and Fair et al. [30] found reduced functional connectivity between the vmPFC and PCC. Others found decreased connectivity between the dACC and PCC [70, 76]. This decreased connectivity was associated with age in controls, supporting the theory that impaired cognitive control is related with delayed neuromaturation in ADHD [30]. Increased volume on the PCC was also found in ADHD [52].

In this study, several connectivity differences between ADHD and control subjects were found, for example, it was seen higher connectivity strength for controls, using PTEU, regarding the connection between PCC and the insula, which is a component of the frontoparietal control network(anterior insula). This is in agreement with previous findings on connectivity patterns between these two networks.

Central structures:

The central structures were also registered to have connectivity differences between the control and the ADHD groups. For example, when it comes to metrics from the frequency domain, using BCohF, these structures were seen to have stronger connections for controls, regarding the frontal lobe, and, when using BCohW, they had stronger connections for the ADHD group for connections with regions from the insula.

In particular, the putamen had connectivity differences pointed out when using Hsquare and Time Basic families, showing both positive and negative mean group differences regarding connections with regions from all the brain.

The putamen is structurally connected with cortical motor areas and is involved in working memory and language processing. It is a component of the frontostriatal system which, as mentioned before, is critical for behavioural responses according to environmental demands. This area was shown to have several structural and functional abnormalities in ADHD subjects, such as reduced volume associated with symptoms, or association between lesions and symptoms [16].

Cao et al. found decreased connectivity in ADHD subjects between the left putamen and: the right superior frontal gyrus, and the superior and middle temporal gyrus. In this study, connectivity differences involving the same connections were found, however, having stronger connectivity for the ADHD group.

Parietal lobe:

Connectivity differences between the control and the ADHD groups regarding the parietal lobe were seen across all the metrics specially regarding the temporal and frontal lobes.

The supramarginal gyrus had several connections stronger for ADHD group, when using Time Basic metrics, and was even present in a network obtained that involves the

rolandic operculum, the anterior cingulate and paracingulate gyri, and the middle temporal gyrus (temporal pole). The supramarginal gyrus is a component of the ventral attentional network which monitors behaviourally salient stimuli and whose intranetwork decreased connection was correlated with executive attention deficits [64]. Nothing was stated about its increased connection in the same study.

The precuneus had connectivity differences between the two groups registered when using BMITU and PH2D, having several stronger connections for controls when using the first metric. This region is one of the components from DMN and, in previous studies, it was found to have decreased correlation with dACC [20] and with dlPFC [43].

The angular gyrus also had several group differences registered with several metrics, including: PH2D, BTEU, PCorrD, and metrics from the frequency domain. In particular, the left angular gyrus was found in several significant networks that can be found in figures: 5.15, 5.28a, 5.28d, and 5.30a.

Temporal lobe:

The temporal lobe also had several connectivity differences between the control and the ADHD groups. It was found increased connectivity for the ADHD group between the temporal lobe and the central structures (BH2U and BCohW) and between the temporal lobe and both the frontal and parietal lobes (BTEU). It was found several connectivity differences for connections across the whole brain regarding this area, when using BCohF1.

Concerning particular regions from the temporal lobe it was found several connections that were stronger for the ADHD group, such as: left fusiform - left superior frontal and right superior occipital gyrus (PH2U); left heschl gyrus - right inferior temporal gyrus, left precuneus, and right supplementary motor area (PH2D); right heschl gyrus - vermis 1 and 2 (PH2D). Using transfer entropy metrics, it was found several connectivity differences involving the amygdala and the left superior temporal gyrus. In addition, it was also found significant group differences involving hippocampus and fusiform gyrus, using Time Basic metrics. The amygdala and the hippocampus are both components of the emotional regulation system and its impaired connection with other brain areas have been correlated with altered arousal and appraisals of emotional stimuli and deficits in motivation and reward which are found in ADHD subjects [64].

Stronger connections for the control group between the occipital and temporal lobes were found with BTEU. The right heschl gyrus also had several stronger connections for controls seen with: PCorrD (right insula) and BCohF2 (right rolandic operculum). In particular, regarding the parahippocampal, significant group differences were found with: bivariate Transfer Entropy metrics, BMITU, BCorr, and BH2U. Stronger connections were found for controls for areas from occipital lobe (BTED and BTEU) and vermis and cerebellum (BTEU, BTED, and BCorrU) as well as for several regions (Mutual Information and Hsquare families).

Cerebellum and Vermis:

Stronger connections for the ADHD group were found within cerebellum and vermis (BH2U, metrics from Mutual Information, BCohW, and BCohF), and between cerebellum and other areas, such as temporal regions (BH2U, PTEU, and BTED), occipital regions (PH2U), and insula (PH2U and PTED).

Stronger connections for the control group were found between the cerebellum and both the frontal lobe (BTEU, BCohF2, and bivariate Time Basic metrics) and the temporal lobe (bivariate Transfer Entropy and Time Basic metrics).

Several significant networks involving areas from vermis and cerebellum were found, in particular, the ones depicted in figures 5.15, 5.25, 5.30b, and 5.29b.

The cerebellum is involved in autonomic functions and has been suggested to play an act in facilitating cortical modulation of brainstem autonomic nuclei. Due to this function, Tian et al. suggested that its increased connection with dACC in ADHD subjects suggests abnormalities in autonomic control. In the literature not much information is found regarding these areas when it comes to functional connectivity studies on ADHD, however, reduced volume and underdevelopment was also reported [27].

CHAPTER 6

Conclusion

The purpose of this study was to identify useful tools for brain image classification. In particular, to study if certain metrics of brain functional connectivity led to a better characterization of certain brain connections. It was indeed clear that regional specificity exists and different metrics detect in a distinct way the association between different brain regions. To our knowledge this was never shown in such a systematic way.

It was followed two independent procedures that showed that there is variability between different metrics in what regards different brain connections. The reason for this difference is beyond the scope of this study and we suggest that future work may assess to what extent the results of inter-metric comparisons depend on connection types (i.e. association, projection, and commissural), connection lengths or even fiber density.

We further suggest that, in future research, parameter optimization prior to matrix construction should be done in order to guarantee a proper application to the data under analysis. In the present study, it was used parameters that were already optimized by Wang et al. but its proper adaptation to the data under analysis is not guaranteed and may not be ideal. In fact, we suspect that undefined weights that were obtained and led to the exclusion of some matrices may have been caused by improper parameter application. This specific problem, however, may be, in part, related with the short duration of each sliding window which is known to affect metric's performance.

In approach A, it was performed a pairwise metric comparison. Here, due to the type of comparison that was done and the fact that different metrics have different ranges, a normalization procedure was undertaken. We suggest that future studies apply different normalization procedures in order to see in what extent the results are affected.

It was found substantial differences between the metrics, but few significant patterns stood out. We propose that, in the future, comparison between the results from each metric and another type of data, such as structural data may be done. Hence, it could

be studied if a given metric better correlates with connectivity distance or white tracts density than others. Simulated data can also be used, as this is already an usual procedure used to compare different metrics.

The use of simple methods such as Pearson's correlation facilitates communication [92] as it is easy to understand and fast to compute, justifying its almost universal use. Furthermore, previous studies have shown that brain connections are almost Gaussian in the healthy brain. For instance, in a study with a healthy sample, non-linearities neglected by the use of linear correlation were seen to be minor [42]. Furthermore, in another study, also performed with healthy subjects, metrics based on higher order statistics, phase or temporal lag performed poorer than the others, which is an indicative that the BOLD signal is close to gaussianity [72] .

However, it is known that non-linearities exist in neural dynamics and have been reported on several studies [42]. A small contribution of non-linearities associations are known to affect the BOLD signal in both timing and amplitude [92]. There are even suggestions that they may play an important role in pathological tissues. In fact, in a recent study with epileptic children, this small amount of non-linearities made a significant difference in terms of group distinction [92]. In this study, authors stated that the use of generalized measures, such as mutual information, that do not assume any relationship between the variables, is important, as there are suggestions that the dynamics of the pathological brain may involve even more complex associations than the normal brain. This group warned that this may not apply to other diseases and future work should study the generalization of this finding.

In approach B, we looked for impaired connections regarding a well studied disease (ADHD). To do so, we compared diseased an healthy subjects using different metrics. Then, the obtained results were confronted with the known affected areas described among the literature. Here, several limitations arised.

First, almost every study found in the literature used Pearson's correlation coefficient to characterize connections. So, the comparison with our results was not ideal and may even be considered very incomplete. Second, due to the large number of brain areas, this was an exhaustive work where only general patterns were seen and mentioned. It must be said that some affected areas might have been unmentioned as it was impossible to name all the significant connections with group differences. Another problem concerns the different parcellations used in the literature which were sometimes very different from the AAL parcellation. Thus, it was difficult to compare results as a given AAL area sometimes corresponded to a portion of a given area from another atlas, or even more than one area.

Results from group comparison were often very different from the literature and not even in what regards metrics directly related to Pearson's correlation coefficient, that is, metrics from Time Basic family, results were the same. However, this happened even amongst the literature itself and it must be said, as some authors have done, that different sample size and sample features may significantly affect the results.

For example, some studies, used subjects that did not ever take medication, others

used subjects that were in medication hold for a given amount of time before taking part of the study. In fact, several authors stated that medication influences brain dynamics. In addition, age was also seen to influence results from group comparison, as neural dynamics are not the same in different maturation stages.

Furthermore, metrics' performance is affected by the size of the time-series and the strength of the connection under analysis [87]. Another factor that affects functional connectivity metrics is noise, and some studies have already assessed that different metrics have different behaviours concerning different types of noise and different levels of signal-to-noise ratios. Regarding the types of noise, Wang et al. [84] saw that metrics were more robust to white noise, followed by pink, pink mixtures, and brown mixtures. They also saw that all the metrics were sensitive to noise that came either from the equipment or the environment whereas system noise did not affect metrics' performance. Other authors have seen that non-linear metrics are extremely susceptible to noise [69]. Future work should further analyse metrics' resilience to noise as, besides understanding the type of dependency each metric quantifies, it is important to know how stable they are [31].

As a matter of fact, true connections are unknown and complex, so the ideal confrontation with reality is not possible. In an attempt to mitigate this fault, we tried to compare functional connectivity differences that were found with disease models and suggest that a more detailed analysis may be done.

Comparisons from the present work led to a great number of significant results, some, easy to explain, others requiring further study. In addition, as widely recommended, correction for multiple comparisons should have been performed, as spurious false positives easily arise as the number of comparisons rise. Some authors, however, argue that correction methods may yield results that are too conservative when searching for general patterns.

The employment of graph theoretical methods could lead to a better comparison between different metrics, allowing, for example, to study how network construction is affected by the use of different metrics. Graph theory provides tools to quantify global and local topological networks proprieties and have already been used to compare some functional connectivity metrics [54].

Concluding, no optimal metric exists and they complement each other as different information is captured by different metrics [69], which are based on distinct assumptions. We suggest, as several authors, that it is better to use general metrics that not only detect linear relationships but also non-linearities, which is even more important when it is the pathological brain that is being studied. Nevertheless, we believe, that the best situation, is to use ensemble tools, such as the one used in [85], which have into account information from different metrics to characterize each connection in an attempt to capture different features of the underlying mechanism of brain functioning.

We hope that this study will lay the ground for further assessment of the specificities and complementary of connectivity metrics, paving the way for approaches that, instead of being limited to correlation, explore the wealth of available functional connectivity measures, thereby leading to a better grasp of the intricacies of the human connectome.

Bibliography

[1] *ACPI Scan Parameters*. URL: https://s3.amazonaws.com/fcp-indi/data/Projects/ACPI/ScanParameters/mta_1_scan_parameters.pdf (visited on 06/06/2018).

[2] *Addiction Connectome Preprocessed Initiative*. URL: http://fcon_1000.projects.nitrc.org/indi/ACPI/html/index.html (visited on 06/06/2018).

[3] L. An, X. H. Cao, Q. J. Cao, L. Sun, L. Yang, Q. H. Zou, R. Katya, Y. F. Zang, and Y. F. Wang. "Methylphenidate normalizes resting-state brain dysfunction in boys with attention deficit hyperactivity disorder." In: *Neuropsychopharmacology* 38.7 (2013), pp. 1287–1295. ISSN: 0893133X. DOI: 10.1038/npp.2013.27. URL: http://www.nature.com/doifinder/10.1038/npp.2013.27.

[4] O. J. Arthurs and S. Boniface. "How well do we understand the neural origins of the fMRI BOLD signal?" In: *Trends in Neurosciences* 25.1 (2002), pp. 27–31. ISSN: 01662236. DOI: 10.1016/S0166-2236(00)01995-0. arXiv: NIHMS150003.

[5] L. Badea, M. Onu, T. Wu, A. Roceanu, and O. Bajenaru. "Exploring the reproducibility of functional connectivity alterations in Parkinson's disease." In: *PLoS ONE* 12.11 (2017), pp. 1–21. ISSN: 19326203. DOI: 10.1371/journal.pone.0188196.

[6] A. M. Bastos and J.-M. Schoffelen. "A Tutorial Review of Functional Connectivity Analysis Methods and Their Interpretational Pitfalls." In: *Frontiers in Systems Neuroscience* 9.175 (2016). ISSN: 1662-5137. DOI: 10.3389/fnsys.2015.00175. URL: http://journal.frontiersin.org/Article/10.3389/fnsys.2015.00175/abstracthttp://www.ncbi.nlm.nih.gov/pubmed/26778976http://www.pubmedcentral.nih.gov/articlerender.fcgi?artid=PMC4705224.

[7] M Bear, M; Connors, B; Paradiso. *Neuroscience Exploring the Brain*. Fourth. 2016. ISBN: 9780874216561. DOI: 10.1007/s13398-014-0173-7.2. arXiv: arXiv:1011.1669v3.

[8] T. E. Behrens and O. Sporns. "Human connectomics." In: *Current Opinion in Neurobiology* 22.1 (2012), pp. 144–153. ISSN: 09594388. DOI: 10.1016/j.conb.2011.08.005. URL: http://dx.doi.org/10.1016/j.conb.2011.08.005.

[9] J. I. Bloch, E. T. Chou, and J. A. Carrino. "Magnetic Resonance Imaging." In: *Pain Management*. W.B. Saunders, 2007. Chap. 10, pp. 106–117. ISBN: 9780721603346. DOI: 10.1016/B978-0-7216-0334-6.50014-5. URL: https://www.sciencedirect.com/science/article/pii/B9780721603346500145.

[10] S. L. Bressler and V. Menon. "Large-scale brain networks in cognition: emerging methods and principles." In: *Trends in Cognitive Sciences* 14.6 (2010), pp. 277–290. ISSN: 13646613. DOI: 10.1016/j.tics.2010.04.004. arXiv: 1011.4916 [stat.ME].

[11] A. Brovkin, L. Waller, L. Dorfschmidt, D. Bzdok, H. Walter, and J. D. Kruschwitz. "GraphVar 2.0: A user-friendly toolbox for machine learning on functional connectivity measures." In: *pre-print (Arxiv)* (2018). arXiv: 1803.00082. URL: https://arxiv.org/abs/1803.00082.

[12] R. L. Buckner, F. M. Krienen, and B. T. Yeo. "Opportunities and limitations of intrinsic functional connectivity MRI." In: *Nature Neuroscience* 16.7 (2013), pp. 832–837. ISSN: 10976256. DOI: 10.1038/nn.3423.

[13] R. B. Buxton. "The physics of functional magnetic resonance imaging (fMRI)." In: *Reports on Progress in Physics* 76.9 (2015), pp. 1–61. DOI: 10.1088/0034-4885/76/9/096601.The.

[14] M. Cao, N. Shu, Q. Cao, Y. Wang, and Y. He. "Imaging Functional and Structural Brain Connectomics in Attention-Deficit/Hyperactivity Disorder." In: *Molecular Neurobiology* 50.3 (2014), pp. 1111–1123. ISSN: 15591182. DOI: 10.1007/s12035-014-8685-x.

[15] Q. Cao, Y. Zang, L. Sun, M. Sui, X. Long, Q. Zou, and Y. Wang. "Abnormal neural activity in children with attention deficit hyperactivity disorder: a resting-state functional magnetic resonance imaging study." In: *Neuroreport* 17.10 (2006), pp. 1033–1036. ISSN: 0959-4965. DOI: 10.1097/01.wnr.0000224769.92454.5d. URL: http://afni.nimh.nih.gov/.

[16] X. Cao, Q. Cao, X. Long, L. Sun, M. Sui, C. Zhu, X. Zuo, Y. Zang, and Y. Wang. "Abnormal resting-state functional connectivity patterns of the putamen in medication-naïve children with attention deficit hyperactivity disorder." In: *Brain Research* 1303 (2009), pp. 195–206. ISSN: 00068993. DOI: 10.1016/j.brainres.2009.08.029.

[17] M. Carlén. "What constitutes the prefrontal cortex?" In: *Science* 358.6362 (2017), pp. 478–482. ISSN: 10959203. DOI: 10.1126/science.aan8868.

[18] S. B. Carlyle and G. Clarke. *Magnetic Ressonance Imaging: Physical and Biological Principles*. Fourth. Elsevier, 2015. ISBN: 9780323073547.

[19] F. X. Castellanos and E. Proal. "Large-scale brain systems in ADHD: Beyond the prefrontal-striatal model." In: *Trends in Cognitive Sciences* 16.1 (2012), pp. 17–26. ISSN: 13646613. DOI: 10.1016/j.tics.2011.11.007.

[20] F. X. Castellanos, D. S. Margulies, C. Kelly, L. Q. Uddin, M. Ghaffari, A. Kirsch, D. Shaw, Z. Shehzad, A. Di Martino, B. Biswal, E. J. Sonuga-Barke, J. Rotrosen, L. A. Adler, and M. P. Milham. "Cingulate-Precuneus Interactions: A New Locus of Dysfunction in Adult Attention-Deficit/Hyperactivity Disorder." In: *Biological Psychiatry* 63.3 (2008), pp. 332–337. ISSN: 00063223. DOI: 10.1016/j.biopsych.2007.06.025.

[21] P. Ciuciu, P. Abry, and B. J. He. "Interplay between functional connectivity and scale-free dynamics in intrinsic fMRI networks." In: *NeuroImage* 95 (2014), pp. 248–263. ISSN: 10959572. DOI: 10.1016/j.neuroimage.2014.03.047. arXiv: NIHMS150003.

[22] L. Cocchi, I. E. Bramati, A. Zalesky, E. Furukawa, L. F. Fontenelle, J. Moll, G. Tripp, and P. Mattos. "Altered Functional Brain Connectivity in a Non-Clinical Sample of Young Adults with Attention-Deficit/Hyperactivity Disorder." In: *Journal of Neuroscience* 32.49 (2012), pp. 17753–17761. ISSN: 0270-6474. DOI: 10.1523/JNEUROSCI.3272-12.2012. URL: http://www.jneurosci.org/cgi/doi/10.1523/JNEUROSCI.3272-12.2012.

[23] J. B. Colby, J. D. Rudie, J. A. Brown, P. K. Douglas, M. S. Cohen, and Z. Shehzad. "Insights into multimodal imaging classification of ADHD." In: *Frontiers in Systems Neuroscience* 6 (2012). ISSN: 1662-5137. DOI: 10.3389/fnsys.2012.00059. URL: http://journal.frontiersin.org/article/10.3389/fnsys.2012.00059/abstract.

[24] R. C. Craddock, S. Jbabdi, C. G. Yan, J. T. Vogelstein, F. X. Castellanos, A. Di Martino, C. Kelly, K. Heberlein, S. Colcombe, and M. P. Milham. "Imaging human connectomes at the macroscale." In: *Nature Methods* 10.6 (2013), pp. 524–539. ISSN: 15487091. DOI: 10.1038/nmeth.2482. arXiv: NIHMS150003.

[25] R. C. Craddock, R. L. Tungaraza, and M. P. Milham. "Connectomics and new approaches for analyzing human brain functional connectivity." In: *GigaScience* 4 (2015). ISSN: 2047-217X. DOI: 10.1186/s13742-015-0045-x. URL: https://academic.oup.com/gigascience/article-lookup/doi/10.1186/s13742-015-0045-x.

[26] A. Cubillo and K. Rubia. "Structural and functional brain imaging in adult attention-deficit/hyperactivity disorder." In: *Expert Review of Neurotherapeutics* 10.4 (2010), pp. 603–620. ISSN: 1473-7175. DOI: 10.1586/ern.10.4. URL: http://www.tandfonline.com/doi/full/10.1586/ern.10.4.

[27] A. De La Fuente, S. Xia, C. Branch, and X. Li. "A review of attention-deficit/hyperactivity disorder from the perspective of brain networks Angelica." In: *Frontiers in Human Neuroscience* 7.192 (2013). DOI: doi.org/10.3389/fnhum.2013.00192.

[28] G. Deco and M. L. Kringelbach. "Great expectations: Using whole-brain computational connectomics for understanding neuropsychiatric disorders." In: *Neuron* 84.5 (2014), pp. 892–905. ISSN: 10974199. DOI: 10.1016/j.neuron.2014.08.034. URL: http://dx.doi.org/10.1016/j.neuron.2014.08.034.

[29] G. Deco, V. K. Jirsa, and A. R. McIntosh. "Emerging concepts for the dynamical organization of resting-state activity in the brain." In: *Nature Reviews Neuroscience* 12.1 (2011), pp. 43–56. ISSN: 1471003X. DOI: 10.1038/nrn2961.

[30] D. A. Fair, J. Posner, B. J. Nagel, D. Bathula, T. G. Dias, K. L. Mills, M. S. Blythe, A. Giwa, C. F. Schmitt, and J. T. Nigg. "Atypical default network connectivity in youth with attention-deficit/ hyperactivity disorder." In: *Biological Psychiatry* 68.12 (2010), pp. 1084–1091. ISSN: 00063223. DOI: 10.1016/j.biopsych.2010.07.003.

[31] M. Fiecas, H. Ombao, D. van Lunen, R. Baumgartner, A. Coimbra, and D. Feng. "Quantifying temporal correlations: A test-retest evaluation of functional connectivity in resting-state fMRI." In: *NeuroImage* 65 (2013), pp. 231–241. ISSN: 10538119. DOI: 10.1016/j.neuroimage.2012.09.052. URL: http://dx.doi.org/10.1016/j.neuroimage.2012.09.052.

[32] G. Fitzmaurice and M. G. Kenward. *Handbooks of Neuroimaging Data Analysis*. 2017. ISBN: 9781439854624.

[33] A. Fornito and E. T. Bullmore. "Connectomics: A new paradigm for understanding brain disease." In: *European Neuropsychopharmacology* 25.5 (2015), pp. 733–748. ISSN: 18737862. DOI: 10.1016/j.euroneuro.2014.02.011.

[34] M. D. Fox and M. Greicius. "Clinical applications of resting state functional connectivity." In: *Frontiers in Systems Neuroscience* 4.19 (2010), pp. 1–13. ISSN: 1662-5137. DOI: 10.3389/fnsys.2010.00019.

[35] M. D. Fox, M. Corbetta, A. Z. Snyder, J. L. Vincent, and M. E. Raichle. "Spontaneous neuronal activity distinguishes human dorsal and ventral attention systems." In: *Proceedings of the National Academy of Sciences* 103.26 (2006), pp. 10046–10051. ISSN: 0027-8424. DOI: 10.1073/pnas.0604187103. URL: http://www.ncbi.nlm.nih.gov/pubmed/16788060http://www.pubmedcentral.nih.gov/articlerender.fcgi?artid=PMC1480402http://www.pnas.org/cgi/doi/10.1073/pnas.0604187103.

[36] K. J. Friston. "Functional and Effective Connectivity: A Review." In: *Brain Connectivity* 1.1 (2011), pp. 13–36. ISSN: 2158-0014. DOI: 10.1089/brain.2011.0008. URL: http://www.liebertonline.com/doi/abs/10.1089/brain.2011.0008.

[37] P. M. Gleiser and V. I. Spoormaker. "Modelling hierarchical structure in functional brain networks." In: *Philosophical Transactions of the Royal Society A: Mathematical, Physical and Engineering Sciences* 368.1933 (2010), pp. 5633–5644. ISSN: 1364503X. DOI: 10.1098/rsta.2010.0279. URL: http://www.ncbi.nlm.nih.gov/pubmed/21078639.

[38] N. Gogolla. "The insular cortex." In: *Current Biology* 27.12 (2017), R580–R586. ISSN: 09609822. DOI: 10.1016/j.cub.2017.05.010.

[39] P. Hagmann. "From Diffusion MRI to Brain Connectomic." Doctoral dissertation. École Polytechnique Fédérale de Lausanne, 2005. ISBN: 9783642312083. DOI: 10.5075/epfl-thesis-3230. URL: http://library.epfl.ch/theses/?nr=3230.

[40] J. J. Harris, C. Reynell, and D. Attwell. "The physiology of developmental changes in BOLD functional imaging signals." In: *Developmental Cognitive Neuroscience* 1.3 (2011), pp. 199–216. ISSN: 18789293. DOI: 10.1016/j.dcn.2011.04.001.

[41] M. P. van den Heuvel and H. E. Hulshoff Pol. "Exploring the brain network: A review on resting-state fMRI functional connectivity." In: *European Neuropsychopharmacology* 20.8 (2010), pp. 519–534. ISSN: 0924977X. DOI: 10.1016/j.euroneuro.2010.03.008. arXiv: 0811.3721. URL: http://dx.doi.org/10.1016/j.euroneuro.2010.03.008.

[42] J. Hlinka, M. Paluš, M. Vejmelka, D. Mantini, and M. Corbetta. "Functional connectivity in resting-state fMRI: Is linear correlation sufficient?" In: *NeuroImage* 54.3 (2011), pp. 2218–2225. ISSN: 10538119. DOI: 10.1016/j.neuroimage.2010.08.042. arXiv: NIHMS150003.

[43] E. Hoekzema, S. Carmona, J. A. Ramos-Quiroga, V. Richarte Fernández, R. Bosch, J. C. Soliva, M. Rovira, A. Bulbena, A. Tobeña, M. Casas, and O. Vilarroya. "An independent components and functional connectivity analysis of resting state FMRI data points to neural network dysregulation in adult ADHD." In: *Human Brain Mapping* 35.4 (2014), pp. 1261–1272. ISSN: 10970193. DOI: 10.1002/hbm.22250.

[44] C. J. Honey, R. Kötter, M. Breakspear, and O. Sporns. "Network structure of cerebral cortex shapes functional connectivity on multiple time scales." In: *Proceedings of the National Academy of Sciences* 104.24 (2007), pp. 10240–10245. ISSN: 0027-8424. DOI: 10.1073/pnas.0701519104. URL: http://www.pnas.org/cgi/doi/10.1073/pnas.0701519104{\%}5Cnpapers3://publication/doi/10.1073/pnas.0701519104.

[45] R. M. Hutchison, T. Womelsdorf, E. A. Allen, P. A. Bandettini, V. D. Calhoun, M. Corbetta, S. Della Penna, J. H. Duyn, G. H. Glover, J. Gonzalez-Castillo, D. A. Handwerker, S. Keilholz, V. Kiviniemi, D. A. Leopold, F. de Pasquale, O. Sporns, M. Walter, and C. Chang. "Dynamic functional connectivity: Promise, issues, and interpretations." In: *NeuroImage* 80 (2013), pp. 360–378. ISSN: 10538119. DOI: 10.1016/j.neuroimage.2013.05.079. arXiv: NIHMS150003. URL: http://www.ncbi.nlm.nih.gov/pubmed/23707587http://www.pubmedcentral.nih.gov/articlerender.fcgi?artid=PMC3807588http://linkinghub.elsevier.com/retrieve/pii/S105381191300579X.

[46] R. Iannaccone, T. U. Hauser, J. Ball, D. Brandeis, S. Walitza, and S. Brem. "Classifying adolescent attention-deficit/hyperactivity disorder (ADHD) based on functional and structural imaging." In: *European Child and Adolescent Psychiatry* 24.10 (2015), pp. 1279–1289. ISSN: 1435165X. DOI: 10.1007/s00787-015-0678-4.

[47] O. Karim. *Statistical Signal Processing for Neuroscience and Neurotechnology*. Elsevier, 2010. ISBN: 9780123750273. DOI: 10.1016/C2009-0-20215-7. URL: https://linkinghub.elsevier.com/retrieve/pii/C20090202157.

[48] K. Konrad and S. B. Eickhoff. "Is the ADHD brain wired differently? A review on structural and functional connectivity in attention deficit hyperactivity disorder." In: *Human Brain Mapping* 31.6 (2010), pp. 904–916. ISSN: 10659471. DOI: 10.1002/hbm.21058.

[49] J. D. Kruschwitz, D. List, L. Waller, M. Rubinov, and H. Walter. "GraphVar: A user-friendly toolbox for comprehensive graph analyses of functional brain connectivity." In: *Journal of Neuroscience Methods* 245 (2015), pp. 107–115. ISSN: 1872678X. DOI: 10.1016/j.jneumeth.2015.02.021. URL: http://dx.doi.org/10.1016/j.jneumeth.2015.02.021.

[50] J. H. Krystal and M. W. State. "Psychiatric disorders: Diagnosis to therapy." In: *Cell* 157.1 (2014), pp. 201–214. ISSN: 10974172. DOI: 10.1016/j.cell.2014.02.042. URL: http://dx.doi.org/10.1016/j.cell.2014.02.042.

[51] J.-P. Lachaux, A. Lutz, D. Rudrauf, D. Cosmelli, M. Le Van Quyen, J. Martinerie, and F. Varela. "Estimating the time-course of coherence between single-trial brain signals: an introduction to wavelet coherence." In: *Neurophysiologie Clinique/Clinical Neurophysiology* 32.3 (2002), pp. 157–174. ISSN: 09877053. DOI: 10.1016/S0987-7053(02)00301-5. URL: http://linkinghub.elsevier.com/retrieve/pii/S0987705302003015.

[52] R. Leech and D. J. Sharp. "The role of the posterior cingulate cortex in cognition and disease." In: *Brain* 137.1 (2014), pp. 12–32. ISSN: 14602156. DOI: 10.1093/brain/awt162.

[53] K. Li, L. Guo, J. Nie, G. Li, and T. Liu. "Review of methods for functional brain connectivity detection using fMRI." In: *Computerized Medical Imaging and Graphics* 33.2 (2009), pp. 131–139. ISSN: 08956111. DOI: 10.1016/j.compmedimag.2008.10.011.

[54] C. Lithari, M. A. Klados, C. Papadelis, C. Pappas, M. Albani, and P. D. Bamidis. "How does the metric choice affect brain functional connectivity networks?" In: *Biomedical Signal Processing and Control* 7.3 (2012), pp. 228–236. ISSN: 17468094. DOI: 10.1016/j.bspc.2011.05.004. URL: http://dx.doi.org/10.1016/j.bspc.2011.05.004.

[55] F. Lopes Da Silva, J. P. Pijn, and P. Boeijinga. "Interpedence of EEG signals - linear vs nonlinear associations and the significance of time delays and phase shifts." In: *Brain Topography* 2 (1989), pp. 9–17. URL: papers2://publication/uuid/8A7E9298-5A32-44AF-89D6-CFC0B1DE3B1B.

[56] S. Marek and N. U. F. Dosenbach. "The frontoparietal network: function, electrophysiology, and importance of individual precision mapping." In: *Dialogues in clinical neuroscience* 20.2 (2018), pp. 133–140. ISSN: 1958-5969. URL: http://www.ncbi.nlm.nih.gov/pubmed/30250390http://www.pubmedcentral.nih.gov/articlerender.fcgi?artid=PMC6136121.

[57] D. W. McRobbie, E. A. Moore, M. J. Graves, and M. R. Prince. *MRI: From Picture to Proton*. 3rd. Cambridge University Press, 2017. ISBN: 978-1-107-64323-9.

[58] K. L. Mills, D. Bathula, T. G. Dias, S. P. Iyer, M. C. Fenesy, E. D. Musser, C. A. Stevens, B. L. Thurlow, S. D. Carpenter, B. J. Nagel, J. T. Nigg, and D. A. Fair. "Altered cortico-striatal-thalamic connectivity in relation to spatial working memory capacity in children with ADHD." In: *Frontiers in Psychiatry* 3.JAN (2012). ISSN: 16640640. DOI: 10.3389/fpsyt.2012.00002.

[59] J. C. Mostert, E. Shumskaya, M. Mennes, A. M. H. Onnink, M. Hoogman, C. C. Kan, A. Arias Vasquez, J. Buitelaar, B. Franke, and D. G. Norris. "Characterising resting-state functional connectivity in a large sample of adults with ADHD." In: *Progress in Neuro-Psychopharmacology and Biological Psychiatry* 67 (2016), pp. 82–91. ISSN: 18784216. DOI: 10.1016/j.pnpbp.2016.01.011. arXiv: 15334406.

[60] K. Murphy and M. D. Fox. "Towards a consensus regarding global signal regression for resting state functional connectivity MRI." In: *NeuroImage* 154 (2017), pp. 169–173. ISSN: 10959572. DOI: 10.1016/j.neuroimage.2016.11.052.

[61] H. Namkung, S. H. Kim, and A. Sawa. "The Insula: An Underestimated Brain Area in Clinical Neuroscience, Psychiatry, and Neurology." In: *Trends in Neurosciences* 40.4 (2017), pp. 200–207. ISSN: 1878108X. DOI: 10.1016/j.tins.2018.05.004. arXiv: 15334406.

[62] S Ogawa, T. M. Lee, A. R. Kay, and D. W. Tank. "Brain magnetic resonance imaging with contrast dependent on blood oxygenation." In: *Proceedings of the National Academy of Sciences of the United States of America* 87.24 (1990), pp. 9868–72. ISSN: 0027-8424. DOI: 10.1073/pnas.87.24.9868. arXiv: NIHMS150003. URL: http://www.pubmedcentral.nih.gov/articlerender.fcgi?artid=55275{\&}tool=pmcentrez{\&}rendertype=abstract.

[63] E. Pereda, R. Q. Quiroga, and J. Bhattacharya. "Nonlinear multivariate analysis of neurophysiological signals." In: *Progress in Neurobiology* 77.1-2 (2005), pp. 1–37. ISSN: 03010082. DOI: 10.1016/j.pneurobio.2005.10.003. arXiv: 0510077 [nlin].

[64] J. Posner, V. Rauh, A. Gruber, I. Gat, Z. Wang, and B. S. Peterson. "Dissociable attentional and affective circuits in medication-naïve children with attention-deficit/hyperactivity disorder." In: *Psychiatry Research - Neuroimaging* 213.1 (2013), pp. 24–30. ISSN: 09254927. DOI: 10.1016/j.pscychresns.2013.01.004. arXiv: NIHMS150003.

[65] J. Posner, C. Park, and Z. Wang. "Connecting the dots: A review of resting connectivity MRI studies in attention-deficit/hyperactivity disorder." In: *Neuropsychology Review* 24.1 (2014), pp. 3–15. ISSN: 10407308. DOI: 10.1007/s11065-014-9251-z. arXiv: NIHMS150003.

[66] M. E. Raichle, A. M. MacLeod, A. Z. Snyder, W. J. Powers, D. A. Gusnard, and G. L. Shulman. "A default mode of brain function." In: *Proceedings of the National Academy of Sciences of the United States of America* 98.2 (2001), pp. 676–82. ISSN: 0027-8424. DOI: 10.1073/pnas.98.2.676. arXiv: 0402594v3 [arXiv:cond-mat]. URL: http://www.pubmedcentral.nih.gov/articlerender.fcgi?artid=14647{\&}tool=pmcentrez{\&}rendertype=abstract.

[67] D Rangaprakash, G. R. Wu, D. Marinazzo, X. Hu, and G. Deshpande. "Hemodynamic response function (HRF) variability confounds resting-state fMRI functional connectivity." In: *Magnetic Resonance in Medicine* 80.4 (2018), pp. 1697–1713. ISSN: 15222594. DOI: 10.1002/mrm.27146.

[68] D. N. Reshef, Y. A. Reshef, H. K. Finucane, S. R. Grossman, G. McVean, P. J. Turnbaugh, E. S. Lander, M. Mitzenmacher, and P. C. Sabeti. "Detecting novel associations in large data sets." In: *Science* 334.6062 (2011), pp. 1518–1524. ISSN: 10959203. DOI: 10.1126/science.1205438. arXiv: arXiv:1401.7645v1. URL: http://science.sciencemag.org/http://www.sciencemag.org/cgi/doi/10.1126/science.1205438.

[69] V. Sakkalis. "Review of advanced techniques for the estimation of brain connectivity measured with EEG/MEG." In: *Computers in Biology and Medicine* 41.12 (2011), pp. 1110–1117. ISSN: 00104825. DOI: 10.1016/j.compbiomed.2011.06.020.

[70] J. R. Sato, M. Q. Hoexter, X. F. Castellanos, and L. A. Rohde. "Abnormal Brain Connectivity Patterns in Adults with ADHD: A Coherence Study." In: *PLoS ONE* 7.9 (2012). ISSN: 19326203. DOI: 10.1371/journal.pone.0045671. arXiv: 1208.2976.

[71] T. Schreiber. "Measuring information transfer." In: *Physical Review Letters* 85.2 (2000), pp. 461–464. ISSN: 00319007. DOI: 10.1103/PhysRevLett.85.461. arXiv: 0001042v1 [nlin].

[72] S. M. Smith, K. L. Miller, G. Salimi-Khorshidi, M. Webster, C. F. Beckmann, T. E. Nichols, J. D. Ramsey, and M. W. Woolrich. "Network modelling methods for FMRI." In: *NeuroImage* 54.2 (2011), pp. 875–891. ISSN: 10538119. DOI: 10.1016/

j.neuroimage.2010.08.063. URL: http://dx.doi.org/10.1016/j.neuroimage.2010.08.063.

[73] K. Smitha, K Akhil Raja, K. Arun, P. Rajesh, B. Thomas, T. Kapilamoorthy, and C. Kesavadas. "Resting state fMRI: A review on methods in resting state connectivity analysis and resting state networks." In: *The Neuroradiology Journal* 30.4 (2017), pp. 305–317. ISSN: 1971-4009. DOI: 10.1177/1971400917697342. URL: http://journals.sagepub.com/doi/10.1177/1971400917697342.

[74] O. Sporns, G. Tononi, and R. Kötter. *The human connectome: A structural description of the human brain*. 2005. DOI: 10.1371/journal.pcbi.0010042. arXiv: arXiv:1011.1669v3.

[75] F. T. Sun, L. M. Miller, and M. D'Esposito. "Measuring interregional functional connectivity using coherence and partial coherence analyses of fMRI data." In: *NeuroImage* 21.2 (2004), pp. 647–658. ISSN: 10538119. DOI: 10.1016/j.neuroimage.2003.09.056.

[76] L. Sun, Q. Cao, X. Long, M. Sui, X. Cao, C. Zhu, X. Zuo, L. An, Y. Song, Y. Zang, and Y. Wang. "Abnormal functional connectivity between the anterior cingulate and the default mode network in drug-naïve boys with attention deficit hyperactivity disorder." In: *Psychiatry Research - Neuroimaging* 201.2 (2012), pp. 120–127. ISSN: 09254927. DOI: 10.1016/j.pscychresns.2011.07.001.

[77] B. T. Thomas Yeo, F. M. Krienen, J. Sepulcre, M. R. Sabuncu, D. Lashkari, M. Hollinshead, J. L. Roffman, J. W. Smoller, L. Zöllei, J. R. Polimeni, B. Fischl, H. Liu, and R. L. Buckner. "The organization of the human cerebral cortex estimated by intrinsic functional connectivity." In: *Journal of Neurophysiology* 106.3 (2011), pp. 1125–1165. ISSN: 0022-3077. DOI: 10.1152/jn.00338.2011. arXiv: NIHMS150003. URL: http://jn.physiology.org/cgi/doi/10.1152/jn.00339.2011http://www.physiology.org/doi/10.1152/jn.00339.2011http://www.physiology.org/doi/10.1152/jn.00338.2011.

[78] L. Tian, T. Jiang, Y. Wang, Y. Zang, Y. He, M. Liang, M. Sui, Q. Cao, S. Hu, M. Peng, and Y. Zhuo. "Altered resting-state functional connectivity patterns of anterior cingulate cortex in adolescents with attention deficit hyperactivity disorder." In: *Neuroscience Letters* 400.1-2 (2006), pp. 39–43. ISSN: 03043940. DOI: 10.1016/j.neulet.2006.02.022.

[79] D. Tomasi and N. D. Volkow. "Abnormal Functional Connectivity in Children with Attention-Deficit/Hyperactivity Disorder." In: *Biological Psychiatry* 71.5 (2012), pp. 443–450. DOI: 10.1016/j.biopsych.2011.11.003.

[80] C. Torrence and G. P. Compo. "A Practical Guide to Wavelet Analysis." In: *Bulletin of the American Meteorological Society* 79.1 (1998), pp. 61–78.

[81] L. Q. Uddin, A. M. Kelly, B. B. Biswal, D. S. Margulies, Z. Shehzad, D. Shaw, M. Ghaffari, J. Rotrosen, L. A. Adler, F. X. Castellanos, and M. P. Milham. "Network homogeneity reveals decreased integrity of default-mode network in ADHD." In: *Journal of Neuroscience Methods* 169.1 (2008), pp. 249–254. ISSN: 01650270. DOI: 10.1016/j.jneumeth.2007.11.031. arXiv: arXiv:0810.5560v1.

[82] K. Ugurbil. "What is feasible with imaging human brain function and connectivity using functional magnetic resonance imaging." In: *Philosophical Transactions of the Royal Society B: Biological Sciences* 371.1705 (2016). ISSN: 14712970. DOI: 10.1098/rstb.2015.0361.

[83] R. Vicente, M. Wibral, M. Lindner, and G. Pipa. "Transfer entropy-a model-free measure of effective connectivity for the neurosciences." In: *Journal of Computational Neuroscience* 30.1 (2011), pp. 45–67. ISSN: 09295313. DOI: 10.1007/s10827-010-0262-3. URL: http://www.ncbi.nlm.nih.gov/pubmed/20706781http://www.pubmedcentral.nih.gov/articlerender.fcgi?artid=PMC3040354.

[84] H. E. Wang, C. G. Bénar, P. P. Quilichini, K. J. Friston, V. K. Jirsa, and C. Bernard. "A systematic framework for functional connectivity measures." In: *Frontiers in Neuroscience* 8 (2014), pp. 1–22. ISSN: 1662453X. DOI: 10.3389/fnins.2014.00405.

[85] H. E. Wang, K. J. Friston, C. G. Bénar, M. M. Woodman, P. Chauvel, V. Jirsa, and C. Bernard. "MULAN: Evaluation and ensemble statistical inference for functional connectivity." In: *NeuroImage* 166.July 2017 (2018), pp. 167–184. ISSN: 10959572. DOI: 10.1016/j.neuroimage.2017.10.036.

[86] W. Wang, B. Hu, Z. Yao, M. Jackson, R. Liu, and C. Liang. "Dysfunctional neural activity and connection patterns in attention deficit hyperactivity disorder: A resting state fMRI study." In: *Proceedings of the International Joint Conference on Neural Networks*. 2013. ISBN: 9781467361293. DOI: 10.1109/IJCNN.2013.6707011.

[87] X. Wang, Y. Jiao, and Z. Lu. "Discriminative analysis of resting-state brain functional connectivity patterns of Attention-Deficit Hyperactivity Disorder using Kernel Principal Component Analysis." In: *Proceedings - 2011 8th International Conference on Fuzzy Systems and Knowledge Discovery, FSKD 2011*. Vol. 3. 2011, pp. 1938–1941. ISBN: 9781612841816. DOI: 10.1109/FSKD.2011.6019911.

[88] M. Xia, J. Wang, and Y. He. "BrainNet Viewer: A Network Visualization Tool for Human Brain Connectomics." In: *PLoS ONE* 8.7 (2013). Ed. by P. Csermely. ISSN: 19326203. DOI: 10.1371/journal.pone.0068910. URL: https://dx.plos.org/10.1371/journal.pone.0068910.

[89] H. Yang, Q. Z. Wu, L. T. Guo, Q. Q. Li, X. Y. Long, X. Q. Huang, R. C. Chan, and Q. Y. Gong. "Abnormal spontaneous brain activity in medication-naïve ADHD children: A resting state fMRI study." In: *Neuroscience Letters* 502.2 (2011), pp. 89–93. ISSN: 03043940. DOI: 10.1016/j.neulet.2011.07.028.

[90] Z. Yao, B. Hu, Y. Xie, P. Moore, and J. Zheng. "A review of structural and functional brain networks: small world and atlas." In: *Brain Informatics* 2.1 (2015), pp. 45–52. ISSN: 2198-4018. DOI: 10.1007/s40708-015-0009-z. URL: http://link.springer.com/10.1007/s40708-015-0009-z.

[91] Y. F. Zang, H. Yong, Z. Chao-Zhe, C. Qing-Jiu, S. Man-Qiu, L. Meng, T. Li-Xia, J. Tian-Zi, and W. Yu-Feng. "Altered baseline brain activity in children with ADHD revealed by resting-state functional MRI." In: *Brain and Development* 29.2 (2007), pp. 83–91. ISSN: 01560417. DOI: 10.1016/j.braindev.2006.07.002. arXiv: NIHMS150003.

[92] W. Zhang, V. Muravina, R. Azencott, Z. D. Chu, and M. J. Paldino. "Mutual information better quantifies brain network architecture in children with epilepsy." In: *Computational and Mathematical Methods in Medicine* 2018 (2018). ISSN: 17486718. DOI: 10.1155/2018/6142898.

[93] X. Zhong, H. Shi, Q. Ming, D. Dong, X. Zhang, L. L. Zeng, and S. Yao. "Whole-brain resting-state functional connectivity identified major depressive disorder: A multivariate pattern analysis in two independent samples." In: *Journal of Affective Disorders* 218 (2017), pp. 346–352. ISSN: 15732517. DOI: 10.1016/j.jad.2017.04.040. URL: http://dx.doi.org/10.1016/j.jad.2017.04.040.